The Impact of Type Two Diabetes Mellitus on the Cardiac Metabolic Phenotype and Myocardial Perfusion in Patients with Severe Aortic Stenosis and Hypertrophic Cardiomyopathy

Nicholas James George Jex

Submitted in Accordance with the Requirements for the Degree of

Doctor of Philosophy

The University of Leeds

School of Medicine

December 2022

UNIVERSITY OF LEEDS

Intellectual Property and Publication Statement

(A) I can confirm that the work submitted here is my own and that appropriate credit has been given where reference has been made to the work of others.

(B) This copy has been supplied on the understanding that it is copyright material and that no quotation from the thesis may be published without proper acknowledgement.

Declarations

This work is original and my own, Dr David Broadbent provided physics support leading to the results in Chapter 3. Dr Amrit Chowdhary, Dr Sharmaine Thirunavukarasu and Dr Sindhoora Kotha provided help with scanning and study visits leading to the results in Chapters 4 and 5. Dr Amrit Chowdhary and Dr Sindhoora Kotha also provided support with biopsy sample collection leading to the results in chapter 6. Dr Henry Procter provided help with blinded analysis leading to the results in Chapters 4 and 5. David Shelly, Lizette Cash, Julian Tongue, Margaret Saysell, Lisa Lewis, and Gavin Bainbridge provided support with patient scanning leading to the results in chapters 4 and 5. Mr Sotiris Papaspyros, Ms Betsy Evans, Mr Kalyana Javangula, Ms Antonella Ferrara, Mr Pankaj Kaul, and Mr Walid Elmahdy performed intra-operative myocardial biopsy sampling leading to the results in chapter 6. Ms Amanda Maccannell, Ms Anna McGrane and Ms Marcella Conning-Rowland aided with biopsy sample collection and analysis leading to the results in Chapter 6.

Acknowledgements

I will be forever indebted to my amazing primary supervisor Dr Eylem Levelt, without whose continued guidance and unwavering support this work would not have been possible. It was a real honour to work with such a talented and caring individual.

Additional thanks to my secondary supervisors Prof John Greenwood and Prof Sven Plein for all their support and advice during my thesis. I would also like to thank the following colleagues in my research group, Dr Amrit Chowdhary, Dr Sharmaine Thirunavukarasu, Dr Sindhoora Kotha, Dr Henry Procter, and Dr Marilena Giannoudi for their friendship, help with the day to day running of my projects and for making my time spent as a research fellow a fun and rewarding experience I will forever look back on fondly.

I am also very grateful to my colleagues David Shelly, Lizette Cash, Julian Tongue, Margaret Saysell, Lisa Lewis, and Gavin Bainbridge for their support with scanning and to Dr David Broadbent for his technical support and troubleshooting.

I would like to thank Mr Sotiris Papaspyros, Ms Betsy Evans, Mr Kalyana Javangula, Ms Antonella Ferrara, Mr Pankaj Kaul, and Mr Walid Elmahdy for their collaboration on the myocardial biopsy study.

I would also like to place on record my thanks to my colleagues in the LIGHT laboratory, Amanda Maccannell, Anna McGrane and Marcella Conning-Rowland for their collaboration with biopsy sample analysis.

Thesis Abstract

It is well established that type 2 diabetes mellitus (T2DM) in isolation is associated with increased cardiovascular morbidity and mortality, even in the absence of coronary artery disease. However, despite epidemiological evidence showing increased morbidity and mortality when T2DM co-exists in states of acquired or inherited cardiac hypertrophy, such as severe aortic stenosis (AS) and hypertrophic cardiomyopathy (HCM) respectively, a more detailed assessment of the metabolic, structural, and functional phenotypic alterations associated with co-morbid T2DM in these common cardiovascular conditions remains to be established. Cardiac magnetic resonance (CMR) and phosphorus magnetic resonance spectroscopy (^{31}P-MRS) are powerful tools which can aid the characterisation of the myocardial sequelae of these common co-morbidities.

The aims of this thesis were to use CMR and ^{31}P-MRS to define the impact of co-morbid T2DM in severe AS and in HCM respectively, with regard to the alterations in myocardial phosphocreatine to ATP ratio (PCr/ATP) as a sensitive indicator of myocardial energetic state, perfusion, structure, and function.

To the best of my knowledge this thesis is the first to report that severe AS or HCM-associated abnormalities in myocardial PCr/ATP and in stress indices of myocardial perfusion including stress myocardial blood flow and myocardial perfusion reserve are exacerbated by T2DM comorbidity. Moreover, in a longitudinal cohort study this thesis is the first to report that while aortic valve replacement reverses myocardial abnormalities and limitations in exercise capacity in patients with severe AS alone, despite a similar degree of improvement in aortic valve gradient, the recovery in myocardial features were nevertheless undermined by T2DM comorbidity. In addition, in patients with HCM, the work in this thesis shows that despite matching for sarcomeric mutations and left ventricular mass, patients with T2DM comorbidity displayed a greater degree of fibrosis burden with higher scar percentage than patients with HCM alone.

This work has also demonstrated that the energetic impairment in T2DM seen with non-invasive imaging, translates to impairment in myocardial mitochondrial oxidative phosphorylation with use of high resolution respirometry technique on myocardial biopsy

sample analysis. Additionally, a modified phosphorous spectroscopy technique is presented, with improved patient comfort and a higher degree of reproducibility, which might allow for the wider application of this technique.

In summary, the work in this thesis demonstrates the significant impact of T2DM on myocardial PCr/ATP, perfusion, and function in states of cardiac hypertrophy and demonstrates the potential for advanced MR imaging techniques to allow for improved patient risk stratification and a more refined approach to assessing and treating these common co-morbidities.

Table of Contents

Abbreviations

ACE-I	Angiotensin-converting enzyme inhibitors
ADP	Adenosine diphosphate
AF	Atrial fibrillation
AS	Aortic stenosis
ATP	Adenosine triphosphate
AVR	Aortic valve replacement
AW	Acquisition Weighting
BMI	Body Mass Index
CAD	Coronary artery disease
CCCP	Carbonyl cyanide m-chlorophenyl hydrazone
CFS	Clinical frailty score
CSI	Chemical shift imaging
CK	Creatine kinase
CMR	Cardiovascular Magnetic Resonance
COV	Coefficient of variance
CSI	Chemical shift imaging
CV	Cardiovascular
DM	Diabetes mellitus
EDV	End diastolic volume
ECV	Extra cellular volume fraction
ECG	Electrocardiogram
ESC	European Society of Cardiology
ESV	End systolic volume
FFA	Free fatty acids
HbA1c	Glycated hemoglobin
HOMA-IR	Homeostatic Assessment of Insulin Resistance
iECV	Indexed extra cellular volume
LDL	Low density lipoprotein
LGE	Late gadolinium enhancement
LV	Left ventricle

MBF	Myocardial blood flow
MOLLI	Modified look locker inversion recovery
MPRI	Myocardial perfusion reserve index
MRI	Magnetic resonance imaging
NO	Nitric oxide
NT-pro BNP	N-terminal pro hormone B-type natriuretic peptide
NYHA	New York Heart Association
^{31}P-MRS	^{31} Phosphorus magnetic resonance spectroscopy
PPA	Phenyl phosphoric acid
PCr	Phosphocreatine
RF	Radio frequency
ROT	Rotenone
RPP	Rate pressure product
RV	Right ventricle
SNR	Signal to noise ratio
SSFP	Steady State Free Precession
SAVR	Surgical aortic valve replacement
SV	Stroke volume
Svi	Stroke volume indexed to body surface area
T	Tesla
TE	Echo time
TG	Triglyceride
TR	Repetition time
T1DM	Type 1 Diabetes Mellitus
T2DM	Type 2 Diabetes Mellitus

Presentations

International

August 2022 - **Coexistent Diabetes Is Associated With the Presence of Adverse Phenotypic Features in Patients With Hypertrophic Cardiomyopathy –** Oral poster presentation, European Society Cardiology, Barcelona, Spain

February 2022 – **Deteriorating coronary microvascular function despite normal coronary angiography in a patient with co-morbid hypertrophic cardiomyopathy and type two diabetes mellitus** – Oral presentation 25th Annual SCMR Scientific Sessions, Florida, USA

February 2022 – **Comorbid diabetes worsens myocardial energetics, perfusion and contractility in patients with severe aortic stenosis -** Oral presentation 25th Annual SCMR Scientific Sessions, Florida, USA

National

June 2022 - **Coexistent diabetes is associated with residual myocardial abnormalities after aortic valve replacement in patients with severe aortic stenosis.** Oral presentation BCS annual conference, Manchester, UK

October 2021 - **Coexistent Diabetes Is Associated with the Presence of Adverse Phenotypic Features in Patients with Hypertrophic Cardiomyopathy.** Oral presentation BSCMR annual conference, London, UK

Publications

H-index: 5; i10-index: 4; total publications: 17

Peer reviewed papers

1. Brown LAE, Gulsin GS, Onciul SC, Broadbent DA, Yeo JL, Wood AL, Saunderson CED, Das A, **Jex N**, Chowdhary A, Thirunavukarasu S, Sharrack N, Knott KD, Levelt E, Swoboda PP, Xue H, Greenwood JP, Moon JC, Adlam D, McCann GP, Kellman P, Plein S. **Sex- and age-specific normal values for automated quantitative pixel-wise myocardial perfusion cardiovascular magnetic resonance.**
   Eur Heart J Cardiovasc Imaging. 2022 Dec

2. Brown LAE, Wahab A, Ikongo E, Saunderson CED, **Jex N**, Thirunavukarasu S, Chowdhary A, Das A, Craven TP, Levelt E, Dall'Armellina E, Knott KD, Greenwood JP, Moon JC, Xue H, Kellman P, Plein S, Swoboda PP. **Cardiovascular magnetic resonance phenotyping of heart failure with mildly reduced ejection fraction.** *Eur Heart J Cardiovasc Imaging*. 2022 Oct
3. Chowdhary A, Javed W, Thirunavukarasu S, **Jex N**, Kotha S, Kellman P, Swoboda P, Greenwood JP, Plein S, Levelt E. **Cardiac Adaptations to Acute Hemodynamic Stress in Function, Perfusion, and Energetics in Type 2 Diabetes with Overweight and Obesity.** *Diabetes Care.* 2022 Oct
4. Thirunavukarasu S, Ansari F, Cubbon R, Forbes K, Bucciarelli-Ducci C, Newby DE, Dweck MR, Rider OJ, Valkovič L, Rodgers CT, Tyler DJ, Chowdhary A, **Jex N**, Kotha S, Morley L, Xue H, Swoboda P, Kellman P, Greenwood JP, Plein S, Everett T, Scott E, Levelt E. **Maternal Cardiac Changes in Women with Obesity and Gestational Diabetes Mellitus**. *Diabetes Care*. 2022 Sep
5. Gorecka M, **Jex N,** Thirunavukarasu S, Chowdhary A, Corrado J, Davison J, Tarrant R, Poenar AM, Sharrack N, Parkin A, Sivan M, Swoboda PP, Xue H, Vassiliou V, Kellman P, Plein S, Halpin SJ, Simms AD, Greenwood JP, Levelt E. **Cardiovascular magnetic resonance imaging and spectroscopy in clinical long-COVID-19 syndrome: a prospective case-control study**. *J Cardiovasc Magn Reson*. 2022 Sep
6. **Jex N,** Chowdhary A, Thirunavukarasu S, Levelt E. **A case report of refractory angina in a patient with diabetes and apical hypertrophic cardiomyopathy**. *Eur Heart J Case Rep*. 2022 Aug
7. **Jex N,** Chowdhary A, Thirunavukarasu S, Procter H, Sengupta A, Natarajan P, Kotha S, Poenar AM, Swoboda P, Xue H, Cubbon RM, Kellman P, Greenwood JP, Plein S, Page S, Levelt E. **Coexistent diabetes is associated with the presence of adverse phenotypic features in patients with hypertrophic cardiomyopathy**. *Diabetes Care.* 2022 Aug
8. Chowdhary A, Thirunavukarasu S, **Jex N,** Coles L, Bowers C, Sengupta A, Swoboda P, Witte K, Cubbon R, Xue H, Kellman P, Greenwood J, Plein S, Levelt E. **Coronary microvascular function and visceral adiposity in patients with normal body weight and type 2 diabetes**. *Obesity.* 2022 May
9. Malik A, Garland E, Drozd M, Palin V, Giannoudi M, Straw S, **Jex N,** Walker AM, Gierula J, Paton M, Witte KK, Kearney MT, Levelt E, Cubbon RM. **Diabetes mellitus**

and the causes of hospitalisation in people with heart failure. *Diab Vasc Dis Res*. 2022 Jan

10. Chowdhary A, **Jex N,** Thirunavukarasu S, MacCannell A, Haywood N, Almutairi A, Athithan L, Jain M, Craven T, Das A, Sharrack N, Saunderson CED, Sengupta A, Roberts L, Swoboda P, Cubbon R, Witte K, Greenwood J, Plein S, Levelt E. **Prospective longitudinal characterization of the relationship between diabetes and cardiac structural and functional changes**. *Cardiol Res Pract.* 2022 Feb
11. Das A, Kelly C, Teh I, Nguyen C, Brown LAE, Chowdhary A, **Jex N,** Thirunavukarasu S, Sharrack N, Gorecka M, Swoboda PP, Greenwood JP, Kellman P, Moon JC, Davies RH, Lopes LR, Joy G, Plein S, Schneider JE, Dall'Armellina E. **Phenotyping hypertrophic cardiomyopathy using cardiac diffusion magnetic resonance imaging: the relationship between microvascular dysfunction and microstructural changes.** *Eur Heart J Cardiovasc Imaging*. 2022 Feb
12. Thirunavukarasu S, **Jex N**, Chowdhary A, Hassan IU, Straw S, Craven TP, Gorecka M, Broadbent D, Swoboda P, Witte KK, Cubbon RM, Xue H, Kellman P, Greenwood JP, Plein S, Levelt E. **Empagliflozin treatment is associated with improvements in cardiac energetics and function and reductions in myocardial cellular volume in patients with type 2 diabetes**. *Diabetes*. 2021 Dec
13. **Jex, N.,** Farley, J., Thirunavukarasu, S., Chowdhary, A., Sengupta, A., Greenwood, J.P, Schlosshan, D., Plein, S., Levelt, E. **A 30-Year-old man with primary cardiac angiosarcoma,** *JACC: Case Reports,* 2021
14. Craven, T.P., **Jex, N.**, Chew, P.G. *et al.* **Exercise cardiovascular magnetic resonance: feasibility and development of biventricular function and great vessel flow assessment, during continuous exercise accelerated by Compressed SENSE: preliminary results in healthy volunteers**. *Int J Cardiovasc Imaging*, 2021
15. Das, A., Chowdhary, A., Kelly, C., Teh, I., Stoeck, C.T., Kozerke, S., Maxwell, N., Craven, T.P., **Jex, N.J**., Saunderson, C.E., Brown, L.A., Ben-Arzi, H., Sengupta, A., Page, S.P., Swoboda, P.P., Greenwood, J.P., Schneider, J.E., Plein, S. and Dall'Armellina, E. (2021), **Insight into myocardial microstructure of athletes and hypertrophic cardiomyopathy patients using diffusion tensor imaging**. *J Magn Reson Imaging*
16. Thirunavukarasu, S.A., Brown, L.A., Chowdhary, A., **Jex, N**., et al. **Rationale and design of the randomised controlled cross-over trial: Cardiovascular effects of empaglifozin in diabetes mellitus.** *Diab Vasc Dis Res*; 20
    Das,A., Kelly,C., Teh,I., Stoeck,CT., Kozerke,S., Chowdhary,A., Brown,L.A., Saunderson,C.E., Craven,T.P., Chew,P.G., **Jex,N**., Swoboda,P.P., Levelt,E., Greenwood, J.P., Schneider, J.E., Plein, S. and Dall'Armellina, E. **Acute microstructural changes after ST-segment elevation myocardial infarction assessed with diffusion tensor imaging**, *Radiology* 2021
17. Athithan, L., Chowdhary,A., Swarbrick,D., Gulsin,S.G., Singh,A., **Jex,N.,** Jain,M., et al. **"Male sex adversely affects the phenotypic expression of diabetic heart disease."** *Therapeutic Advances in Endocrinology and Metabolism***,** (January 2020)

Manuscripts currently undergoing rebuttal process

Jex, N et al. **Coexistent diabetes is associated with residual myocardial abnormalities after aortic valve replacement in patients with severe aortic stenosis.** *Circulation*

Manuscripts undergoing internal review process

Jex, N et al. **Type 2 diabetes is associated with sarcopenic obesity in subjects with severe aortic stenosis and is associated with a residual impairment in post operative exercise capacity following aortic valve replacement**

Chapter 1

Introduction

1.1 Diabetic Cardiomyopthy

1.11 Background

The concept of a distinct cardiomyopathy independent of coronary artery disease, valvular heart disease and hypertension was first proposed by Rubler et al in 1972[1]. This was subsequently born out in epidemiological data from the Framingham Heart Study in 1974 which showed a higher incidence of heart failure in diabetic men (2.4:1) and women (5:1), even after adjusting for traditional risk factors such as age, coronary artery disease and hypertension[2]. However, it was not until 2013 that a joint position statement from the American Heart Association and the European Society of Cardiology defined diabetic cardiomyopathy as 'a condition of ventricular dysfunction that occurs in the absence of coronary artery disease and hypertension in patients with diabetes mellitus'[3]. Whilst initial focus centred on macro myocardial structural abnormalities such as fibrosis, hypertrophy and microangiopathy, there is emerging evidence that the diabetic cardiomyopathy phenotype involves a complex process of molecular and metabolic derangement[4,5].

1.12 Epidemiology

In the context of a global obesity pandemic, the prevalence of type 2 diabetes mellitus (T2DM) is increasing at an alarming rate in all age groups, with 5 million UK citizens expected to have diabetes by 2025[6]. Contemporary European data shows the incidence of heart failure to be as high as 21% in the diabetic population[6,7], with an increased relative risk of developing heart failure in both individuals with clinically defined diabetes (OR 2.8) but also those with the so-called 'pre-diabetic' state of abnormal glucose regulation (OR 1.7)[8]. The challenges in demonstrating a causal link between diabetes and heart failure (HF), however, remain formidable. Inferred evidence for a diabetic cardiomyopathy in humans rests on a number of structural, functional, and metabolic observations.

1.13 Macroscopic Structural and Functional Alterations

T2DM represents a serious disruption of fuel homeostasis with ravaging consequences throughout the body. Echocardiographic screening shows combined diabetes and heart failure to be associated with increased left ventricular wall thickness, mass and reduced left ventricular cavity volume, a process of concentric remodelling, with resultant reduction in LV systolic performance and increased arterial stiffness[9,10]. Increasing LV mass and concentricity, as defined by LV mass:volume, is associated with increased mortality and incidence of heart failure events (HR 1.4, per 10% increment)[11,12]. The increased hypertrophic response seen in T2DM is associated with myocardial fibrosis, a well-recognised independent predictor of cardiovascular mortality [13,14].

1.14 Molecular Mechanisms of Diabetic Cardiomyopathy

The primary cardiac metabolic alterations in T2DM include impaired insulin metabolic signalling and decreased GLUT-4 recruitment to the myocyte plasma membrane, with resultant reduced myocardial glucose uptake, from which numerous alterations in underlying myocyte homeostasis occur[4,15]. On the microscopic level, histological studies demonstrate that diabetes is associated with myocyte hypertrophy, stiffness, perivascular fibrosis, and increased quantities of matrix collagen, cellular triglyceride, and cell membrane lipid[4,9,16,17].
Myocyte stiffness is thought to result from decreased GLUT-4 expression and increased intra-cellular calcium, with impaired insulin signalling also resulting in decreased coronary mediated nitric oxide (NO) production which increases titin phosphorylation, an additional contributor to myocyte stiffness[4,18].
Hyperglycaemia, insulin resistance and oxidative stress, the central metabolic disturbances seen in T2DM, contribute to cardiomyocyte hypertrophy through hypertrophic gene expression via β-myosin heavy chain (MYH7), insulin-like growth factor 1 (ILG-1) and B type natriuretic peptide (BNP)[19]. Myocardial fibrosis, increasingly recognised as a significant independent risk factor for cardiovascular mortality, is increased in T2DM[14,20,21]. Hyperinsulinemia, hyperglycaemia and renin-angiotensin- aldosterone (RAAS) system activation leads to activation of transforming growth factor β-1, inducing interstitial and peri-vascular fibrosis, collagen cross-linking and basement membrane thickening[22,23].

1.15 Normal myocardial high energy phosphate metabolism

The heart consumes more energy than any other organ per gram of tissue and must continually produce significant quantities of ATP to maintain contractile function[24]. If not replaced the heart would become deficient of ATP in between 2-10 seconds resulting in contractile failure[25,26]. Therefore, just as the heart has a large contractile reserve, a significant metabolic reserve exists to meet changes in energy demand [27]. The heart can increase its pump work three-fold despite a limited capacity for energy storage, changes in energy demand thus require a rapid response from mitochondria [27,28].

Cardiac energy metabolism has four principal components

1. Adequate perfusion: An adequate blood supply, with appropriate hyperaemic response during exercise allows sufficient delivery of both substrate and oxygen to the myocardium[29].

2. Substrate utilisation: The heart is a metabolic omnivore, demonstrating flexibility in its ability to use a variety of substrates to meet energy demands[30]. Under normal conditions 85% of cardiac ATP is derived from fatty acids (FA), (57% from free fatty acids (FFA) and 28% from lipoprotein derived FA's), in-addition, glucose, ketones, glutamate and branch chain amino acids (BCAA) can all be utilised to varying degrees, dependent on the physiological conditions [26,31-33]. Substrates are ultimately broken down, predominantly via beta oxidation and glycolysis, with the entry of resultant intermediary metabolites into the tricarboxylic acid (TCA) cycle (Fig 1).

3. Oxidative phosphorylation: The production of energy via the mitochondrial respiratory-chain complexes I through IV, which transfer electrons from NADH to oxygen, thereby creating a proton electrochemical gradient across the inner mitochondrial membrane as well as NAD and water. This gradient drives ATP synthase, which produces ATP by phosphorylating ADP (adenosine diphosphate)[26].

4. ATP transfer and utilisation: Energy transfer occurs via the creatine kinase (CK) energy shuttle. Mitochondrial creatine kinase catalyses the transfer of the high energy phosphate bond in ATP to creatine to form phosphocreatine (PCr). This molecule is smaller and less polar, diffusing out of the mitochondria into the cytoplasm. At the

site of energy usage, the sarcomere, ATP is reformed in the reverse reaction. Creatine, which is not produced in the heart, is taken up by the creatine transporter[34].

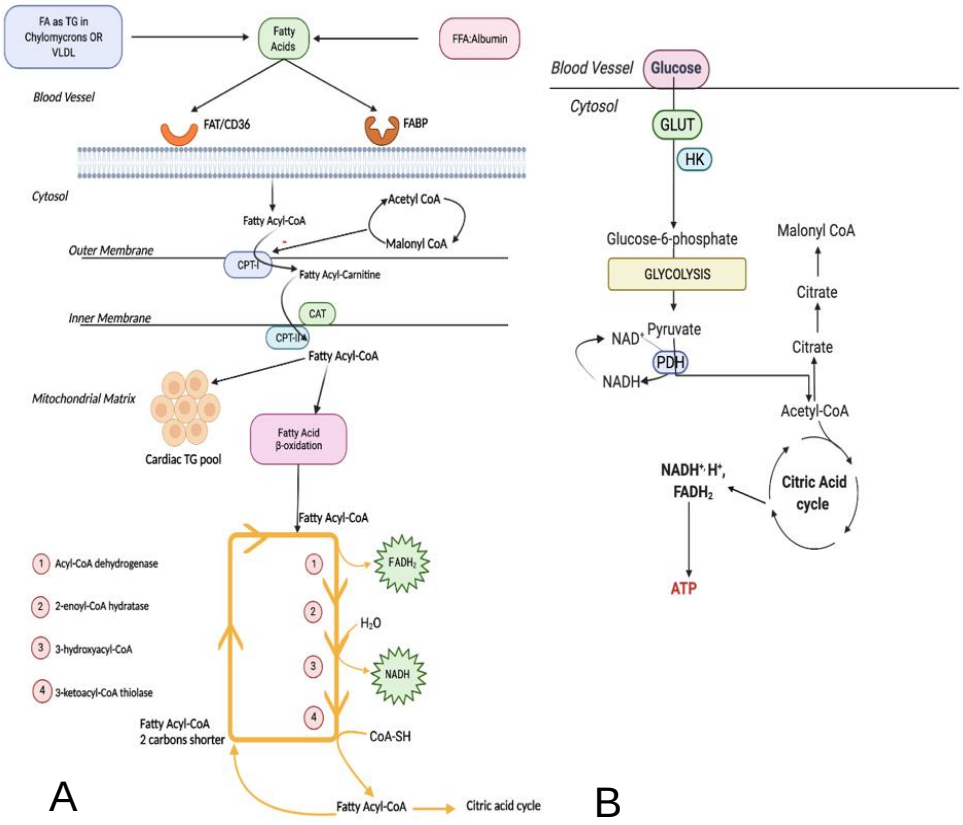

Figure 1.1: Schematic representation of myocardial fatty acid (A) and glucose (B) metabolism. Adapted from Lopaschuk, G. et al. Myocardial fatty acid metabolism in health and disease. Physiological Reviews. 2010 Jan : A: FA, fatty acid; TG, triglyceride; VLDL, very low-density lipoproteins; FFA, free fatty acid; FAT, FA translocase; FABP, FA binding protein; CPT (I and II) and carnitine palmitoyltransferase B: GLUT, glucose transporter and PDH, pyruvate dehydrogenase

Various signalling pathways co-ordinate energy metabolism and contractile function, with both insulin and contraction induced signalling acutely affecting the quantitative utilisation of FA's and glucose[15,25]. Additionally, an important function of the CK energy shuttle is to act as an energy buffer, when energy demand exceeds supply, phosphocreatine levels fall maintaining ATP levels at a constant [26,35].

1.16 Myocardial Energy Depletion in Type 2 Diabetes

Impaired myocardial energy metabolism is a well-established feature of both type 1 and 2 diabetes [6,36-39]. Although incompletely understood, myocardial energy depletion in subjects with T2DM is thought to relate to three principal disturbances in metabolic function. Firstly, glucose, lactate and ketone metabolism are thought to be reduced with an overreliance on FA metabolism and a loss of the heart's usual metabolic flexibility (Fig 2) [40-42]. Secondly hyperglycaemia and insulin resistance increase mitochondrial oxidative stress, increased NAD and FAD flux results in hyperpolarisation of the inner mitochondrial membrane and inhibition of the electron transport chain (ETC) at complex II and III and excess reactive oxygen species (ROS) production [43,44]. Thirdly increased FA uptake via attenuated AMPK activation and increased CD36 expression, wasteful cycling of FFA through intramyocardial lipolysis and esterification with accumulation of toxic lipid intermediates such as ceramides and diacylglycerols, results in lipotoxicity, a further aggravation of the energetic impairment [45-47].

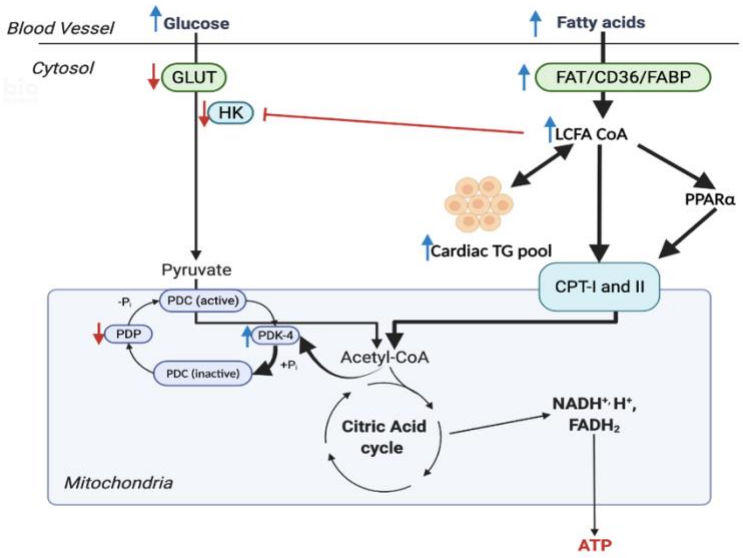

Figure 1.2: Cardiac metabolic perturbations in type 2 diabetes (T2D). Adapted from Lopaschuk, G. et al. Myocardial fatty acid metabolism in health and disease. Physiological Reviews. 2010 Jan

Fatty acid (FA) metabolism is increased in T2D, mediated through increased free FA concentrations and increased activity of FA transporters (FA translocase FAT/CD36 and FA binding protein (FABP)). Long chain FA co-enzyme A (LCFA CoA) accumulates and increases mitochondrial β-oxidation flux through CPT-I (carnitine palmitoyltransferase-I). This activates the transcription factor peroxisome proliferator-activated receptor α (PPARα) and increases the esterification into triglycerides (TG). Despite increased plasma glucose

concentrations, there is a decrease in the activity of glucose transporters (GLUT). Glucose metabolism is inhibited at the level of hexokinase (HK) by LCFA CoA accumulation. An increase in acetyl CoA generation activates pyruvate dehydrogenase kinase (PDK) enzymes, and inhibits pyruvate dehydrogenase phosphatase (PDP) enzymes, resulting in an inactivation of the pyruvate dehydrogenase complex (PDC); a key step in glucose oxidation. As a result, energy is shifted away from glucose metabolism and towards FA metabolism in T2D. Thick and thin lines represent increased and decreased flux, respectively. Red line indicates inhibition. Blue arrows indicate an increase in activity/abundance and red arrows indicate a decrease in activity/abundance.

1.17 Additional Maladaptive Features of The Diabetic Heart

Several important additional contributory factors should be considered in the mechanism of the diabetic cardiomyopathy phenotype.

Hyperglycaemia and insulin resistance are thought to lead to the increased accumulation of advanced glycation end products (AGE), resulting in myocardial structural alterations through non-enzymatic glycation, oxidation of lipids and proteins, connective tissue cross-linking and fibrosis [48].

A maladaptive proinflammatory innate immune response is seen in individuals with diabetes, where activation of proinflammatory cytokines contribute to oxidative stress, remodelling and fibrosis[4]. In animal models, high circulating FFA levels and impaired insulin metabolic signalling activate the NLRP3 inflammasome, a potential novel marker of diabetic cardiomyopathy [49]. Additionally, it is thought that interaction of AGE's with their surface receptor on cardiomyocytes may be linked to the proinflammatory response seen in T2DM[48]. Cytosolic Ca^{2+} levels regulate cellular metabolism, contraction, and cell signalling [50]. Impaired mitochondrial Ca^{2+} handling in T2DM increases cardiac action potential duration and prolongs diastolic relaxation time [18,51].

Activation of both the sympathetic nervous system (SNS) and RAAS, fundamental therapeutic targets of heart failure treatment, are seen in response to states of hyperglycaemia and insulin resistance[23,52]. The autonomic neuropathy seen in T2DM, whereby sustained hyperglycaemia impairs parasympathetic activity, leading to imbalanced SNS activation, enhances β-1 adrenergic receptor signalling, promoting cardiac hypertrophy, interstitial fibrosis, and cardiomyocyte apoptosis[52].

T2DM is associated with an array of microvascular complications and the coronary micro-circulation is no exception [17]. Impaired coronary flow reserve is seen in T2DM, which is a

strong independent risk factor for cardiovascular mortality [53]. Structural microcirculatory abnormalities in T2DM include luminal obstruction, inflammation, vascular re-modelling and peri-vascular fibrosis [22]. Functionally, NO mediated vasodilation is impaired early in T2DM, initially vascular function may be preserved through normal or enhanced activity of endothelial derived hyper-polarising factor, in the later stages however both vasodilators are impaired with significant impairment of micro-vascular function [54]. The persistently elevated plasma endothelin-1 and reduced NO activity inherent to coronary microvascular dysfunction may also be additional contributory factors to the development of cardiac fibrosis and diastolic dysfunction [55].

1.18 Ectopic and Visceral Adiposity

Accumulating evidence suggests that the increased cardiovascular risk associated with diabetes and obesity is not exclusively the result of increased adiposity but is also affected by the distribution of the excess fat[45,56-60]. Visceral adipose tissue may have more of an adverse influence on cardiovascular health as it is metabolically more active than subcutaneous adipose tissue and secretes a different profile of adipokines associated with inflammation, insulin resistance and diabetes[61-63]. Epicardial adipose tissue (EAT) is a visceral fat depot which through paracrine and/or autocrine signalling pathways may play a significant role in diabetic heart disease, given the absence of anatomical barriers with the myocardium[64,65]. Supporting this, human EAT secreted adipokines were shown to promote cardiomyocyte contractile dysfunction and fibrosis of the atrial myocardium in animal models[66]. Furthermore, it was also confirmed in a small study that diabetes is associated with a different secretory profile of EAT, and low-grade inflammation in patients with T2DM[67].

1.2 Measuring Myocardial Energy Metabolism

Myocardial ATP levels are kept relatively constant over a range of cardiac loads, buffered by the transfer of energy from PCr with the equilibrium constant of the CK reaction favouring the synthesis of ATP over PCr by a factor of approximately 100[35,68]. Hence when energy production is impaired in disease, ATP levels remain constant at the expense of PCr, therefore

the ratio of PCr/ATP can be used as a sensitive index of the energetic state of the myocardium [26,69]. In the healthy myocardium PCr is present in concentrations above twice that of ATP, ensuring PCr/ATP is maintained >2 consistently [26,69].

Due to the labile phosphoryl bond, direct measurement of PCr/ATP in myocardial biopsies ex-vivo is extremely challenging, in-direct measures of mitochondrial oxidative capacity at different complexes within the electron transport chain (ETC) can be inferred from myocardial biopsy samples using high resolution respirometry techniques [70]. These techniques will be discussed in more detail in chapter 6.

31 phosphorous magnetic resonance spectroscopy (^{31}P-MRS) is the only technique that allows for a validated, non-invasive measurement of high energy phosphate metabolism in-vivo [71,72]. Studies using ^{31}P-MRS have shown reductions in PCr/ATP to be a feature of diabetic cardiomyopathy [36,39], inherited cardiomyopathies [73,74], valvular heart disease [75] and systolic heart failure [26].

1.3 Cardiac Hypertrophy

In order to maintain peripheral organ perfusion in the presence of increased pre-load or afterload individual myocytes undergo enlargement. Hypertrophy increases contractility, through the addition of sarcomere units in parallel with increased left ventricular (LV)wall thickness decreasing wall stress and maintaining cardiac efficiency [76]. Cardiac hypertrophy is accompanied by an array of changes in gene expression, metabolism and cardiomyocyte survival. Cardiac hypertrophy may be physiological or pathological, physiological hypertrophy is classically eccentric in nature, with proportional increases in both LV wall thickness and cavity size, pathological hypertrophy in contrast is usually defined by concentric re-modelling, in which wall thickness occurs at the expense of LV cavity volume[76]. Both develop as a response to cardiac stress but display significantly different underlying molecular mechanisms, phenotype and prognosis[77]. Whether physiological or pathological hypertrophy develops, depends on the nature rather than the duration of the stimuli [78].

1.31 Physiological Cardiac Hypertrophy

In response to athletic training, mild (10-20%), eccentric increases in LV mass occur, accompanied by cardiomyocyte growth in both length and width. This leads to preserved or increased contractile function without the presence of interstitial or replacement fibrosis, of note physiological hypertrophy is typically fully reversible after withdrawal of the initiating stimuli[76].

For cardiac hypertrophy to be fully adaptive it must be accompanied by various additional compensatory mechanisms, including cell survival signalling, increased energy production, angiogenesis proportional to LV wall growth, antioxidant systems, mitochondrial quality and control[76,78].

Insulin and insulin like growth factor 1

Insulin and insulin like growth factor 1 (IGF-1) regulate cell growth, proliferation, differentiation, apoptosis, contractility and metabolism[79]. IGF-1 is predominantly synthesised and secreted in the liver but also in additional organs including the heart, physiological hypertrophy in athletes has been shown to be associated with increased cardiac IGF-1 levels [80].

IGF-1 is also linked to the RAS-RAF-MEK-MAPK signalling axis, leading to synthesis of serine/threonine kinase-1 (AKT-1)[81]. AKT-1, a crucial player in inducing physiological and preventing pathological hypertrophy, inhibits fork head box protein 3 (FOX03), which reduces catabolism and promotes cardiomyocyte growth[81,82].

Nitric Oxide

Exercise has been shown to activate β-3 adrenergic receptors in endothelial cells, leading to an increased NO production. NO activates protein kinase G, suppressing pathological and attenuating physiological cardiac hypertrophy[83,84]. As discussed, disturbances in nitric oxide synthases (NOS) impair maintenance of myocardial calcium homeostasis, distensibility and protection from abnormal stress stimuli[85].

Cyclic guanosine monophosphate (cGMP) is a secondary messenger molecule that transduces NO and natriuretic peptide coupled signalling, stimulating phosphorylation by protein kinase G. Enhancing cGMP synthesis, or blocking its degradation by phosphodiesterase type 5A

(PDE5A) therefore protects against a pathological hypertrophic response in cardiovascular disease processes[86].

MTOR Signalling

MTOR is a serine protein kinase that functions as part of two distinct complexes (MTORc1+2) to co-ordinate growth factor signalling and amino acid bioavailability with cell metabolism and growth, this is done by controlling protein synthesis and degradation[87]. Despite increasing protein synthesis and mitochondrial quality control, through MTOR signalling, being essential adaptive mechanisms for the heart during acute pressure overload[88], sustained activity is detrimental, in part due to suppression of autophagy and reduced protein quality control mechanisms[88,89]. Pharmacological suppression of MTORc1 attenuates angiotensin-II induced and pressure over-load related pathological hypertrophy[90], additionally, the MTOR inhibitors used in humans to prevent organ transplant rejection, have been shown to modify cardiac hypertrophy[91].

Natriuretic Peptides

Expression of genes encoding atrial natriuretic peptide (ANP) and brain natriuretic peptide (BNP) are induced in response to pathological stimuli, with the key stimulant for release being myocardial stretch, classically ANP and BNP exert natriuretic, diuretic and hypotensive action and offer anti-hypertensive and anti-hypertrophic protective effects[92,93].

Angiogenesis

Capillary density is an important factor contributing to the development of both physiological and pathological hypertrophy[94]. Vascular endothelial growth factor (VEGF) is a critical angiogenic molecule involved in the adequate maintenance of myocardial capillary density[95]. The importance of VEGF in normal cardiac function can be seen by the increased incidence of cardiomyopathy in anti-VEGF agents used in cancer treatment[96], with decreased circulating VEGF levels shown to correlate with poor recovery from peripartum cardiomyopathy[97].

Hypoxia inducible factor 1- α (HIF1- α) is a major transcription factor that controls oxygen homeostasis by regulation of angiogenesis, vascular remodelling and glucose metabolism[98]. Exercise training leads to upregulation of MTOR and stimulation of HIF1- α responsive angiogenic factors, including VEGF, which in-turn lead to a well-co-ordinated cardiomyocyte growth and angiogenic response[99,100].

Micro RNA's

Micro-RNA's (mi-R) are a class of small, non-encoding RNA's that modulate gene expression at the post-transcriptional level[101], miR-22 is a cardiac and skeletal muscle enriched mi-RNA which is up-regulated during myocyte differentiation and physiological hypertrophy[102]. Mouse models demonstrate that over-expression of miR-22 induces hypertrophy, conversely, loss of miR-22 leads to increased susceptibility to development of a dilated cardiomyopathy phenotype[102].

Neuregulin-1

Neuregulin 1-4 are members of the epidermal growth factor, of which neuregulin-1 is most abundant in the heart[103]. Signalling via neuregulin-1 and its receptors, the tyrosine protein kinase ERBB2 family, has a crucial role in the adaptation to physiological and pathological hypertrophic stimuli[103,104]. In the situation of endurance training, neuregulin-1 is increased, inducing cardiomyocyte differentiation and proliferation, which protects the heart from ischaemic injury[105-107]. In mouse models, post-natal over-expression of ERBB2 induces cardiac hyperplasia with increased cardiomyocyte hypertrophy and proliferation, akin to the HCM phenotype[108].

1.32 Pathological Cardiac Hypertrophy

Pathological left ventricular hypertrophy (LVH) is common to a variety of cardiac disease processes, including, chronic hypertension, aortic stenosis (AS), storage diseases, sarcomeric gene mutations such as hypertrophic cardiomyopathy (HCM), obesity and diabetes[109]. Initially

a compensatory response, in contrast to physiological hypertrophy, pathological LVH swiftly becomes maladaptive and may eventually lead to contractile dysfunction and heart failure syndrome[76].

Pathological hypertrophy can be seen to be a distinct entity from physiological re-modelling, with a return to a state of foetal metabolic programming[110], with increased expression of the genes ANP, BNP, MYHC- β and skeletal muscle- α actin[111], and accompanying interstitial and peri-vascular fibrosis, increased levels of type-1 collagen and myofibroblast activation[78,112]. These genetic and structural changes may be seen in response to a number of underlying stress stimuli and maladaptive signalling pathways.

Pressure Overload

Whilst many signalling molecules are implicated in the development of pathological hypertrophy in the pressure loaded ventricle, a key pathway which has shown promise as a therapeutic target in animal models, is calmodulin dependent kinase II (CaMKII)[113]. CaMKII is a unique mediator of beat-to-beat cardiac function, activated and de-activated with the rise and fall of Ca^{2+} allowing for a dynamic response to varying metabolic needs. Under states of pathological stress, with increased ROS, CaMKII activation is prolonged and induces hypertrophic and inflammatory transcriptional pathways and promotes apoptosis[114]. The hypertrophic response is mediated as CaMKII induces the nuclear exit of class-II histone deacetylase-4[115], class-II histones (4,5,9) act as repressors of hypertrophy, whereas class-I histones (1,2,3) are pro-hypertrophic[115,116].

Sympathetic Nervous System Activation

Catecholamines are neuroendocrine hormones, modulating cytosolic Ca^{2+} levels through protein kinase A[76]. Prolonged, imbalanced activation of the sympathetic nervous system, as seen in hypertension, myocardial infarction, and heart failure, leads to chronic stimulation of β adrenergic receptors, promoting pathological hypertrophy and receptor desensitisation, mediated by GPCR kinase[117-119].

Genetic Mutations and Epigenetic Modifications

Pathogenic mutations causing HCM have been identified in genes encoding numerous sarcomere proteins, including ACT1, MYBPC3, MYH7, MYC2,3, TNNI2,3 and TPM1[120]. In-addition, epigenetic modifications regulate pathological hypertrophy by modulating genome architecture, stability, and gene expression[78,120]. Specifically, a genome wide study identified a role for Histone-3 and miR-217 mediated gene re-programming in pathological hypertrophy[121,122].

1.33 Metabolic Remodelling in Cardiac Hypertrophy

It is proposed that impaired adaptation of energy metabolism during the hypertrophic response exacerbates pathological hypertrophy and increases cardiomyocyte death[26,76], and that under stress certain metabolic responses become maladaptive.

The hypertrophied heart is characterised by a switch to foetal type metabolic programming, with increased glucose and reduced FA metabolism[31]. Cardiac specific deletion of the gene encoding CD36 reduces FA uptake and utilisation, this reduced substrate flexibility may exacerbate pressure overload induced dysfunction[123]. Therefore, during pathological hypertrophy, cardiomyocytes are thought to re-model, with increased glycolysis, ketone and BCCA utilisation with reduced energy derived from FA's[76,110,124].

Deficiency of oestrogen related receptor alpha (ERR α) is thought to be a polymorphism that may promote transition to heart failure in the hypertrophied heart. Under normal conditions, ERR α interacts to activate mitochondrial energy metabolism by increasing expression of genes encoding proteins involved in the TCA cycle and OxPhos[125].

1.4 Aortic Stenosis

1.41 Background and Clinical Context

Aortic stenosis (AS) is the most frequent degenerative valvular heart disease in the Western world with a prevalence of 5% in people aged >65, with ageing demographics in most populations, the burden of AS on global health systems is likely to continue to increase[126].
A gradient at rest between the LV and aorta occurs once the aortic valve area (AVA) is less than 1.5cm^2 and AS is considered severe once the AVA falls to below 0.6cm^2/m^2 [127] . Even in the absence of symptoms or LV systolic dysfunction, once AS progresses to severe it is associated with increased mortality, with rates of sudden cardiac death (SCD) approaching 1% per annum[128,129]. Once symptoms develop clinical deterioration may be rapid, with SCD rates 4% at 1-month and 12% at 6-months [128,130,131]. Although both transcatheter (TAVR) and surgical aortic valve replacement (SAVR) are highly effective treatments for severe AS, 30-day post procedural mortality rates following aortic valve replacement (AVR) approach 1% in contemporary data[129], therefore the identification of additional prognostic markers, either to allow disease modulation or improved risk stratification, forms much of current research into the AS phenotype.

1.42 Cardiac Magnetic Resonance Imaging in Aortic Stenosis

Cardiac magnetic resonance (CMR) imaging is the reference standard assessment of LV volumes and mass[132], allowing for full characterisation of LV remodelling[133]. Development of a pattern of concentric remodelling, normalising shear wall stress in severe AS, has been shown to be associated with adverse outcomes regardless of clinical management[134]. However the LV displays a heterogenous response to increasing AS severity, with several patterns of LV hypertrophy and adaptation[135], indeed asymmetric patterns of wall thickening are at least as common as concentric re-modelling and have shown to be independent predictors of AVR and death[135,136]. Additionally, insights from CMR suggest that pattern and degree of LVH do not correlate well with the severity of valve stenosis in AS[135]. Sexual dimorphisms in AS remodelling have been shown with women tending towards increased concentricity and lower indexed LV mass[137,138].

CMR is the only non-invasive method for assessment of LV fibrosis and whilst health economic barriers remain, an emerging body of evidence suggests that use of CMR assessment and quantification of fibrosis in AS patients may soon be more widely incorporated into clinical

guidelines and risk stratification[139,140]. Presence of LV mid-wall late gadolinium enhancement (LGE), has been shown to confer an 8-fold increased risk of all-cause mortality[141], and combined CMR and myocardial biopsy data suggests that a gradient of fibrosis from the endocardium to epicardium exists in AS[142]. However, the degree to which this fibrosis is a response to reduced capillary density and ischemia (replacement fibrosis) or pressure overload induced fibroblast activation (reactive fibrosis) has yet to be fully ascertained[142-144]. CMR T1 mapping techniques and extra cellular volume (ECV) quantification, in combination with LGE imaging, may allow for a more comprehensive assessment of the multi-pattern fibrosis seen in AS[142].

1.43 Development and Progression of Aortic Stenosis

Long considered a passive degenerative phenomenon, related to 'wear and tear' of the valve, histopathological evidence suggests AS is an active and complex process, involving chronic inflammation, lipoprotein deposition, RAAS activation and osteoblastic transformation of valvular interstitial cells[145-148].

The normal aortic valve is composed of three leaflets, these usually thin, mobile and flexible structures become thickened, fibrosed and calcified upon the development of AS. Whereby reduced valve leaflet mobility leads to progressive valvular obstruction[146,149]. AS pathophysiology can be broadly divided into two phases.

Early Initiation Phase

In this early initiation phase, which shares commonality with atherosclerosis, valvular lipid deposition, injury and inflammation predominate[149,150]. In AS, as seen in atherosclerosis, following initial damage to the endothelium, infiltration of lipids, low density lipoprotein (LDL) and lipoprotein a, is seen. Subsequently lipid oxidation leads to a pro-inflammatory response[149,151]. Despite sharing common features and indeed risk factors with atherosclerosis[150], trials using statin, lipid lowering therapy have failed to arrest AS progression[152,153]. This is likely due to AS usually becoming clinically manifest after the early initiation phase[149].

Propagation Phase

The later stage of AS, during which most patients come to the attention of clinicians, is driven by a self-perpetuating cycle of calcium formation and valvular injury[149]. An initial fibrotic process occurs within the valve, in part mediated by reduced NO expression [154], and also RAAS activation[155,156]. Angiotensin converting enzyme (ACE) is delivered to the valve by LDL, where it converts angiotensin I to angiotensin II, which mediates pro-fibrotic effects[156,157], in support of this, small, randomised placebo controlled trials using ACE inhibitors in AS, have shown modest reductions in LV mass and trends towards slower AS progression[158].

Following fibrosis, valvular calcification dominates, driven by osteoblastic cells[149]. It is thought that differentiation of myofibroblasts into osteoblasts occurs, driven initially by macrophages via pro-inflammatory cytokines (IL-1, IL-6, IL-8, TNF- *α, ILG-1)*[159]*,* and laterally by calcific pathways[160]*.*

1.44 Aortic Stenosis and Cardiac Metabolism

AS is a prototype model for afterload-induced heart failure[161]. Histological studies have shown that significant myocardial steatosis in patients with severe AS is linked to abnormalities in cardiac contractile function and steatosis may regress and contractile function improve after AVR[162]. However, the mechanisms underlying cardiac steatosis in AS are incompletely understood. It is likely that impaired myocardial FA oxidation contributes to lipid accumulation in the pressure overloaded ventricle. Confirming this, in patients with severe AS undergoing surgical AVR, coordinated downregulation of sequential steps involved in FA oxidative metabolism was shown in cardiac biopsies[163]. This was accompanied by upregulation of the glucose transporters confirming the metabolic shift from FA to glucose utilisation[163]. Further, a negative correlation between the FA translocase (FAT/CD36) levels and LV mass index was demonstrated, thus confirming that the patients with the greatest cardiac hypertrophy had the lowest FA translocase (FAT/CD36) protein levels; while in contrast there was a positive correlation with the extent of hypertrophy and glucose-transporter-4 (GLUT-4) levels[163].

The hypoxic environment of the hypertrophied heart favours the use of glucose, which affords more contractile power for a given rate of oxygen consumption[164], although initially thought to be entirely maladaptive, animal studies suggest this increase in glucose uptake may result

in a more favourable metabolic profile, affording some protection against myocardial susceptibility to ischemic injury[165]. However in the long term, this switch to glucose metabolism is likely to lead to negative physiological effects, as FA oxidation yields overall greater ATP production compared to glucose[31]. Indeed, studies using ^{31}P-MRS have shown an energetic impairment to be present in both moderate and severe AS, one that appears to reverse following AVR and relief of pressure overload and hypertrophy regression[75].

1.45 Co-morbidity of Aortic Stenosis and Type 2 Diabetes Mellitus

In parallel with ageing demographics and the obesity epidemic, AS and T2DM are increasingly frequent comorbidities[166] with 22 to 36% of severe symptomatic AS patients having coexisting T2DM[167-173,174]. Comorbidity with T2DM influences the prognosis of AS with increased morbidity and mortality following aortic valve replacement (AVR) even after adjustment for comorbidities such as vascular disease or renal dysfunction[130,175-178]. Although distinct pathological entities, AS and T2DM share common features of altered myocardial energy metabolism, left ventricular concentric remodeling and coronary microvascular dysfunction[75,170,179,180]. The mechanism underlying the poor prognosis of patients with AS and T2DM comorbidity are incompletely understood. One potential explanation is the collective impact of the two conditions on cardiac metabolism, structure and perfusion. Supporting this clinical observation, more pronounced LV hypertrophy and dysfunction after aortic banding was shown in a mouse model of diet-induced obesity with insulin resistance and hyperglycemia, compared to mice fed a standard diet[181].

1.5 Hypertrophic Cardiomyopathy

1.51 Background and Clinical Context

Cardiomyopathies encompass a diverse spectrum of inherited and acquired disorders characterised by impaired myocardial contractility and pathological ventricular remodelling[182,183]. Identification of genetic mutations as well as insight into cellular metabolism in these cardiomyopathies has provided insight into disease aetiology. Deranged

cardiac energy metabolism has been implicated in both hypertrophic [184, 123, 185,186] and dilated cardiomyopathy [187,188, 189] .

HCM affects 1 in 200 to 1 in 500 individuals and is the commonest cause of sudden cardiac death in the young (including competitive athletes) and this is perhaps the most devastating component of its natural history[182,183,190-192].

Despite being a common genetic cardiomyopathy, determining disease progression and risk stratification remains a clinical dilemma.

Over 1500 gene mutations encoding sarcomeric proteins are associated with HCM, however genotype negative cases predominate in registry studies with an identifiable mutation being present in around 36% of cases[193]. The vast majority of genotype positive patients carry a heterozygous mutation, hence HCM is considered a disease with autosomal dominant inheritance[194].

The disease course for the majority of patients is relatively benign with 5 year survival rates of 82% and pooled 10 year survival of 76%[195]. However, there is significant heterogeneity in terms of outcomes with a relatively poor prognosis in a subset of patients who rapidly progress to heart failure or succumb to sudden cardiac death[196]. Equally, current risk stratification tools to identify patients who are at the greatest risk of SCD and may benefit from protection with implantable cardiac defibrillator (ICD) are suboptimal, with appropriate device therapy rates of only 17% over 5 years compared with inappropriate shock rates of 27%[197].

In this context, advances are needed to allow for more refined risk stratification to reduce morbidity and mortality. The identification of additional prognostic markers or greater understanding of the influence of modifiable cardiometabolic co-morbidities, such as T2DM, may offer an additional avenue for improving disease outcomes.

1.52 Pathophysiology of Hypertrophic Cardiomyopathy

The heterogeneity in terms of clinical outcomes is reflective of a significant variance in disease penetrance. The dose of the mutant sarcomere protein, which is regulated at RNA level, determines the onset and severity of cardiomyopathy[198-200]. Based on the observation that the presence alone of a heterozygous mutation is not enough to confer disease initiation or indeed progression, it has been suggested that the development of HCM is linked to additional disease modifying factors. This is most likely through the affectation of cell systems

that maintain myocyte homeostasis, disrupting the ability to prevent accumulation of the mutant protein[201].

Histologically the hallmarks of HCM are cardiomyocyte hypertrophy and disarray, fibrosis and reduced capillary density[182,196,202,203]. Physiologically mutations in sarcomere proteins cause increased Ca^{2+} sensitivity of the myofilaments, increased tension cost and altered myosin sequestration which combine to result in increased ATP use. Increased Ca^{2+} sensitivity induces myofilament activation at relatively low Ca^{2+} levels and delays the dissociation of Ca^{2+} from troponin C, this results in prolonged cross bridge activation and impaired relaxation. This increased tension cost denotes that in HCM more ATP is hydrolysed in order to generate the same force[185,204-207].

1.53 Structural and Functional Changes

At a macroscopic level HCM is defined by increased LV wall thickness, with diagnostic criteria in adulthood requiring ≥ 15mm in one or more myocardial segment that cannot be explained solely by loading conditions[196]. In first degree relatives of patients with unequivocal disease an increase in LV wall thickness above 13mm is considered sufficient to make the diagnosis[196]. Functionally HCM is characterised by LV diastolic impairment and coronary microvascular dysfunction, this leads to local ischemia, tissue death and replacement fibrosis[202,203,205,208,209].

1.54 Hypertrophic Cardiomyopathy and Cardiac Metabolism

Little is known about the specific changes in substrate utilisation, oxidative phosphorylation and energy transfer in HCM but it is well established that the energy cost of force production is increased[210].

Traditionally it was thought that the mutant HCM proteins depressed cardiac function and that subsequently activated neuroendocrine and mechanical responses, leading to compensatory hypertrophy. However in vitro and mouse models have subsequently shown increased contractility of the mutant myofilaments due to altered myosin kinetics, increased thin filament calcium sensitivity or changes in myosin binding regulation[211,212]. Mutations in myosin can alter cycling rates of myosin heads thus leading to more cross bridge detachment before completion of the power stroke[200]. Most HCM mutations in thin filament regulatory proteins increase calcium sensitivity, this increases force at submaximal calcium

concentrations[198,199,213]. In addition, mutations in these regulatory proteins can also alter velocity of cross bridge formation[214].

The energy depletion hypothesis proposes that the increased energy demand compromises the cardiomyocyte's ability to maintain energy levels necessary for contraction, pump function and homeostatic function such as calcium re up-take. This myocyte dysfunction results in compensatory hypertrophy. This hypothesis is supported by findings of abnormal resting energetics in patients with HCM[184,185] even in the pre hypertrophied state[184]. Further support comes from the observation that diseases which directly affect glucose transport (GLUT 4 knockout); free fatty acid transport (CD36 deficiency) and mitochondrial function cause HCM phenocopies.

Furthermore, abnormal energetics may be compounded by the microvascular dysfunction which occurs in HCM with possible resultant tissue hypoxia. Microvascular dysfunction in HCM has been extensively investigated using many modalities including MRI[215,216], positron emission tomography (PET) [217] and thallium scanning[218]. Ischaemia has been assumed as a result of perfusion deficits.

Angina and symptoms suggesting myocardial ischemia are frequent features in the natural history of HCM, and there is pathological evidence that ischemia can be related to sudden death even in young asymptomatic patients[219]. Two possible mechanisms may be responsible for de-oxygenation in HCM. Firstly, abnormal intramural coronary arteries, with a reduction in the size of the lumen and thickening of the vessel wall are a consistent feature in HCM[220]. The prominence of abnormal intramural coronary arteries in areas of extensive myocardial fibrosis is consistent with the hypothesis that these abnormalities are responsible for the development of myocardial de-oxygenation. Secondly, capillary density and distribution are of crucial importance for the process of oxygen exchange between blood and tissue. Thus, perfusion abnormalities might also exist in HCM due to an increased oxygen diffusion distance caused by an inadequate growth of capillaries[202] .

1.55 Co-morbidity of Hypertrophic Cardiomyopathy and Type 2 Diabetes Mellitus

T2DM co-exists in around 9% of HCM cases, HCM patients with T2DM tend to be older at age of diagnosis and have greater prevalence of AF, lower functional capacity and increased HF symptoms with worsened 15-year survival rates (22% vs 15%)[221].

Studies with echocardiography suggest that combined T2DM and HCM leads to increased rates of diastolic dysfunction and a higher prevalence of left atrial (LA) enlargement. Studies do not suggest any significant difference in LV dimensions, wall thickness or systolic function. Interestingly the apical variant of HCM occurs more frequently in the T2DM population (15% vs 7%) although the reasons for this are not well understood[221,222].

Obesity has been proposed to induce and aggravate HCM via numerous mechanisms including metabolic over-fuelling, endothelial dysfunction and cardiac adiposity, in addition metabolic status independent of body mass index (BMI) has been shown to predispose to HCM with the presence of T2DM, hypertension or hyperlipidaemia increasing the chance of being diagnosed with HCM, even in individuals with normal or low BMI[223-225]. It has been suggested that the endothelial inflammation and pro-fibrotic signalling that occurs in T2DM may provide a trigger initiating the pathological remodelling seen in HCM[201].

With the potential relationship between T2DM and HCM suggesting co-existence not only confers increased mortality risk but also potentially triggering increased disease penetrance, greater understanding of the cardiomyopathic process that occurs in this subset of patients may offer an additional opportunity to modify disease progression.

1.6 Aims of PhD Studies

This PhD project is focussed on the combined impacts of T2DM and cardiac comorbidities associated with left ventricular hypertrophy (acquired in severe AS cohort and inherited in HCM cohort) on cardiac phosphocreatine to ATP ratio, function and perfusion. The relationship between T2DM and severe AS and additionally the relationship between T2DM and HCM will be investigated. This will be done using the techniques detailed below.

The changes assessed will include:

1. *Structural changes*

Left ventricular hypertrophy, left ventricular wall thickness and mass will be assessed using cine imaging; fibrosis using T1 mapping and gadolinium imaging with CMR.

2. *Functional changes*

Systolic function will be assessed using cine MRI technique as well as myocardial strain analysis. Diastolic function will be characterized using MRI strain parameters.

3. *Metabolic changes*

Myocardial energetics will be assessed using ^{31}P-MRS at 3T.

4. *Microvascular function*

Microvascular function will be assessed using adenosine stress CMR imaging and quantitative perfusion analysis. Furthermore, the relationship between myocardial energetics and myocardial microvascular function will be assessed.

5. *Mitochondrial function - Myocardial biopsy*

Myocardial mitochondrial function in the AS study will be assessed ex-vivo from cardiac biopsy samples using respirometry techniques. Furthermore, the relationship between mitochondrial function on respirometry analysis and myocardial energetics as assessed by ^{31}P MRS will also be explored.

6. *Epicardial adipose tissue characteristics -Epicardial fat biopsy*

The differences in the histopathological characteristics of epicardial adipose tissue between diabetics and non-diabetics will be assessed ex-vivo in the AS study.

7. *Skeletal muscle changes*

The influence of T2DM co-morbidity on skeletal muscle mass and exercise capacity in patients undergoing AVR will be explored using MR thigh imaging and 6-minute walk test assessments in the AS study.

The aim of this thesis include:

1. To assess the reproducibility of a modified scan protocol allowing for robust assessment of coil position, and for chemical shift imaging grid positioning. (Chapter 3)

   In this study, I showed that ^{31}P-MRS can be performed in the supine position with a high degree of reproducibility using an optimised protocol with improved coil positioning thereby maximizing patient comfort and increasing the scope for tolerance of the technique by a wider patient cohort.

2. To investigate if hypertrophic cardiomyopathy patients with type 2 diabetes mellitus comorbidity exhibit adverse cardiac alterations in myocardial energetics, function, perfusion, or tissue characteristics. (Chapter 4)

   In this study, I showed for the first time that HCM patients with T2DM comorbidity display greater reductions in myocardial energetics, perfusion, contractile function

and higher myocardial scar burden and serum NT-proBNP levels compared to patients with isolated HCM despite similar LV mass and wall thickness and presence of sarcomeric mutations. These adverse phenotypic features may be important components of the adverse clinical manifestation attributable to a combined presence of HCM and T2DM.

3. To establish if T2DM comorbidity is associated with altered myocardial recovery after aortic valve replacement (AVR) in severe AS. (Chapter 5)

   In this study, I showed that while AVR is effective in reversing myocardial alterations in AS patients without T2DM, AS patients with T2DM comorbidity show residual myocardial abnormalities and continued limitations in exercise capacity after AVR.

4. To better understand if the presence of T2DM in patients with severe AS is associated with impaired mitochondrial oxidative capacity. (Chapter 6).

   In this study we showed that worsening glycaemic control is associated with reduced mitochondrial oxidative capacity with impaired ETC activity at complex II. These findings supported the previous work done in the field and may go some way to explain to explain the energetic impairment and adverse prognostic association seen in subjects with combined severe AS and T2DM.

5. To better understand the impact of T2DM on skeletal muscle mass and functional exercise capacity in patients with severe AS undergoing AVR (Chapter 7).

   In this study I showed T2DM to be associated with sarcopenia and impairment of functional exercise capacity following AVR. This work suggests sarcopenia in T2DM patients following aortic valve intervention may contribute to limitations in exercise capacity and adverse prognostic outcomes.

In conclusion, the work in this thesis demonstrates the potential power of both CMR and cardiac ^{31}P-MRS as tools to identify sub-clinical structural, functional, and metabolic derangements that may allow for more refined identification of high-risk patients with cardiometabolic co-morbidities.

Chapter 2

General Methods

2.1 General Methods

The DAS study (Diabetes and Aortic Stenosis) was approved by the Yorkshire and Humber Research Ethics Committee (IRAS ID 252633). Subjects were recruited from across the Yorkshire region via the Leeds Teaching Hospitals NHS trust specialist valve service. The HCM patients and Healthy volunteers were recruited under a separate study which was also approved by the Yorkshire and Humber Research Ethics Committee (REC Ref:18/YH/0168). Patients with HCM were recruited from Leeds Teaching Hospital NHS trust inherited cardiac conditions (ICC) clinic. Healthy volunteers were recruited via word of mouth and through email advertisement to local cycling, running and golf clubs. Each participant gave written, informed consent to be involved.

2.2 Eligibility Criteria

Patients were considered eligible for inclusion in the DAS study investigating the hypotheses related to T2DM and severe AS under the following criteria.

Inclusion Criteria:

1. Men and women >18 years of age.
2. Severe AS based on transthoracic echo with an AVA of ≤1.0 cm^2 or peak velocity >4 m/s.
3. Ability and willingness to provide written and informed consent and to comply with the requirements of the study.
4. For patients diagnosed with AS and T2DM, the following is also required: T2DM diagnosis in accordance with WHO criteria (fasting plasma glucose ≥ 7.0 mmol/L or 2-h plasma glucose ≥11.1 mmol/L), on any type of glucose lowering treatment.

Exclusion Criteria:

1. Significant CAD (>50% luminal stenosis or evidence of large vessel ischemia), previous CABG, angioplasty or myocardial infarction.
2. Known HF or reduced LV EF (<50%).
3. Participation in a Clinical trial of an investigational medicinal product in the preceding 12 weeks.
4. Contra-indications to CMR (pacemaker, cranial aneurysm clips, metallic ocular foreign bodies, severe claustrophobia), adenosine or gadolinium-based contrast agents.
5. Significant renal impairment (eGFR<30 ml/min/1.73m^2).
6. More than mild aortic regurgitation or other moderate or above valvular pathology.
7. For patients diagnosed with severe AS and T2DM the following is also grounds for exclusion: diagnosis of any other type of diabetes other than T2DM.
8. Patients who are on Insulin therapy.

Patients were considered eligible for inclusion in the HCM-DM study investigating the hypotheses related to HCM and T2DM under the following criteria.

Inclusion Criteria:

1. Men and women >18 years of age.
2. Established diagnosis of HCM based on presence of unexplained left ventricular (LV) hypertrophy (maximum wall thickness ≥15 mm).
3. Ability and willingness to provide written and informed consent and to comply with the requirements of the study.
4. For patients diagnosed with HCM and T2DM, the following is also required: T2DM diagnosis in accordance with WHO criteria (fasting plasma glucose ≥ 7.0 mmol/L or 2-h plasma glucose ≥11.1 mmol/L), on any type of glucose lowering treatment.

Exclusion Criteria:

1. Established coronary artery disease (>50% luminal stenosis or evidence of large vessel ischemia), previous CABG, angioplasty or myocardial infarction.
2. Known HF or reduced LV EF (<50%).
3. Participation in a Clinical trial of an investigational medicinal product in the preceding 12 weeks.
4. Contra-indications to CMR (pacemaker, cranial aneurysm clips, metallic ocular foreign bodies, severe claustrophobia), adenosine or gadolinium-based contrast agents.
5. Significant renal impairment (eGFR<30 ml/min/1.73m^2).
6. Permanent pacemaker and implantable cardiac defibrillator (ICD).
7. Anderson-Fabry disease.
8. For patients diagnosed with HCM and T2DM the following is also grounds for exclusion: diagnosis of any other type of diabetes other than T2DM.
9. Patients who are on Insulin therapy.

Healthy volunteers were considered eligible for inclusion in all studies under the following criteria.

Inclusion Criteria:

1. Men and women >18 years of age.
2. Ability and willingness to provide written and informed consent and to comply with the requirements of the study.
3. Age-matched healthy volunteers with no known history of cardiac disease, hypertension or diabetes.
4. Able in the investigators opinion to comply with all study requirements

Exclusion Criteria:

1. Pregnancy, or lactating mothers.
2. Contra-indications to CMR (pacemaker, cranial aneurysm clips, metallic ocular foreign bodies, severe claustrophobia).
3. Presence of severe asthma (contraindication to adenosine).
4. Known hypersensitivity to adenosine or gadolinium.
5. Patients who were diagnosed with hypertension previously, or blood pressure measurement at screening revealing systolic levels >140 mmHg and diastolic levels of >85mmHg.
6. Estimated glomerular filtration rate (eGFR) <30ml/min/1.73m^2 (stage 3-5 renal disease) were excluded from the study. Participants had a blood test to assess kidney function at the study visit.
7. Current smoker or a history of smoking in the past 5 years.
8. Any other significant disease or disorder which, in the opinion of the investigator, may either put the participant at risk because of participation in the study, or may influence the result of the study, suitability as a healthy control subject or the participant's ability to participate.

2.3 Clinical Assessments

Of note prior to study enrolment all patients with severe AS recruited to the DAS study had undergone trans-thoracic echocardiography to confirm the diagnosis of severe AS and obtain an up-to-date assessment left ventricular systolic function. Echocardiography assessments were undertaken by the cardiac physiology department at Leeds Teaching Hospitals NHS Trust as part of usual work up for aortic valve replacement (AVR). In addition, all subjects with severe AS underwent diagnostic coronary angiography to exclude significant coronary artery disease as part of work-up for AVR.

On **visit 1** and **2** all subjects underwent clinical assessment which included history for:

- The presence of exclusion criteria as documented above.
- Past medical history
- Drug history including allergies
- Weekly alcohol level (units)

- Smoking history
- Diabetes history, including duration since the diagnosis, symptoms, presence of diabetic complications

The following measurements were carried out:

- Blood pressure measurements using a manual sphygmomanometer
- Height (cm) and weight (kg) using calibrated scales.
- 12 lead electrocardiogram (ECG)

6 Minute Walk Test

At both **visit 1** and **2** the participants were instructed to walk along a 30-meter corridor and cover the maximum achievable distance in 6-minutes under the supervision of study investigators with medical training and with experience in conducting the test. At the end of 6-minutes, participants were asked to stop, and the distance walked was measured in meters[226].

Serum Biochemistry

At both **visit 1** and **2** a fasting blood sample was taken for assessments of full blood count, eGFR, lipid profile, glycated hemoglobin (HbA1c), insulin, free fatty acid, beta hydroxybutyrate, and N-terminal pro hormone B-type natriuretic peptide (NT-proBNP).

2.4 Scan Protocols

All subjects underwent comprehensive CMR protocol which included the following.

i) ^{31}P MRS at rest
ii) Visceral fat assessment

iii) Cardiac volumes, mass and function

iv) Pre-contrast T1 mapping of the 3 short axis slices of the heart (base, mid and apex)

v) Rest and stress adenosine quantitative perfusion

vi) Late gadolinium enhancement, (LGE)

vii) Post-contrast T1 mapping (15 minutes after gadolinium injection)

All scans were conducted on a Siemens 3 Tesla PRISMA MR system (Erlangen, Germany). The average scan time was 90 minutes, schematic representation of the multi-parametric scan protocol can be seen in *Figure 1.*

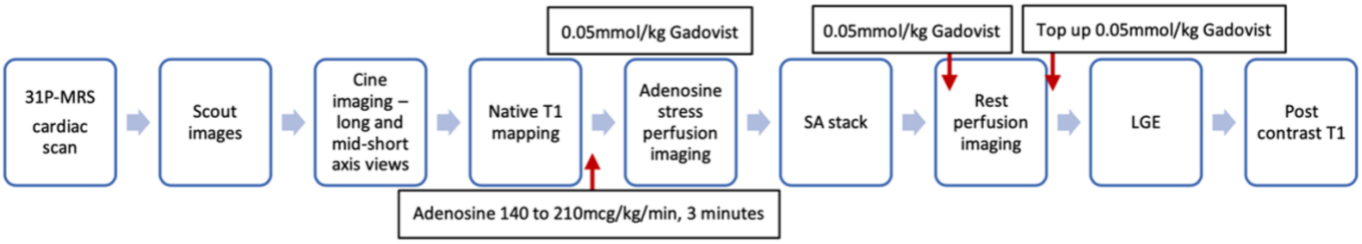

Figure 2.1: Multiparametric scan protocol

2.4.1 ^{31}Phosphorous Magnetic Resonance Spectroscopy

Prior to commencing my research project, the ^{31}P-MRS technique had not yet been established in Leeds Teaching Hospitals. In conjunction with my supervisor and the medical physics team, we developed a modified, reproducible ^{31}P-MRS protocol which allowed for supine scanning and improved patient comfort. This work is discussed in further detail in chapter 3.

2.4.2 Left Ventricular Function and Mass

CMR is accurate, reproducible and well validated for measuring left ventricular volumes and mass[132,227]. Cardiac volumes were acquired using Steady State Free Precession (SSFP) imaging. Pilot, horizontal long axis, vertical long axis and short axis stack images were acquired with the patient in the supine position. Each slice was 8mm thick with a 3mm gap and is prospectively gated with echo time, 1.5 ms; repetition time, 3 ms; flip angle, 50°. The slices were obtained during a breath-hold at the end of normal expiration to minimize the effects of respiratory motion.

LV short axis epicardial and endocardial borders were manually contoured at end diastole and end systole, for determining end diastolic volume (EDV); end systolic volumes (ESV); stroke volume (SV) using cvi42© (Circle Cardiovascular Imaging Inc., Calgary, Canada). Ejection fraction (EF) and cardiac output (CO) are calculated (EF = SV/EDV, CO=SV x heart rate. Myocardial mass is also calculated by subtracting the endocardial volume from the epicardial volume. Left ventricular mass is calculated based on prior knowledge of myocardial specific gravity (1.05 g/cm^3).

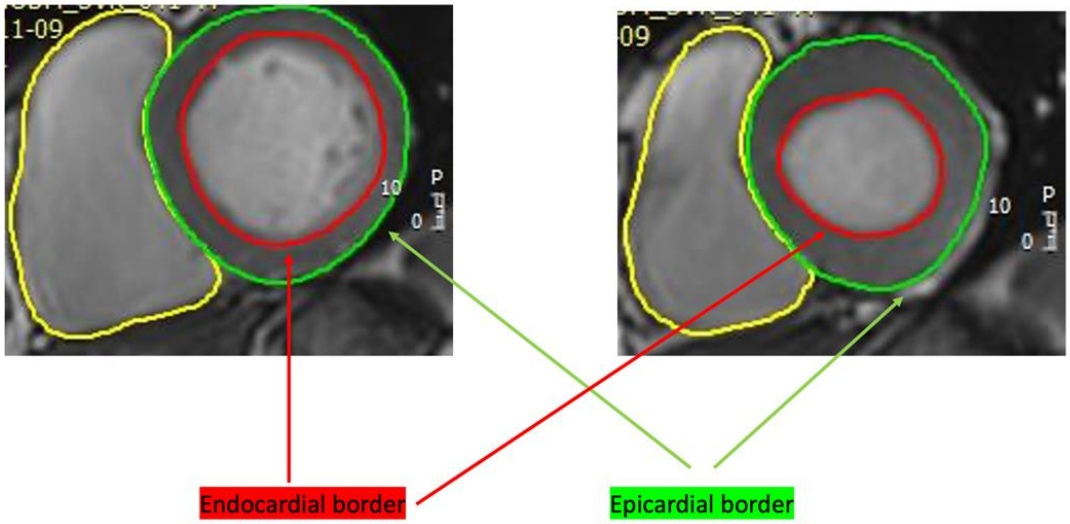

Figure 2.2: Epicardial and endocardial contours are drawn at end diastole and end systole.

2.4.3 Left Atrial Volumes and Function

CMR provides a gold standard technique for in-vivo LA volumetric assessment, demonstrating improved reproducibility compared with echocardiography[228,229]. Cardiac volumes were obtained using SSFP imaging as outlined above. Bi-plane volumetric measurements were undertaken offline using commercially available software, cvi42© (Circle Cardiovascular Imaging Inc., Calgary, Canada), Maximal LA volume (LA max) was defined visually as the phase with the largest LA dimension and minimal LA volume (LA min) defined as the phase with the smallest LA dimension. Manual tracing of the endocardial border from the apex of the LA to the atrioventricular junction, was performed in the vertical long axis (VLA) and horizontal long axis (HLA) views (Fig 3). Of note, the LA appendage was included in LA volume whereas the pulmonary veins were excluded at their ostia.

LA ejection fraction was then calculated as:

$$\frac{End\ diastolic\ volume - End\ systolic\ volume}{End\ diastolic\ volume} \times 100$$

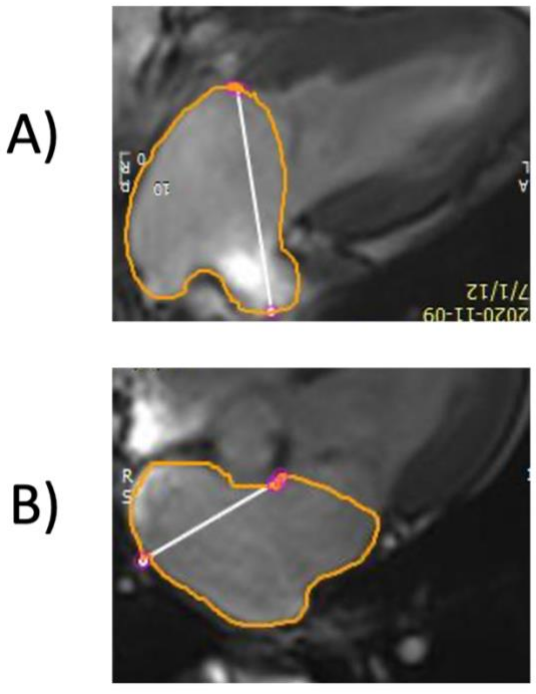

Figure 2.3: Bi-plane left atrial endocardial contours in the vertical and horizontal long axis views.

2.4.4 Left Ventricular Strain

Aside from volumetric assessment, CMR can derive deformation parameters including myocardial strain which is defined as the percentage change of myocardial fiber length with respect to the diastolic phase in a certain direction[230]. Strain is 3D and thought to be a sensitive diagnostic index to detect early, subtle alterations in myocardial function, prior to deterioration in LV ejection fraction, which may be preserved or even increased, particularly in states of left ventricular hypertrophy[231,232]. 3D global longitudinal strain (GLS) has been shown to be a robust index for predicting adverse cardiac events in patients with severe AS[233]. Cardiac volumes were obtained using SSFP imaging as outlined above, feature tracking analysis was then performed offline using cvi42 software. Longitudinal strain was assessed in three long axis views, 4 chamber, 3 chamber and 2 chamber views respectively, circumferential strain was assessed using full coverage short axis stack of the LV. Endocardial and epicardial contours were manually drawn in end diastolic and end systolic phases, the left ventricular outflow tract (LVOT), papillary muscles and epicardial fat were excluded from contouring. The cvi42 software automatically propagates manual contours and tracked myocardial features throughout the cardiac cycle, allowing for assessment of systolic and diastolic circumferential and longitudinal strain, with segmentation via the American Heart Association (AHA) 17 segment model[234].

The algorithms used for tissue tracking have been previously well described [235]. Briefly, 2D CMR tissue tracking determines the myocardial deformation by a set of reference points placed on the mid myocardial wall, which are then tracked over the cardiac cycle in short and long axis images. With the contraction and relaxation of the myocardium, these 2D reference points can be traced to provide 2D motion data for short and long axis images. 3D CMR tissue tracking relies on a 3D deformation model generated by combining 2D short and long axis images into a single 3D motion field[230,236].

2.4.5 Epicardial and Visceral Fat Assessment

Epicardial and abdominal visceral fat area measurements single-shot acquisition of thoracic and abdominal non-breath-hold images were performed using multi-echo GRE sequence with gradient flyback for monopolar readout to acquire 3 echoes for each phase encode (parallel imaging rate 3 using GRAPPA with separate reference line acquisition, 32 channel cardiac array, bandwidth=1184 Hz/pixel, TE=1.33, 3.35, and 5.37ms, TR=6.71ms, readout flip angle=20°, matrix=192x108, single shot duration=242ms, FOV=300x225mm^2, slice thickness=6mm) as previously described[237].

2.4.6 Modified Look Locker Inversion (MOLLI) T1 Mapping

T1 maps were acquired in 3 short axis slices using breath held, modified look locker inversion recovery (MOLLI) acquisition (ECG triggered 5s(3s;single shot, SENSE factor 3; pre-pulse delay 350ms, trigger delay set for end diastole, echo time (TE)/ repetition time (TR)= 1.09/774ms, flip angle 20^o, acquisition matrix 380x380mm, slice thickness 8mm, giving a re-constructed voxel size of 1.5x1.5x8mm). Shimming and center frequency adjustments were performed to generate images free from off resonance artefacts.

T1 maps were analysed using cvI42 software, short axis images were manually contoured to define the endocardial and epicardial borders and then divided into six segments per slice using the anterior RV-LV insertion points as a reference, providing an average myocardial T1 value for each individual and for each of the three slices. For the purposes of data analysis, only the native T1 values from the mid myocardial segment for each participant were used. Consistent with established methods for estimating myocardial extra cellular volume (ECV) a delayed, post-contrast bolus protocol was used[238], allowing for measurement of pre and post contrast T1 values in the blood and myocardium. Estimation of ECV and lambada (λ) was based on multi-point regression, whereby the gadolinium contrast partition co-efficient (λGd) in the myocardium is calculated from the change in relaxation rate in myocardium and blood after contrast injection, multiple T1 measurements can then be used to calculate the partition co-efficient from the slope using a linear regression line for the measured values of relaxation

in the blood and myocardium[239]. Incorporating all available pre and post contrast data points increases the robustness of the data[239], final ECV values were calculated as (*1-haematocrit*).

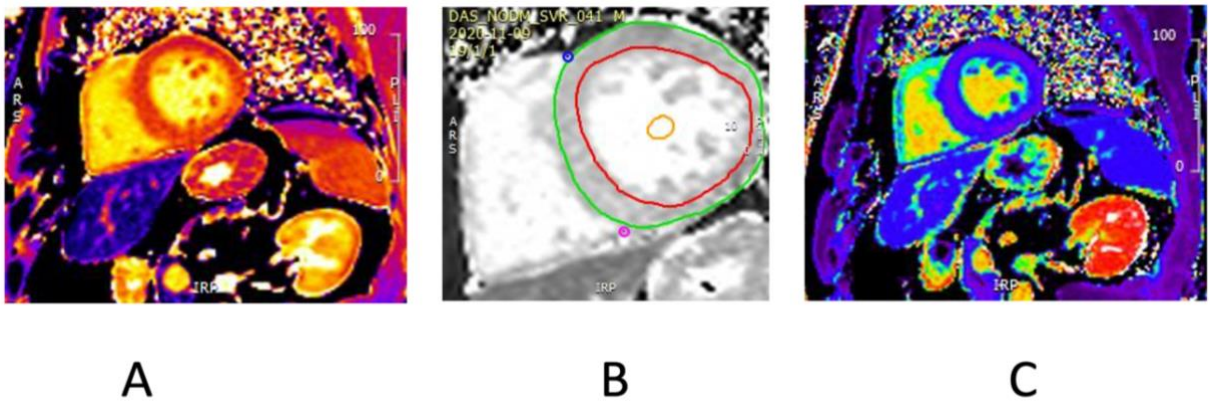

Figure 2.4: Representative images from a patient with isolated severe AS showing, A: Native T1 maps, B: T1 maps with manual epicardial, endocardial and blood pool contouring and C: Post contrast T1 maps.

2.4.7 Late Gadolinium Enhancement

For late gadolinium enhancement (LGE) CMR, a top-up bolus of 0.06 mmol/kg of body weight of a gadolinium-based contrast agent gadobutrol (Gadovist, Leverkusen, Germany) was administered at 5ml/s followed by a 20ml saline flush, given through an intravenous cannulae in the anti-cubital fossa, using an automated injection pump (Medrad MRXperion Injection System, Bayer). The scan parameters used were: slice thickness 8 mm, flip angle 20°, Repetition time/ Echo time =3 ms/7.5 ms.

Areas of LGE were visually scored as absent or present by consensus of 2 experienced operators, additionally LV LGE volume was quantified as a percentage of the total LV myocardial volume, which was computed by summing the percentage area of LGE in each short axis stack slice, multiplied by the slice thickness along the entire LV. LGE was defined by the presence of enhanced areas with signal intensity greater than 6 standard deviations above that of the remote myocardium[240].

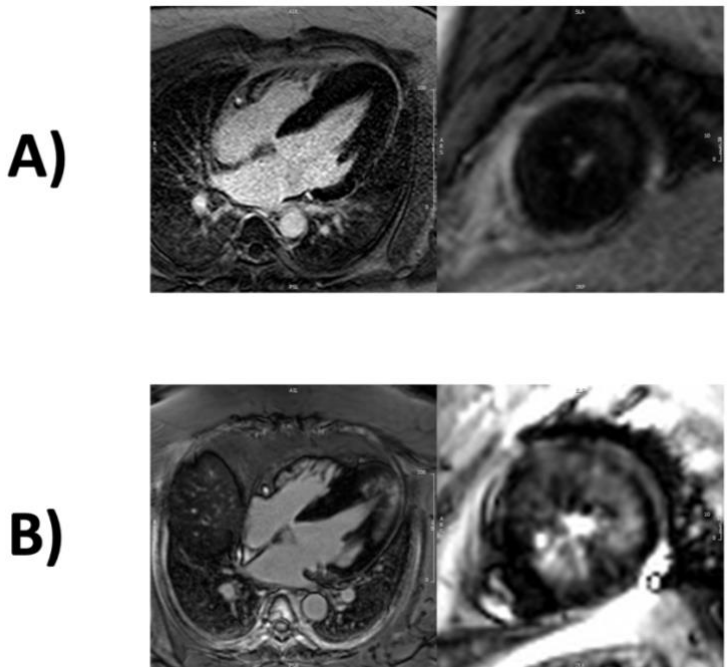

Figure 2.5: Late gadolinium enhanced images in the horizontal long axis and short axis view from a subject with apical HCM showing A: No LGE and B: Diffuse LGE at the LV apex at follow up.

2.4.8 Quantitative Myocardial Perfusion

Perfusion imaging used a free breathing, fast low angle shot (FLASH) magnetic resonance protocol with motion-corrected (MOCO) automated in-line perfusion mapping using the Gadgetron streaming software image reconstruction framework as previously described[241]. For stress perfusion imaging, adenosine was infused at a rate of 140 µg/kg/min and increased up to a maximum of 210 µg/kg/min according to hemodynamic and symptomatic response (a significant hemodynamic response to adenosine stress was defined as >10 beats/min increase in heart rate, or BP drop <10 mm Hg and >1 adenosine-related symptom, (e.g., chest tightness, breathlessness)[242]. A minimum 10-minute interval was kept between perfusion acquisitions to ensure equilibration of gadolinium kinetics and resolution of all hemodynamic effects of adenosine. For each perfusion acquisition, an intravenous bolus of 0.05mmol/kg gadobutrol (Gadovist, Leverkusen, Germany) was administered at 5ml/s followed by a 20ml saline flush using an automated injection pump (Medrad MRXperion Injection System, Bayer). Myocardial perfusion image reconstruction and processing was implemented using the Gadgetron software framework as previously described[241]. Rest/stress myocardial blood flow

(MBF) were measured for each of the 16 segments using the American Heart Association (AHA) classification. MBF values for all remaining segments were averaged to provide a global value. Myocardial perfusion reserve (MPR), was calculated as the ratio of stress to rest MBF, both stress MBF and MPR measured automatically in-line, using artificial intelligence quantification have been shown to provide robust, independent predictors of adverse CVS outcomes[243]. CMR Rest/stress perfusion images were carefully reviewed for each of the 16 segments using the AHA classification to ensure quality control, both evidence of splenic switch off and a regional threshold of stress MBF >1.43ml/min/g were taken as evidence of maximal hyperaemia and adequate stress[244].

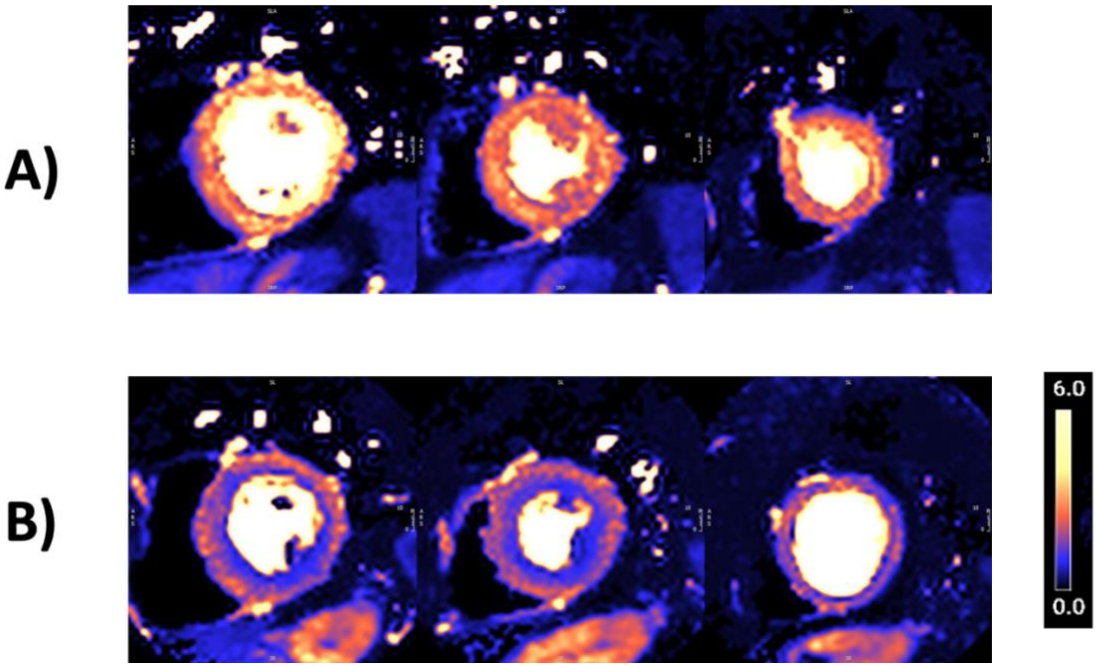

Figure 2.7: Examples of stress myocardial blood flow images at the basal, mid and apical short axis with A: Normal perfusion in a healthy control subject and B: Globally reduced myocardial blood flow in a subject with isolated severe AS.

2.5 Ex-vivo Assessment of Myocardial Mitochondrial Function

In addition to non-invasive assessment via ^{31}P-MRS, mitochondrial function can also be assessed ex-vivo using high-resolution respirometry techniques. All patients enrolled in the DAS study (IRAS ID 252633) who were in the surgical cohort were consented for excision of myocardial tissue during AVR. Further details of the high resolution respirometry technique will be outlined in chapter 6.

2.7 Statistical Analysis

Statistical analysis was performed using GraphPad Prism software (version 9.0.0, San Diego, CA, USA). All data were checked for normality using the Shapiro-Wilks test and presented as mean or median with 95% confidence intervals as appropriate. Categorical data are presented as numbers and percentages and compared with Pearson's chi-square test. Comparisons between multiple groups were performed by 1-way ANOVA with post hoc Bonferroni corrections. Differences in non-parametric variables were assessed using a Kruskal-Wallis test. Student t-test was used for comparison of normally distributed datasets and Mann-Whitney U test was used for non-parametric tests where data were obtained for only two groups. Comparisons between performed with ANOVA with post hoc Bonferroni corrections. $P \leq 0.05$ was used as a threshold of significance.

A 2-sided log-rank test was used to calculate average event rate ratios and confidence intervals. Kaplan-Meier plots were constructed for time-to-event analyses.

Chapter 3

Scan-rescan reproducibility of a modified cardiac ^{31}phosphorus magnetic resonance spectroscopy scan protocol

3.1 Abstract

Background

^{31}Phosphorus magnetic resonance spectroscopy (^{31}P-MRS) allows for non-invasive measurement of the concentration ratio of phosphocreatine (PCr) to ATP, which is a sensitive indicator of the myocardial energetic state. Reduction in variability and higher reproducibility have remained as important goals for wider application of cardiac ^{31}P-MRS. We have assessed reproducibility of a modified scan protocol allowing for robust assessment of coil position, and for chemical shift imaging grid positioning.

Methods

Ten healthy volunteers (four female, 34±3years) were recruited for scan/rescan reproducibility assessments. A separate cohort of five healthy volunteers (two female, 36±7years) were recruited for three sequential scans for further assessment of interscan variability.

Results

The scan-rescan PCr/ATP measured using the modified supine ^{31}P-MRS protocol performed on ten volunteers was highly reproducible achieving variability of <5% and showed excellent agreement (coefficient of variation [CoV] 4.12; bias -0.06±0.13 respectively). In the additional five healthy volunteers who underwent three sequential scans on consecutive days variability was also maintained between the first and second (CoV 5.47; bias -0.006±0.19) and second and third scans (CoV 5.33; bias -0.06±0.15).

Conclusion

^{31}P-MRS can be performed in the supine position with a high degree of reproducibility using an optimised protocol with improved coil positioning thereby maximising patient comfort and increasing the scope for tolerance of the technique by a wider patient cohort.

3.2 Introduction

Cardiac ^{31}phosphorus magnetic resonance spectroscopy (^{31}P-MRS) has become increasingly important in biomedical research owing to its capacity for non-invasive measurement of *in vivo* biochemical information[71,72]. Efficient matching of energy supply to demand in the heart is essential for maintaining cardiac function. In the aerobic setting, more than 90% of the energy currency adenosine triphosphate (ATP) produced by the heart is derived from mitochondrial oxidative phosphorylation[245 33]. Mitochondrial creatine kinase catalyses the transfer of the high energy phosphate bond in ATP to creatine to form phosphocreatine (PCr)[246]. The PCr molecule is smaller and less polar than ATP and therefore able to diffuse out of the mitochondria into the cytoplasm to the site of energy usage, where ATP is reformed in the reverse reaction. The relative concentration of PCr to ATP (PCr/ATP) measured with ^{31}P-MRS is a sensitive index of the energetic state of the myocardium[246]. PCr is present in concentrations above twice that of ATP in the healthy myocardium, providing a PCr/ATP of >2, and is maintained at a constant value due to coordination of ATP utilising and synthesising pathways. Using ^{31}P-MRS, studies have shown reductions in myocardial PCr/ATP to be a feature of diabetic cardiomyopathy[247-249], inherited cardiomyopathies[250,251], valvular heart disease[252], cardiac transplant rejection[253] and systolic heart failure[26,45].

While ^{31}P-MRS allows for unique insights into cardiac energetics, it inherently has a low intrinsic signal-to-noise ratio (SNR). Consequently, clinical applications of ^{31}P-MRS have not yet seen widespread acceptance. The main obstacle for implementation of cardiac ^{31}P-MRS in routine cardiology practice has been, and remains, that it is a tool with significant technical complexity, and with limited signal and resolution. The technical challenges include sensitivity to cardiac and respiratory motion, low MR visibility of ^{31}P nuclei ($^{1}/_{14}$ the molar receptivity of ^{1}H and present in concentrations $\approx$ $^{1}/_{1000}$ that of ^{1}H), low metabolite concentrations and relatively long T1 relaxation times, all of which necessitate long acquisition times for high quality, uncontaminated spectra.

The acquisition of quality spectra in a comfortable scan time by increasing the voxel size was achieved previously reducing the scan time from 30min to ~8min at 3T to acquire metabolite

concentrations in three 5.6mL voxels covering the interventricular septum[254,255]. While this approach reduces the specificity of cardiac signal acquisition, the issue of signal contamination arising from adjacent voxels was also solved in a previous study by the use of saturation pulses issued over neighbouring tissues[256,257].

Despite these improvements in acquisition times, other major limitations of the method have remained, including: i) scan acquisitions in most research centres with subjects laying in a prone position in an attempt to reduce coil distance from the heart, which leads to difficulties scanning symptomatic patients or children; ii) challenging chemical shift imaging (CSI) grid placement with a central voxel in the mid-ventricular septum due to poor quality 3D stack of short axis (SA) images obtainable with the phosphorus coil; iii) undesirable variability in human cardiac PCr/ATP measurements impeding single-subject comparisons[72]; Consequently, reduction in variability (<5%), improved reproducibility, and scanning when subjects lay in a supine position for improved comfort and compliance during the acquisition are important goals for wider application of this technique, as is obtaining data on the effect of feeding status.

To achieve these goals, we have modified the existing 8-minute multi-voxel chemical shift imaging (CSI) sequence at 3T for scanning participants in a supine position. We have increased slice coverage of the proton localisation images to include fiducials and the heart in a coronal orientation for robust assessment of coil position in relation to the heart at the start of the acquisition. This allowed optimisation of coil positioning by adjustments if required to ensure the left ventricle is positioned at the magnet iso-centre. To overcome the shortcoming of the steady-state free precession (SSFP) cine cardiovascular magnetic resonance sequence with a phosphorus coil, we used a real-time cine magnetic resonance sequence[258]. This sequence utilises accelerated imaging and single-shot acquisitions to acquire snapshot images of the heart fast enough to freeze the cardiac and respiratory motion, offering high quality ventricular images without the need for breath-holding or ECG triggering for cardiac voxel selection and CSI grid positioning from short axis left ventricular planes even with a phosphorus coil.

The purpose of this work was to establish scan-rescan reproducibility of this modified cardiac ^{31}P-MRS scan protocol. Two consecutive scan acquisitions with an 8-minute (nominal voxel volume 11.2ml, true voxel volume is 93ml) multi-voxel CSI acquisition protocol were performed[254]. This study protocol maintained myocardial specificity by using acquisition weighting, and by careful placement of muscle and liver saturation bands to reduce potential

contamination[257]. Intrasubject variability of the modified protocol was further assessed using three consecutive scan acquisitions.

3.3 Methods

Participants

The study was approved by the National Research Ethics Committee (REC Ref:18/YH/0168). All work was carried out according to the principles of the Declaration of Helsinki and was approved by the local ethics committee. Each subject gave written informed consent. Ten healthy volunteers (four female, mean age 34±3years, BMI 23±3) were recruited for scan/rescan reproducibility assessments. A separate cohort of five healthy volunteers (two female, 36±7years) were recruited for three sequential scans for further assessment of interscan variability. All healthy volunteers were non-smokers, normotensive, non-diabetic and had no history of cardiovascular disease. Subjects were not asked to fast prior to data acquisition.

Acquisition protocol

All scans were performed on a Siemens 3T Magnetom Prisma system (Erlangen, Germany) using a quadrature ^{31}P transmit/receive cardiac coil (Rapid Biomedical GmbH, Rimpar, Germany) consisting of two overlapping rectangular coil elements with an overall size of 200x200mm within a rigid housing. Subjects lay supine, with their left ventricle positioned centrally at iso-centre. Coil position was standardised to be placed above the mid ventricular septum. Imaging was performed by three operators (EL with 9 years of experience in MR spectroscopy supervised all scans and either NJ or ST with 2 years of experience in MR spectroscopy performed the acquisitions).

Flip angle calibration

A sample of phenylphosphonic acid (PPA) doped with chromium (III) acetylacetonate $Cr(acac)_3$ was located within a well in the coil housing. A series of ten inversion-recovery free induction decay signals were acquired at the PPA frequency, in order to allow correction of

transmit efficiency differences between subjects (due to variable coil loading) during analysis. Additionally, 4 fiducial markers were positioned on the anterior coil surface to allow spatial localisation of the coil relative to the subject's anatomy and spectroscopy acquisition. These data allowed determination of subject-specific flip angle maps to allow correction for the differential RF saturation of metabolites.

Chemical Shift Imaging

All ^{31}P-MRS data were acquired with a non-gated 3D acquisition weighted CSI technique (AW-CSI) with 10 averages at the centre of K-space and ultrashort TE to minimise T_2 effects and first order phase artefacts [257]. An optimised RF pulse, centred 1250Hz below the PPA peak between the γ and α ATP resonance frequencies, was used to ensure uniform excitation of all spectral peaks. The acquisition matrix was 16 x 8 x 8. Field of view was 240 x 240 x 200 mm. ECG gated pilot images of the vertical long axis (VLA), the horizontal long axis (HLA) and a 3D stack of short axis (SA) images were acquired (Figure 3.1). The CSI grid was placed with a central voxel in the mid-ventricular septum, on the first short axis image in which the papillary muscles were visible (Figure 1). The acquisition was run with a fixed TR of 720 ms. Two 50 mm saturation bands were placed over the chest wall muscle and an additional 50 mm saturation band was placed over the liver.

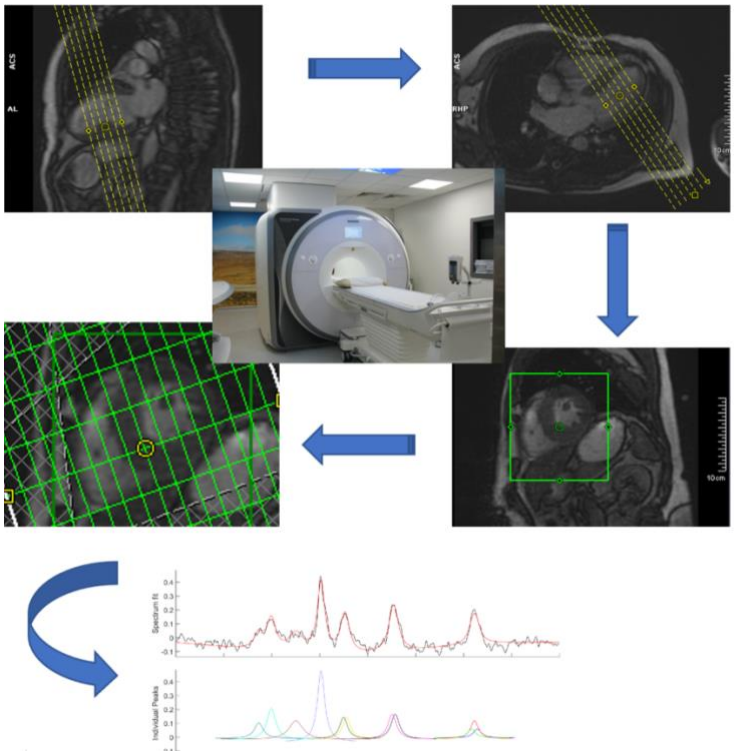

Figure 3.1: Example of voxel acquisition during optimised 31P-MRS protocol

Reproducibility assessments

For the scan-rescan reproducibility assessments, participants underwent two sequential scans within a 1-hour period, with the table repositioned between the interval scans. Intraparticipant variability was further assessed in an additional five healthy volunteers who underwent three sequential scans with patient and coil repositioning between studies and the third scan undertaken on consecutive days.

Data analysis

From the short axis stack images, a single voxel corresponding to the mid inter-ventricular septum voxel was selected for further analysis. ^{31}P-MRS post processing analysis was performed using a custom Matlab (Mathworks, Natick, Mass) implementation of the advanced method for accurate, robust, and efficient spectroscopic (AMARES) fitting with prior

knowledge specifying 11 Lorentzian peaks (α, β, γ-ATP, PCr, phosphodiester, and 2 × 2, 3-diphosphoglycerate), fixed amplitude ratios, and literature values for the scalar couplings for the multiplets as previously described[259]. Saturation and blood pool contamination was corrected using values from the literature. PCr/ATP was reported as the blood and saturation-corrected values of PCr to the average of α-ATP, β-ATP and γ-ATP. All analysis was undertaken by NJ and ST. All analysis was performed blinded.

Statistics

Statistical analysis was performed using GraphPad Prism software (version9.0.0). Continuous variables are presented as mean ± SD and were checked for normality using the Shapiro-Wilks test. Student t-test was used for comparison of normally distributed datasets and Mann-Whitney U test was used for non-parametric tests. P value of ≤0.05 was considered statistically significant. Inter-study reproducibility and bias were assessed using the Bland-Altman method[260], inter-study variability was assessed using the co-efficient of variation (CoV).

3.4 Results

Flip angle calibration

The average flip angle measured at the inter-ventricular septum was 34° ± 11° over all subjects studied.

Assessment of scan-rescan reproducibility

CSI acquisitions were compared by assessing the absolute difference between PCr/ATP values measured by both CSI scans performed on 10 healthy volunteers. The mean PCr/ATP value derived from the spectra acquired from the first scan was 2.35 ± 0.29 and from the second scan was 2.34 ± 0.29, with no significant difference (p=0.69). The absolute difference between

PCr/ATP values acquired via each scan for each subject was 0.05 ± 0.04 (1.86% difference ± 1.8%).

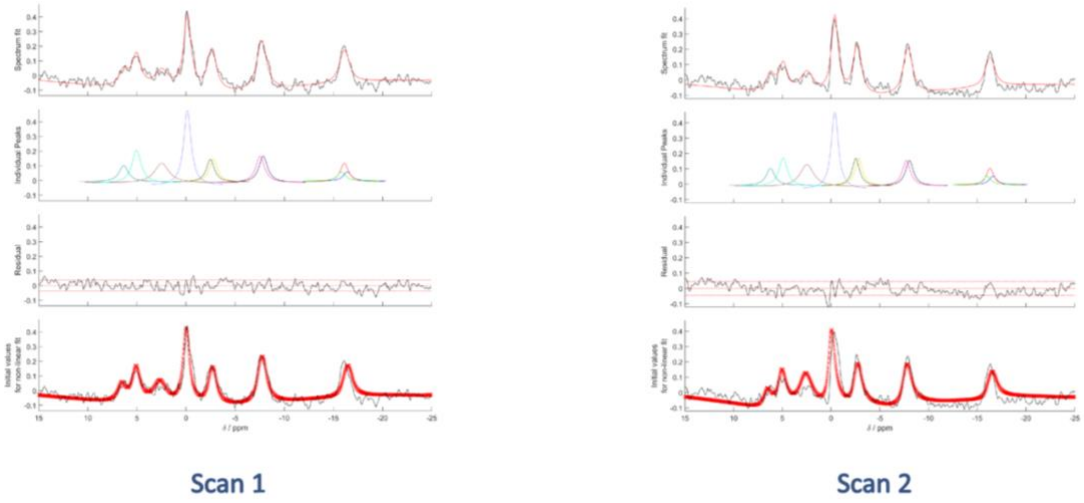

Figure 3.2: Example spectra from healthy volunteer undergoing sequential 31P-MRS scans

A Bland-Altman plot showed the scan-rescan variability of the PCr/ATP measured using our optimised supine ^{31}P-MRS protocol performed on 10 volunteers was 4.12%, r^2=0.95, p=<0.0001, and bias= -0.06±0.13 (Figure 3), showing excellent agreement (Table 1).

Variable		Coefficient of Variance	Upper	Lower	Bias	R^2	Variability
PCr/ATP (n=10)	**scan/rescan**	4.12	0.3	-0.2	0.06	0.95	0.08
PCr/ATP (n=5)	**scan 1-2**	5.47	0.4	-0.4	-0.006	0.79	0.06
PCr/ATP (n=5)	**scan 2-3**	5.33	0.2	-0.3	0.06	0.58	0.06

Table 3.1: Reproducibility and accuracy of cardiac 31P-MRS

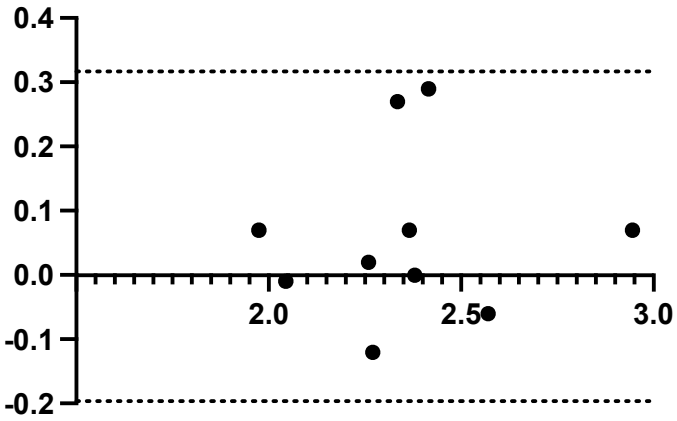

Figure 3.3: Bland-Altman plot of healthy volunteer inter-study variability (PCr/ATP). Dashed lines mark 95% confidence limits of bias.

Assessment of sequential scan-rescan variability

In the separate cohort of 5 participants who underwent three sequential scans variability did not alter significantly ([scan1-2; CoV 5.47; bias -0.006±0.19], [scan2-3 CoV 5.33; bias -0.06±0.15], table 2, fig 4).

Subject Number	**Scan 1 PCr/ATP (n = 5)**	**Scan 2 PCr/ATP (n = 5)**	**Scan 3 PCr /ATP (n=5)**
01	1.83	1.98	2.08
02	2.22	2.34	2.22
03	2.01	2.07	1.83
04	1.80	1.82	1.69
05	2.42	2.10	2.21
Mean	2.06	2.06	2.01

Table 3.2: Sequential variation in 31P-MRS with subject repositioning

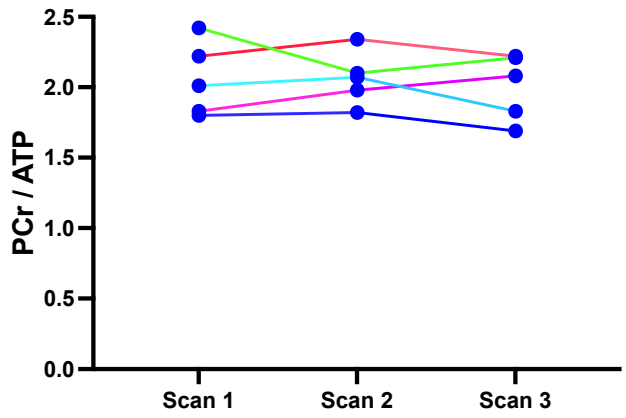

Figure 3.4: Estimation plot of healthy volunteer inter-study variability

3.5 Discussion

Information about reproducibility is necessary for power calculations when making decisions about cohort sizes and for assessing the statistical power of results. Biological variability, variation in voxel selection and coil loading, and participant movement during the scan can all deteriorate the reproducibility of cardiac ^{31}P-MRS. With the measures we have taken to improve reproducibility, we report significant reduction in variability (<5%) of the cardiac PCr/ATP measurements which compares favourably with reported variability of 18% (high spatial resolution 3D-CSI) and 15% (3-D ISIS) [72,261] in previous studies at 3T field strength [72,261]. We have achieved this goal with an optimized scan protocol allowing for robust evaluation of coil positioning and increased cardiac image quality allowing for better visualization of the ventricular septum while positioning the CSI grid. Moreover, this high degree of reproducibility was achieved in the setting of supine scanning thereby maximizing patient comfort. Supine patient position during ^{31}P-MRS scanning offers the possibility of improved patient tolerance in cohorts such as those with advanced heart failure, frailty and the pediatric population.

Limitations

Concurrent measurement of plasma insulin, glucose, ketone and FA levels, which may provide insight into substrate specific relationships to energetics, were not undertaken.

3.6 Conclusion

^{31}P-MRS can be performed at 3T with patients in the supine position with a high degree of reproducibility, allowing for the potential wider application of this technique.

Chapter 4

Coexistent diabetes is associated with the presence of adverse phenotypic features in patients with hypertrophic cardiomyopathy

Jex N**,** Chowdhary A, Thirunavukarasu S, Procter H, Sengupta A, Natarajan P, Kotha S, Poenar AM, Swoboda P, Xue H, Cubbon RM, Kellman P, Greenwood JP, Plein S, Page S, Levelt E. Coexistent Diabetes Is Associated With the Presence of Adverse Phenotypic Features in Patients With Hypertrophic Cardiomyopathy. ***Diabetes Care***. 2022 Aug 1;45(8):1852-1862. doi: 10.2337/dc22-0083. PMID: 35789379

4.1 Abstract

Objective- Type 2 diabetes mellitus (T2DM) is associated with worsened clinical outcomes in hypertrophic cardiomyopathy (HCM) patients. We sought to investigate if hypertrophic cardiomyopathy patients with T2DM comorbidity exhibit adverse cardiac alterations in myocardial energetics, function, perfusion, or tissue characteristics.

Research design and methods- Fifty-five participants with concomitant HCM and T2DM (HCM-DM, n=20), isolated HCM (n=20), and healthy volunteers (HV, n=15) underwent ^{31}phosphorus magnetic resonance spectroscopy and cardiovascular magnetic resonance imaging. The HCM groups were matched for HCM phenotype.

Results- ESC sudden cardiac death risk scores were comparable between the HCM groups (HCM:2.2±1.5%, HCM-DM:1.9±1.2%; p=NS) and sarcomeric mutations were equally common. HCM-DM had the highest NT-proBNP levels (HV:42ng/L[IQR:35-66], HCM:298ng/L[IQR:157-837], HCM-DM:726ng/L[IQR:213-8695]; p<0.0001). Left-ventricular ejection fraction, mass and wall thickness were similar between the HCM groups. HCM patients with T2DM comorbidity displayed a greater degree of fibrosis burden with higher scar percentage, and lower global longitudinal strain compared to the isolated HCM patients. PCr/ATP was significantly lower in the HCM-DM group than both the isolated HCM patients and the healthy controls (HV:2.17±0.49, HCM:1.93±0.38, HCM-DM:1.54±0.27; p=0.002). In a similar pattern, stress myocardial blood flow was significantly lower in the HCM-DM group than both the isolated HCM patients and the healthy controls (HV:2.06±0.42ml/min/g, HCM:1.74±0.44ml/min/g, HCM-DM:1.39±0.42ml/min/g; p=0.002).

Conclusions- We show for the first time that HCM patients with T2DM comorbidity display greater reductions in myocardial energetics, perfusion, contractile function and higher myocardial scar burden and serum NT-proBNP levels compared to patients with isolated HCM despite similar LV mass and wall thickness and presence of sarcomeric mutations. These adverse phenotypic features may be important components of the adverse clinical manifestation attributable to a combined presence of HCM and T2DM.

4.2 Introduction

Hypertrophic cardiomyopathy (HCM) is the most common inherited cardiomyopathy with a population prevalence of 1 in 500[191,196]. HCM is associated with sudden cardiac death and may lead to heart failure at any age, although significant heterogeneity in phenotypic expression exists[191,196]. Type 2 diabetes mellitus (T2DM) occurs concomitantly in 9% of patients with hypertrophic cardiomyopathy (HCM) and is associated with worsened clinical manifestation of HCM[195,262]. HCM patients with T2DM comorbidity (HCM-DM) were shown to have higher prevalence of diastolic dysfunction and pulmonary hypertension, higher New York Heart Association (NYHA) Class, lower exercise capacity and increased long-term mortality[262]. Although distinct pathological entities, HCM and T2DM were shown to share common features of impaired myocardial energetics[247,248,250], coronary microvascular dysfunction[179,208] and myocardial fibrosis[45,203,263-266] on previous studies investigating these conditions in isolation. The mechanisms for the adverse prognostic association between HCM and T2DM are incompletely understood but likely include the collective impact of HCM and T2DM on myocardial energy metabolism, perfusion and the fibrotic process.

The relative concentration of phosphocreatine to ATP (PCr/ATP) is a sensitive index of the energetic state of the myocardium[246] which can be measured non-invasively by ^{31}phosphorus magnetic resonance spectroscopy (^{31}P-MRS). Moreover, cardiovascular magnetic resonance (CMR) allows comprehensive evaluation of myocardial structure, function, strain, tissue characteristics, fibrosis and perfusion with excellent reproducibility[241,267]. Utilising CMR, previous studies identified factors associated with adverse cardiovascular events and mortality in HCM patients, including replacement fibrosis on late gadolinium enhancement imaging[268]. In addition to replacement fibrosis by LGE, CMR is also established as a tool for quantification of diffuse fibrosis by quantifying the extracellular volume fraction (ECV) by native T1 mapping[172].

Combining ^{31}P-MRS and CMR in an observational prospective case-control study we sought to test the hypothesis that coexistent diabetes is associated with greater reductions in myocardial energetics and perfusion, and higher scar burden in HCM.

4.3 Research Design and Methods

This single centre, prospective case control study complied with the declaration of Helsinki and was approved by the National Research Ethics Committee (Ref:18/YH/0168). Informed written consent was obtained from each participant.

Participants

Fifty-five participants including 20 with isolated-HCM; 20 with HCM-DM; and 15 healthy volunteers (HV) were prospectively recruited. Genetic screening was undertaken for all HCM patients for 21 genes. Diagnosis of HCM was based on the presence of unexplained left ventricular (LV) hypertrophy (maximum wall thickness ≥15 mm)[196]. Anderson-Fabry disease was excluded in all male adult patients with presumed HCM with a blood test for plasma and leucocyte alpha galactosidase A[269], except for patients from families with established genetic forms of HCM or for previously diagnosed mutation carriers. In women with a suspicion for the condition, GLA gene test is performed for exclusion.

Two routes were used for recruitment of the participants with HCM (Figure 1, CONSORT diagram). Eligible HCM patients were recruited from the regional Inherited Cardiac Conditions (ICC) Clinic over two years during their routine clinical appointment (May 2019-May 2021), and from a local registry of 426 HCM patients followed by our regional ICC clinic. This list was pre-screened by an independent investigator (PN) in a non-participant facing role. After each prospective block of 5 HCM-DM participants were successfully recruited and completed the study visit, our regional ICC registry was revisited for identifying isolated HCM patients meeting eligibility criteria as well as for matching to scanned HCM-DM patients for age, sex, ESC risk score profile and hypertension comorbidity (PN). This practice was repeated for each block of 5 patients 4 times over the 2 years while this study was conducted. All data were analysed in a blinded fashion after the completion of the study (last participant last visit). The blinding methodology is described in the methods.

HCM-DM patients had an established diagnosis of DM according to World Health Organization criteria and were free of known diabetes complications[270]. HV were recruited from local golf clubs. Ethnicity group was self-reported by participants.

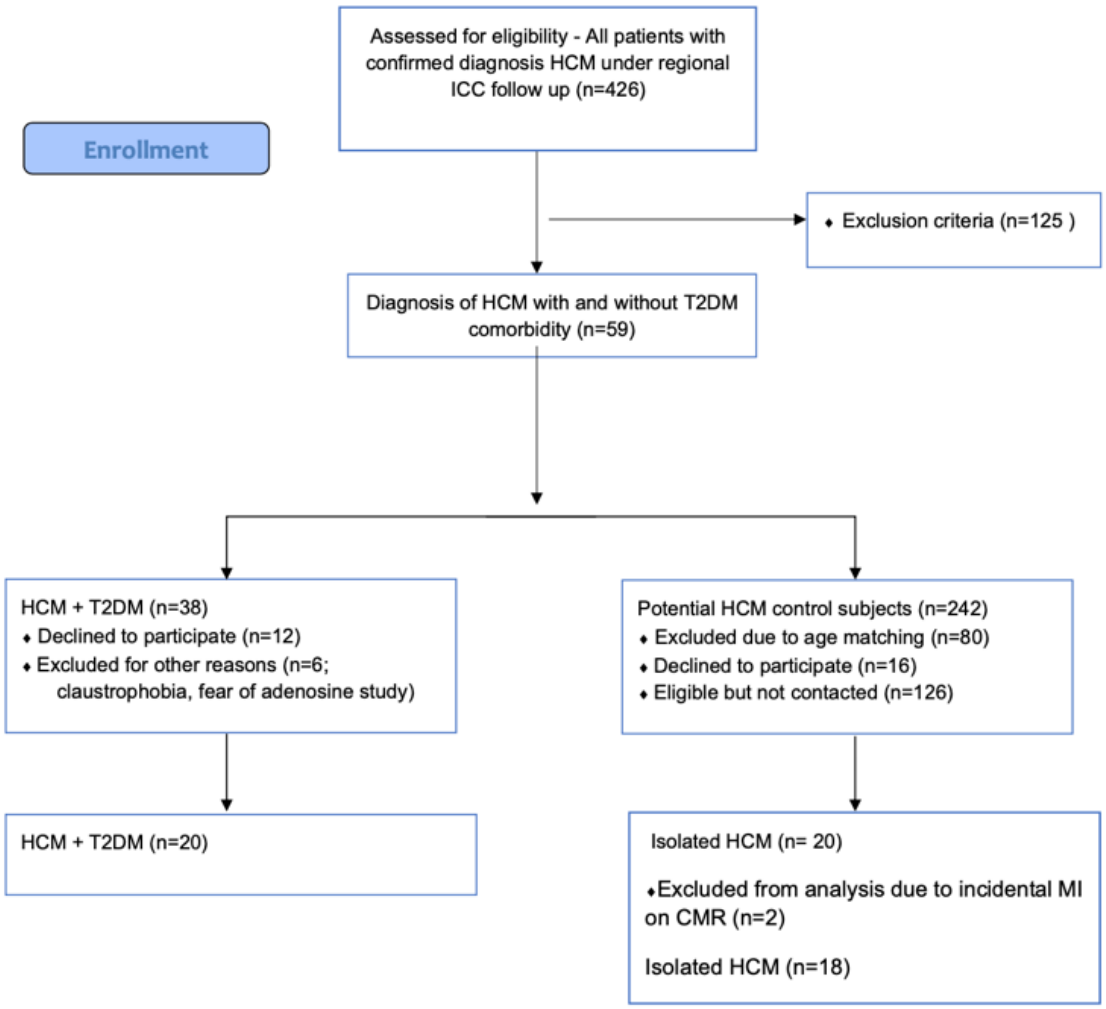

Figure 4.1: Consort flow diagram demonstrating the recruitment pathway for study participants with hypertrophic cardiomyopathy.

Exclusion criteria

Patients with known coronary artery disease (CAD), cardiac surgery, tobacco smoking, amyloidosis, permanent atrial fibrillation, moderate or above valvular heart disease, renal impairment [estimated glomerular filtration rate (eGFR)<30mL/min/1.73m^2], and contraindications to CMR were excluded. For the diabetes cohorts, any other forms of diabetes than patients with type 2 diabetes mellitus were excluded. The safety or feasibility of ^{31}P-MRS has not been assessed in patients with pacemaker or implantable cardioverter defibrillator (ICD), consequently ^{31}P-MRS is not licensed for scanning these cohorts. Therefore, patients with pacemaker or ICD were deemed ineligible for the study.

Anthropometric measurements

Height and weight were recorded, and body mass index (BMI) was calculated. The blood pressure was recorded as an average of 3 measures taken over 10 minutes (DINAMAP-1846-SX, Critikon Corp). 12-lead electrocardiogram (ECG) was recorded. A fasting blood sample was taken for assessments of full blood count, eGFR, lipid profile, HbA1c, insulin, and N-terminal pro hormone B-type natriuretic peptide (NT-proBNP).

^{31}Phosphorus-magnetic resonance spectroscopy

^{31}P-MRS was performed to obtain the PCr/ATP from a voxel placed in the mid-ventricular septum, with subjects lying supine and a ^{31}P transmitter/receiver cardiac coil (Rapid Biomedical GmbH, Rimpar, Germany) placed over the heart, in the iso-center of the magnet on a 3.0 Tesla MR system (Prisma, Siemens, Erlangen, Germany) as previously described[271].

Cardiovascular magnetic resonance

The CMR protocol consisted of cine imaging using a steady state free precession (SSFP) sequence, native pre- and post-contrast T1 mapping, stress and rest perfusion and late gadolinium enhancement imaging.

Native T1 maps were acquired in 3 short-axis slices, including segments with maximal wall thickness, using a breath-held modified look-locker inversion recovery acquisition as previously described[271]. Post-contrast T1 mapping acquisition was performed 15minutes after last contrast injection.

Perfusion imaging used free-breathing, motion-corrected automated in-line perfusion mapping[241]. Adenosine was infused at a rate of 140µg/kg/min, increased to a maximum of 210µg/kg/min according to haemodynamic and symptomatic response (a significant hemodynamic response was defined as >10 beats/min increase in heart rate, or BP drop >10mmHg and >1 adenosine-related symptom e.g., chest tightness, breathlessness)[242]. For perfusion imaging, an intravenous bolus of 0.05mmol/kg gadobutrol (Gadovist, Leverkusen, Germany) was administered at 5ml/s followed by a 20ml saline flush using an injection pump (Medrad MRXperion Injection System, Bayer).

Late gadolinium enhancement imaging was performed using a phase-sensitive inversion recovery sequence in LV short- and long-axis planes >8 minutes after contrast administration[272].

Quantitative analysis

All ^{31}P-MRS analysis was performed off-line blinded to participant details by NJ after completion of the study using software within Matlab version R2012a (Mathworks, Natick, Massachusetts) as previously described[273]. The anonymisation codes were only unlocked once all data analysis was completed.

All CMR image analysis, except for the scar percentage quantification on late gadolinium hyperenhancement imaging, was performed by NJ and scan contours were subsequently reviewed by EL, also blinded to participant details, using cvi42 software (Circle Cardiovascular Imaging, Calgary, Canada). Images for biventricular volumes, function and LV maximal wall thickness were analysed as previously described[274].

Left atrial (LA) volume and ejection fraction (EF) were calculated using the biplane area-length method in the horizontal and vertical long axes as previously described[275]. Strain measurements were performed using cvi42 Tissue Tracking from the short axis images, and the long axis views. Peak circumferential systolic strain, peak early diastolic strain rate and global longitudinal strain (GLS) were measured[276].

Myocardial perfusion image reconstruction and processing was implemented using the Gadgetron software framework[241]. Rest/stress MBF were measured for each of the 16 segments using the AHA classification. T1 maps and ECV were analysed using cvi42 software as previously described[266].

The LV short axis stack of late gadolinium hyperenhancement imaging images was first assessed visually for presence of late gadolinium hyperenhancement, followed by quantification when late gadolinium hyperenhancement was present as previously described(20). Late gadolinium hyperenhancement was defined as areas of signal intensity $\geq$5 standard deviations from normal myocardium and was expressed as the percentage of LV mass, quantified in a blinded fashion.

Statistical analysis

Statistical analysis was performed using GraphPad Prism software (version9.0.0). Categorical data were compared with Pearson's chi-square test. All data were checked for normality using

the Shapiro-Wilks test and presented as mean ±standard deviations, or median (interquartile range) as appropriate. Differences in continuous variables between the cohorts were assessed using 1-way ANOVA with post hoc Bonferroni corrections. Differences in non-parametric variables were assessed using Kruskal-Wallis test. Student t-test was used for comparison of normally distributed datasets and Mann-Whitney U test was used for non-parametric tests where data were obtained for only two groups. P value of ≤0.05 was considered statistically significant.

Prespecified hypotheses were tested on three variables including myocardial PCr/ATP, stress MBF and scar burden on late gadolinium hyperenhancement imaging.

Bi-variate correlations were performed using Pearson's correlation co-efficient for parametric data or Spearman's rank correlation co-efficient for non-parametric data as appropriate.

The correlation analyses were performed to assess the associations between diabetes control (HbA1c) and myocardial energetics (PCr/ATP ratio), and between energetics and perfusion (myocardial perfusion reserve, global rest and stress myocardial blood flows).

These correlation assessments were performed only in the HCM-DM group data. Additionally, these correlation assessments between the scar percentage and the perfusion parameters were performed in the combined data from the two HCM groups not including the healthy volunteer data.

Priori sample size calculations were performed from the data acquired in T2DM patients before the study which suggested to detect a 18% difference in the myocardial energetics (myocardial PCr/ATP ratio in T2DM: 1.74±0.26, controls:2.07±0.35)[179] fourteen participants per group across the 3 cohorts would be needed (with 80% power at α=0.05). These recruitment goals were achieved in the study with 55 participants recruited.

There was only 1 patient in each HCM group with LV outflow tract gradient >30mm Hg at rest. Consequently, results were not adjusted for the presence of LV outflow tract gradient.

4.3 Results

Participant demographics and clinical characteristics:

Demographics, clinical, genetic, and biochemical data are shown in Table-1.

Of the 426 HCM patients screened from the local ICC clinic, 59 (14%) had a diagnosis of concomitant DM (Figure-1). Twenty HCM-DM and 20 age- and sex-matching isolated-HCM patients were prospectively recruited from clinics. Two isolated-HCM patients were found to have previously undiagnosed silent myocardial infarction on CMR imaging and were excluded from the final analysis. In addition, 15 HV completed the study.

Participants across the three groups showed similar ethnicity distribution. The two HCM groups were matched for HCM phenotype (8 apical and 12 asymmetric septal hypertrophy in HCM-DM and 7 apical and 11 asymmetric septal hypertrophy in isolated-HCM). There was no significant difference in European Society of Cardiology (ESC) sudden cardiac death risk score[196] (HCM:2.2±1.5%, HCM-DM:1.9±1.2%; p=NS) and an equal number of participants were confirmed with disease-causing sequence variants in sarcomeric protein genes between the two HCM groups (HCM:33%, HCM-DM:30%; p=NS). Four HCM-DM and 2 isolated-HCM patients had a history of paroxysmal AF and 2 patients in each HCM group had a history of non-sustained ventricular tachycardia on 48-hour ambulatory ECG monitoring. None of the HCM participants had paediatric-onset HCM or had undergone alcohol septal ablation or myectomy. Reflecting the exclusion of participants receiving implantable cardioverter/defibrillators from the study to prevent unlicensed use of ^{31}P-MRS, none of the HCM participants had a previous history of sustained ventricular tachycardia or resuscitated cardiac arrest.

While the majority of isolated-HCM patients described no exertional symptoms (83% NYHA Class-I, 17% Class-II, none Class-III or -IV), 50% of the HCM-DM group were classified as NYHA Class-I, 45% NYHA Class-II and 5% NYHA Class-III based on their symptom status. In symptomatic patients with NYHA Class-II or above, obstructive CAD (>50% of luminal stenosis) was excluded within the last 5 years with invasive coronary angiography in 8 HCM-DM and 5 isolated-HCM patients, and with coronary computed tomographic angiography in 1 HCM-DM patient as part of routine clinical care.

None of the isolated-HCM patients had a history of cerebrovascular events, but 4 HCM-DM patients had this background. HV did not report exertional symptoms.

There were no significant differences in BP or resting heart rate across the groups. The isolated-HCM and HCM-DM groups were matched for hypertension comorbidity. As more participants. in HCM-DM group was receiving a statin treatment, the LDL cholesterol levels were lower in the HCM-DM group compared to HV and isolated-HCM.

There was a stepwise increase in the median NT-proBNP levels in the order of smallest measurements to the greatest respectively (HV:42ng/L[IQR:35-66], HCM:298ng/L[IQR:157-837], HCM-DM:726ng/L[IQR:213-8695]; p<0.0001), with significant increases in both HCM groups compared to the HV groups.

Table 4.1: Clinical characteristics and biochemistry

Variable	**HV** (n=15)	**HCM** (n=18)	**HCM-DM** (n=20)	**P value**
Age, y	60±12	59±10	64±9	0.25
Female, n (%)	5(33)	4(22)	7(35)	0.39
Ethnicity, white, %	10 (67)	12(67)	12 (60)	0.74
Ethnicity, South Asian %	4(27)	5(28)	7(35)	0.67
BMI, kg/m²	25±3¶	29±5	32±6	**0.0003**
Heart rate, bpm	64±11	62±15	69±14	0.11
Systolic BP, mmHg	134±19	123±13	133±18	0.13
Diastolic BP, mmHg	76±8	77±6	76±7	0.91
Creatinine, umol/L	73±10	81±14	77±19	0.23
eGFR, ml/min/1.73m²	83±8	79±9	78±15	0.39
Total cholesterol, mmol/L	5.3±1.1¶	5.3±1.2€	3.8±0.7	**<0.0001**
HDL, mmol/L	1.7±0.4¶	1.5±0.3	1.2±0.2	**<0.0001**
LDL, mmol/L	2.9±0.9¶	3.1±1.1€	1.9±0.6	**0.0005**
TG, mmol/L	1.3±0.6	1.5±0.7	1.6±0.5	0.48
HbA1c, mmol/mol	37±3¶	36±3€	56±7	**<0.0001**
Insulin, pmol/L	35±25¶	53±48€	139±136	**0.001**
NT- proBNP, ng/L	42[35-66]¶†	298[157-837]	725[213-2006]	**<0.0001**
ACEi	-	2(11)	9(45)	**0.01**
ARB	-	2(11)	2(10)	0.91
Beta blocker	-	7(39)	12(60)	0.32
CCB	-	5(28)	8(40)	0.36
Statin	-	4(22)	17(85)	**0.0001**
ASA	-	0(0)	3(17)	0.08
DOAC	-	1(6)	4(20)	0.19
Metformin	-	-	15(75)	0.1
Sulfonylurea	-	-	1(5)	0.29
DPP4i	-	-	3(15)	0.68

GLP-1RA	-	-	1(5)	0.31
SGLT2i	-	-	5(25)	0.08
Genotype +ve	-	6(33)	6(30)	0.83
MYH7	-	4(22)	2(10)	
MYBPC3	-	2(11)	1(5)	
ACTC1	-	0(0)	1(5)	
TNNI3	-	0(0)	1(5)	
Phenotype				
Asymmetric septal hypertrophy	-	11(61)	12(60)	0.94
Apical hypertrophy	-	7(39)	8(40)	0.94
NSVT	-	2(11)	2(10)	0.91
NYHA Class, (%)				
I		15(83)	10(50)	**0.03**
II		3(17)	9(45)	0.06
III		0(0)	1(5)	0.34
IV		0(0)	0(0)	
ESC risk score (%)	-	2.2±1.5	1.9±1.2	0.57
Syncope, n(%)		1(6)	1(5)	0.94
Family history of SCD n(%)		2(11)	1(5)	0.49
Stroke TIA, n(%)	-	0(0)	4(20)	**0.04**
HTN, n(%)	-	6(33)	8(40)	0.3
PAF, n(%)	-	2(11)	4(20)	0.45

€ signifies p<0.05 between HCM-DM and HCM with Bonferroni correction; ¶ signifies p<0.05 between HCM-DM and HV with Bonferroni correction; † signifies p≤0.05 between HCM and HV with Bonferroni correction.
DM indicates type 2 diabetes mellitus; HCM, hypertrophic cardiomyopathy; BMI, Body mass index; bpm, beats per minute; eGFR, estimated glomerular filtration rate; HDL, high density lipoprotein; LDL, low density lipoprotein; TG, triglycerides; ACEI, angiotensin converting enzyme inhibitor; ARB, angiotensin receptor blocker; CCB, calcium channel blocker; ASA, aspirin; DOAC, direct oral anticoagulant; DPP4i, dipeptidyl peptidase-4 inhibitor; GLP-1RA, glucagon-like peptide-1 receptor agonist; SGLT2i, sodium glucose co-transporter-2 inhibitor; MYHY7, myosin heavy chain 7; MYBPC3, myosin binding protein C; ACTC 1, actin alpha cardiac muscle 1; TNNI3, troponin I; NSVT, non-sustained ventricular tachycardia; NYHA, New York Heart Association; ESC, European Society of Cardiology; SCD, sudden cardiac death; TIA, transient ischemic attack; HTN, hypertension; PAF, paroxysmal atrial fibrillation.

Cardiac geometry and function

CMR/^{31}P-MRS results are shown in Table-2.

The HCM groups were comparable in LV volumes, mass and EF, with no significant difference in maximal LV wall thickness between the two groups. As expected, LVEF, LV mass and wall thickness were significantly higher in the HCM groups compared to the HV.

HCM-DM patients showed greater LV concentricity with a higher LV mass over LV end-diastolic volume ratio compared to the HV and HCM groups (supplementary material). Comorbidity with T2DM was associated with greater reductions in GLS (p<0.002), peak systolic circumferential strain (p=0.0005) and diastolic strain rate (p=0.002).

There was no significant difference in LA volumes across the groups, but there was a stepwise decline in LAEF in the order of greatest measurements to the smallest: (HV:62±7%, HCM:45±10%, HCM-DM:34±18%; p<0.0001).

None of the participants with HCM showed a reduction in non-contrast T1 signal or a characteristic pattern of hyperenhancement on LGE suggestive of Anderson-Fabry disease[277,278].

Table 4.2: CMR and 31P-MRS findings

	HV (n=15)	**HCM (**n=18)	**HCM-DM (**n=20)	**P value**
LV end-diastolic volume indexed to BSA, mL/m²	83±18	82±19	76±22	0.08
LV end-systolic volume indexed to BSA, ml/m²	31±7¶	28±15	26±14	**0.02**
LV mass, g	99±27¶†	173±63	187±73	**<0.0001**
LV mass index, g/m²	54±11¶†	90±27	92±40	**<0.0001**
LV mass to LV end-diastolic volume, g/mL	0.65±0.11¶	1.03±0.31	1.24±0.36	**<0.0001**
LV stroke volume, ml	95±23†	118±21	101±22	**0.01**
LV ejection fraction, %	63±4†	70±9	67±9	**0.04**
LV maximal wall thickness, mm	10±1¶†	20±2	21±4	**<0.0001**
RV end-diastolic volume indexed to BSA, mL/m²	86±20¶	79±14€	66±13	**0.001**
RV end-systolic volume indexed to BSA, ml/m²	35±10	30±10	28±13	0.23
RV stroke volume, ml	95±23¶	94±16€	75±21	**0.008**
RV ejection fraction, %	60±6	62±8	58±13	0.42
LA biplane end-systolic volumes, mL	67±17¶†	100±28	113±59	**0.0008**
Biplane LA EF, %	62±7¶†	45±10	34±18	**<0.0001**
Global longitudinal strain, negative (-), %	14±3¶	13±3€	10±4	**0.002**
Peak systolic circumferential strain, (-), %	21±2¶	20±4€	16±4	**0.0005**
Peak circumferential diastolic strain rate, s^{-1}	1.19±0.24¶	0.99±0.21	0.87±0.22	**0.002**

Mean native T1, (ms)	1211±81	1211±65	1209±69	0.99
Extra cellular volume, (%)	25[23-26]¶	27[22-29]€	31[27-43]	**0.006**
LGE scar percentage of LV mass (%)		4±4	10±8	**0.007**
PCr/ATP ratio	2.17±0.49¶	1.93±0.38€	1.54±0.27	**0.002**
Increase in RPP, %	37	33	32	0.3
Stress MBF, ml/min/g	2.06±0.42¶	1.74±0.44€	1.39±0.42	**0.002**
Rest MBF, ml/min/g	0.68±0.03	0.59±0.19	0.69±0.16	0.05
MPR	3.19±0.79¶	3.09±1.06€	2.04±0.82	**0.002**

€ signifies p<0.05 between HCM-DM and HCM with Bonferroni correction; ¶ signifies p<0.05 between HCM-DM and HV with Bonferroni correction; † signifies p≤0.05 between HCM and HV with Bonferroni correction.
Values are mean ±standard deviations or percentages. BSA indicates body surface area; LV, Left ventricle; RV, right ventricle; DM, type 2 diabetes mellitus; HCM, hypertrophic cardiomyopathy; LV, left ventricular; LA, left atrial; LA EF, left atrial ejection fraction; LGE, late gadolinium enhancement; PCr, phosphocreatine; ATP, adenosine tri-phosphate; RPP, rate pressure product; MBF, myocardial blood flow; MPR, myocardial perfusion reserve.

Myocardial energetics

Hypertrophic cardiomyopathy patients with DM comorbidity showed significant reductions in PCr/ATP compared to HV and isolated-HCM (HV:2.17±0.49, HCM: 1.93±0.38, HCM-DM:1.54±0.27; p=0.002). The numeric differences in PCr/ATP between the isolated-HCM and HV were not statistically significant.

Five HCM-DM patients were receiving SGLT2 inhibitors. The myocardial PCr/ATP for the HCM-DM patients receiving SGLT2 inhibitors (1.55, 95% CI, 1.00-1.85) was separately measured.

Myocardial perfusion

Changes in rate pressure product (RPP) from rest to stress, rest and stress MBF and MPR measurements are summarized in Table-2 with representative images from each group in Figure-2. Participants from all groups demonstrated a similar increase in RPP during adenosine stress.

There was again a stepwise decline in stress MBF in the order of the greatest measurements to smallest: [HV:2.06±0.42ml/min/g,HCM:1.74±0.44ml/min/g, HCM-DM:1.39±0.42ml/min/g; p=0.002] with significant reductions in the HCM-DM group compared to the other two groups. The stress MBF was not significantly reduced in the isolated-HCM group compared to the HV.

The rest MBF values were comparable across the groups. Myocardial perfusion reserve (MPR) was also only significantly reduced in the HCM-DM group compared to the other groups.

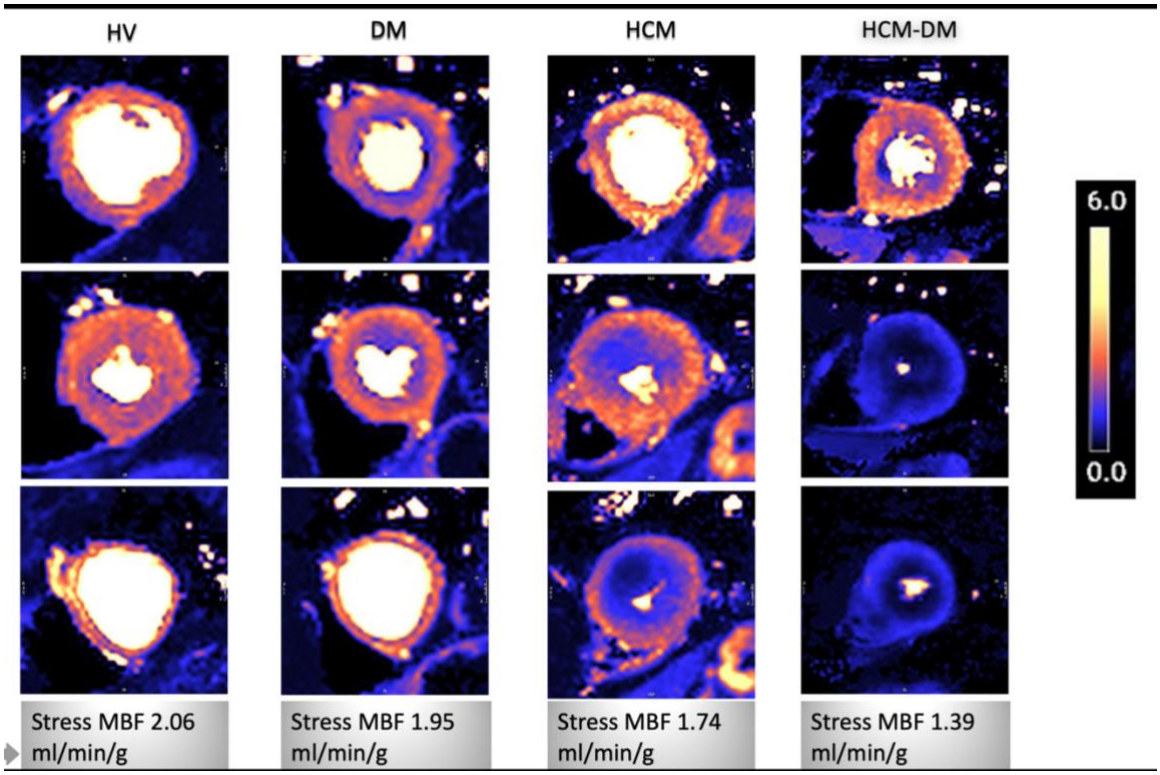

Figure 4.2: Representative examples of mid-left ventricular stress perfusion maps from a healthy volunteer (first column), a patient with HCM (second column) and a patient with HCM-DM (third column).

Myocardial fibrosis and scar burden

Presence of mid-wall hyperenhancement in a non-ischemic pattern was detected in all HCM patients and none of the HV. Two isolated-HCM patients showed evidence of subendocardial hyperenhancement confirming the presence of a silent chronic MI. All their results were excluded from final analysis.

Comorbidity with DM was associated with greater myocardial scar percentage on LGE in HCM patients (HCM:4±4% vs HCM-DM:10±8%, p= 0.002).

While the pre-contrast native T1 map measurements were comparable across the groups, myocardial ECV measurements were significantly higher HCM groups (HV:25%[IQR:23-26], HCM:27%[IQR:22-31], HCM-DM:31%[IQR:27-43]; p=0.006) (Figure 4.3).

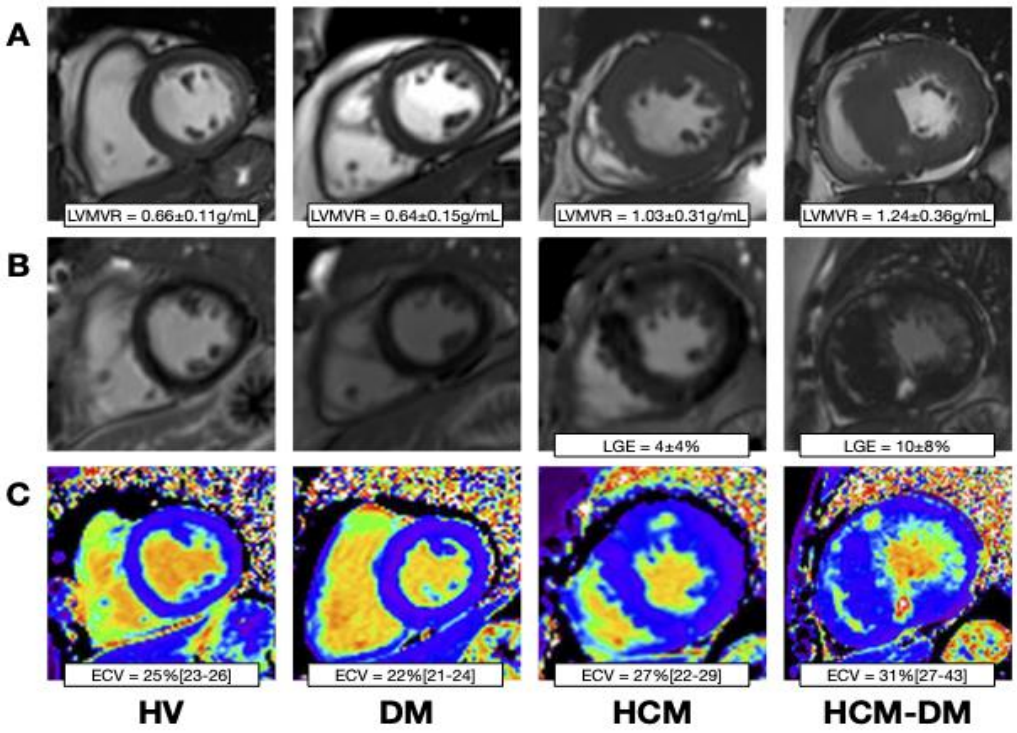

Figure 4.3: Representative examples of structural changes

Representative examples of mid-left ventricular short axis cine imaging (row A with group mean values and standard deviations [SD] provided for the LV mass over LV end-diastolic volume ratios); late gadolinium enhancement imaging (row B, with group mean values and SD provided for the scar percentage of LV mass for the two HCM groups where scar was present); post-contrast native T1 maps (row C, with group mean values and SD provided for the extracellular matrix volume fractions) from a healthy volunteer, a patient with isolated HCM and a patient with HCM-DM.

Comparison of the principal study findings between the HCM patients with and without T2DM

In addition to the myocardial scar percentage comparisons on the LGE, direct comparisons of the principal findings between the two HCM groups were also performed separately. These confirmed significantly higher scar percentage of the LV mass, and significantly lower global longitudinal strain, myocardial PCr/ATP, global stress MBF and MPR in the HCM-DM group compared to isolated HCM group (Figure-4).

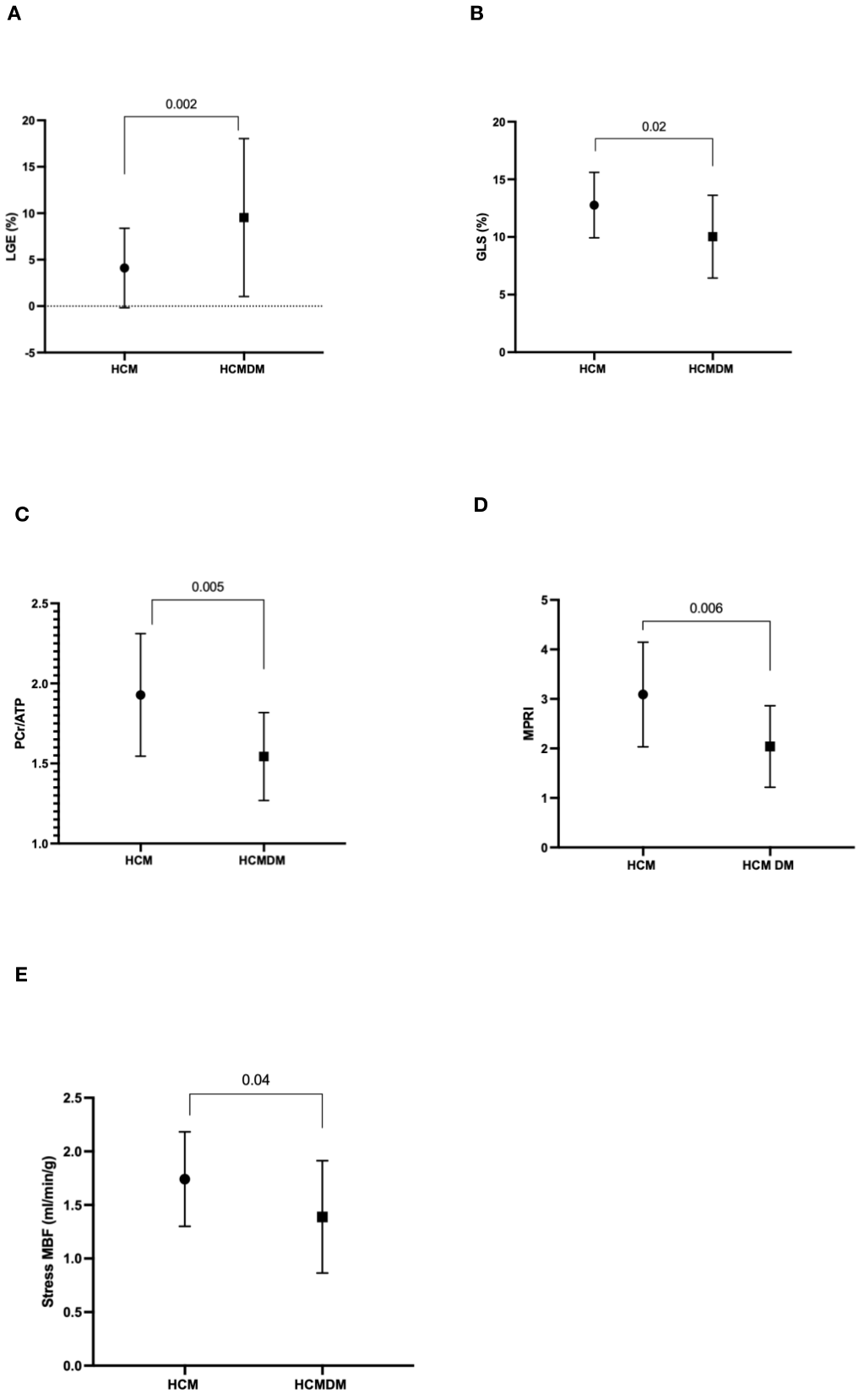

Figure 4.4:Differences in myocardial scar percentage, PCr/ATP ratio, left ventricular global longitudinal strain, myocardial perfusion reserve and global stress myocardial blood flow

and between patients with isolated HCM and patients with HCM and T2DM with group mean values and standard deviations; **(A)** Myocardial scar percentage on late gadolinium enhancement (LGE) scar percentage of left ventricular mass for the two HCM groups where scar was present (%); **(B)** Left ventricular global longitudinal strain (-%); **(C)** Myocardial phosphocreatine to ATP ratio (PCr/ATP); **(D)** Myocardial perfusion reserve; **(E)** Global stress myocardial blood flow (ml/min/g)

Correlations

A correlation between the stress MBF and myocardial scar percentage was detected in the two HCM groups (r=-0.459, p=0.01). There was no significant correlation between the HbA1c and PCr/ATP in the isolated data from the HCM-DM groups (r=-0.4417, p=0.1). There were no significant correlations between the rest or stress MBF and PCr/ATP.

Table 4.3: Linear regression model for dependent variables stress MBF, PCr/ATP and scar burden

LGE	Beta	SE	95% CI lower bound	95% CI upper bound	P value
Constant	15.03	19.50	-25.31	55.36	0.449
Diabetes duration	-0.027	0.060	-0.151	0.096	0.651
HbA1c	-0.196	0.358	-0.937	0.544	0.589
Diabetes	9.570	8.603	-8.227	27.37	0.278
Stress MBF					
Constant	2.516	0.489	1.527	3.505	**<0.0001**
Diabetes duration	-0.008	0.002	-0.004	0.003	0.632
HbA1c	0.005	0.010	-0.016	0.025	0.650
Diabetes	-0.251	0.238	-0.733	0.232	0.299
PCr/ATP					
Constant	2.335	0.388	1.550	3.121	**<0.0001**
Diabetes duration	-0.001	0.001	-0.004	0.002	0.600
HbA1c	0.002	0.008	-0.014	0.017	0.818
Diabetes	-0.436	0.195	-0.829	-0.042	**0.03**

LGE, late gadolinium enhancement; HbA1c, glycated hemoglobin; MBF, myocardial blood flow; PCr/ATP, phosphocreatine to ATP ratio.

4.4 Discussion

Coexistence of T2DM is associated with worsened clinical manifestation of HCM[195,262]. The current study provides insights into this prognostic association by showing adverse cardiac alterations in myocardial energetics, function, perfusion and tissue characteristics in patients with T2DM and HCM comorbidity. It is the first prospective case-control study comparing groups of HCM patients with and without T2DM, carefully matched in HCM phenotype, LV mass, maximal wall thickness, presence of sarcomeric mutations and the ESC sudden cardiac death risk score.

The results of the present study provide several new findings. Firstly, half of the HCM-DM patients described exertional symptoms, were accordingly classified as NYHA Class-II or higher and had significantly increased NT-proBNP levels compared to the isolated-HCM patients, the majority of whom described no exertional symptoms and were NYHA Class-I. Secondly, HCM-DM patients displayed a greater burden of myocardial fibrosis than isolated-HCM patients. Thirdly, reductions in stress MBF and MPR were more pronounced in HCM-DM patients compared to either disease alone. We detected amplified alterations in PCr/ATP in the HCM-DM group compared to the isolated-HCM group. Finally, HCM-DM patients displayed greater reductions in strain parameters and LA function compared to isolated HCM patients. Taken together, while these findings suggest that combined presence of HCM and T2DM may adversely affect the phenotypic expression of HCM, as well as symptom status and plasma biomarkers such as NT-proBNP, our data cannot prove a causal link in line with the cross-sectional observational nature of the study design. The causality of this relationship will need to be investigated in future studies.

This study is limited by a relatively small sample size, in line with its proof-of-principle nature and strict inclusion/exclusion criteria to ensure rigorous matching of the HCM cohorts in HCM phenotype, ESC risk score and presence of sarcomeric mutations. However, using the large dataset of the EURObservational Research Programme (EORP) Cardiomyopathy registry of 1739 patients with HCM, Lopes and colleagues analyzed the relationship between hypertension, T2DM, BMI and clinical traits[279]. They showed the prevalence of hypertension,

DM and obesity was 37%, 10%, and 21%, respectively. In our regional ICC registry prevalence of DM is higher at 14%, broadly in line with the higher T2DM prevalence in the local population of Yorkshire compared the rest of the United Kingdom[280]. In line with our findings, Lopes et al. showed T2DM was associated with higher NYHA class and diastolic dysfunction.

Elevated NT-proBNP concentrations were shown to be a strong predictor of overall prognosis in patients with HCM[281]. A recent retrospective study by Wang and colleagues reporting outcomes of HCM patients with T2DM comorbidity undergoing septal myectomy over a median of 28 year follow-up period[282]. They showed that while HCM patients with and without T2DM have similar 3-year cardiovascular mortality after septal myectomy, there was an association between T2DM comorbidity and the higher sudden cardiac death rate in these patients. While we have excluded patients undergoing septal myectomy in this study, potentially relevant for our findings of higher NTproBNP levels in HCM-DM patients, they showed that NTproBNP was an independent risk factor in their cohort of HCM patients with T2DM comorbidity.

In this study, 33% of the isolated-HCM and 30% of the HCM-DM group were genotype positive for sarcomeric mutations. While early studies from specialist referral centres had suggested that most individuals with HCM (>60%) carried a mutant sarcomere protein, in line with our findings, a large international registry study (Hypertrophic Cardiomyopathy Registry, the HCMR) showed genotype-negative cases to be the majority[193,283]. The participants in the isolated HCM group in this study showed similarities with the HCMR cohort in demographic and clinical characteristics (mean age: 59±10 versus 49±11 years, male participant proportion: 78% versus 71%, ESC risk score: 1.9±1.2 versus 2.48±0.56, maximal wall thickness: 20±2 versus 20.6±4.8mm, LV mass/EDV ratio: 1.03±0.31 versus 1.0 ± 0.3 , scar percentage of the LV mass on LGE: 4±4% versus 3.7±5.2% respectively) suggesting the isolated HCM group in this study can be considered largely representative of the wider HCM population[193].

A previous study had shown higher prevalence of DM comorbidity in patients with an apical HCM phenotype compared to non-apical HCM phenotypes, although the reasons for this are not well understood[221]. Supporting this, the prevalence of apical phenotype was higher in our regional ICC clinic HCM cohort among patients with T2DM comorbidity. However, in this study HCM cohorts were carefully matched in HCM phenotypes to prevent potential biases related to HCM variant differences.

A recent study investigated if genetic variants may contribute to a combined phenotype of HCM and T2DM[284] showing predominant presence of gain-of-function variants in adiponectin

receptor ADIPOR1 in HCM patients with DM comorbidity. ADIPOR1 plays a prominent role in mediating the insulin-sensitizing effects of adiponectin. Of potential significant relevance to our finding of greater reductions in myocardial energetics in patients with concomitant HCM and T2DM the deletion of ADIPOR1 was shown to result in decreased AMP-activated protein activity and the induction of mitochondrial dysfunction[284].

Underscoring the links between early exposure to the diabetic milieu and fetal myocardial structural and functional alterations, elevated neonatal insulin like growth factor 1 levels were shown to be associated with fetal hypertrophic cardiomyopathy phenotype in fetuses of diabetic women[285].

Despite being shown to be predictors of adverse clinical outcomes including arrhythmic events and mortality in HCM[268,286], myocardial fibrosis and reductions in myocardial perfusion are not yet included among the criteria of existing risk scores. We have identified greater reductions in myocardial perfusion and higher scar burden in HCM-DM patients. It was proposed that T2DM associated endothelial inflammation and profibrotic signalling may exacerbate the pathological hypertrophic remodelling in HCM and worsen coronary microvascular function[203,220,223,224]. Our findings of greater reductions in stress MBF and MPR in HCM-DM support this theory. In support of the theory that myocardial ischemia caused by coronary microvascular dysfunction in HCM leads to enhanced scarring[208], we have detected significant correlations between the LGE percentage and the stress MBF measurements in HCM patients.

Although prognostic data related to an impaired energetic state in HCM are lacking, it is believed to hold prognostic relevance in analogy to patients with dilated cardiomyopathy[287]. It has been suggested that the high incidence of exercise-related death in HCM may be explained by a possible further acute impairment of myocardial energetics resulting in ion-pump dysfunction, calcium overload, and ventricular arrhythmias[250]. Supporting this, exacerbation of myocardial energetic compromise has been documented in HCM patients during exercise activity[250]. The correlation analyses were performed to assess the associations between diabetes control (HbA1c) and myocardial energetics (PCr/ATP ratio) only within the HCM-DM group and did not show significance. Larger studies of patients with concomitant diabetes and HCM are needed to assess this relationship.

With regards to comparison of the functional changes, GLS derived from either speckle tracking echocardiography or CMR is a sensitive marker of LV contractile function, especially in the setting of a normal LV EF[288]. A recent meta-analysis of HCM studies showed an

association of abnormal GLS with adverse composite cardiovascular outcomes and ventricular arrythmias[288]. In our study across the four groups HCM-DM patients showed the greatest reductions in GLS. Moreover, while LV circumferential strain is also a sensitive index of regional myocardial function, currently, no studies have assessed its prognostic value in HCM or T2DM populations.

While the prognostic role of changes in LA size is established in HCM patients and increased LA diameter correlates with occurrence of atrial fibrillation in patients with HCM, the prognostic role of LA function has not yet been explored in longitudinal studies. In our study, while the LA size was comparable between the two HCM cohorts, diabetic HCM patients showed significant reductions in LA EF, which may be relevant for future risk of atrial fibrillation occurrence and thromboembolic events. Future studies are needed to explore this.

LIMITATIONS

This study is limited by the small sample size. The ^{31}P-MRS technique is not licensed for scanning patients with a pacemaker or an ICD; therefore, HCM patients with these devices had to be excluded from the study. The mid-septal voxel is the most reproducible cardiac voxel for ^{31}P-MRS[72,289]. Recruiting participants who underwent alcohol septal ablation or septal myectomy could therefore lead to iatrogenic abnormalities in the spectroscopy findings. Therefore, patients who have undergone these procedures had to be excluded from the study. However, the HCM groups were matched for HCM phenotype with similar number of apical or asymmetric septal hypertrophy subgroups.

The study is also limited by the high prevalence of apical HCM which means the results may be affected by selection bias and may not be generalisable to the wider population with HCM. There remain potentially important differences between the HCM and HCM-DM group with respect to age and sex. Due to the small sample size other potentially important differences between groups, for example concomitant medication, cannot be accounted for. The matching of ESC risk score may have introduced additional unexpected confounding.

Obstructive CAD was excluded within the last 5 years as part of routine clinical care in all symptomatic HCM patients who were NYHA II or above. These tests were not repeated for the study to prevent unnecessary ionizing radiation exposure. Therefore, it is possible that occult CAD could be present in the participants.

4.5 Conclusion

Coexistent diabetes is associated with higher NT-proBNP levels, greater reductions in myocardial energetics, perfusion, contractile function, and left atrial function, and higher scar burden in patients with hypertrophic cardiomyopathy. These adverse phenotypic features may be important components of the adverse clinical manifestation attributable to a combined presence of hypertrophic cardiomyopathy and type 2 diabetes mellitus.

Chapter 5

Coexistent diabetes is associated with residual myocardial abnormalities after aortic valve replacement in patients with severe aortic stenosis

5.1 Abstract

Background:

Coexistent aortic stenosis (AS) and type 2 diabetes mellitus (T2DM) are associated with increased cardiovascular morbidity and mortality after aortic valve replacement (AVR). AS and T2DM share common cardiac features of altered energy metabolism and reduction in stress perfusion indices. Cardiac phosphocreatine to ATP ratio (PCr/ATP) is a sensitive index of energetic status defined by phosphorus-magnetic resonance spectroscopy (^{31}P-MRS). Perfusion indices rest and stress global myocardial blood flow (MBF) can be defined by cardiovascular magnetic resonance imaging (CMR). Using ^{31}P-MRS and CMR, we defined myocardial alterations pre-AVR and their recovery post-AVR in patients with severe AS with and without T2DM.

Methods:

Ninety-five consecutive patients with severe AS awaiting AVR, with (n=30) and without (n=65) T2DM, participated in a single-center prospective cohort study. Significant obstructive coronary artery disease (CAD) was excluded by coronary angiography in patients with AS. Thirty healthy volunteers and 30 T2DM patients were controls. Patients with known CAD, left ventricular (LV) ejection fraction <50%, kidney dysfunction, chronic lung disease, significant bystander valve disease, hypertrophic cardiomyopathy and infiltrative diseases were excluded.

Within 1-month before and 6-months post-AVR, we defined: cardiac PCr/ATP by ^{31}P-MRS; rest and adenosine stress MBF, left ventricular (LV) volumes, mass, ejection fraction, peak diastolic strain rate (PDSR), global longitudinal strain (GLS) and myocardial scar on late-gadolinium enhancement imaging by CMR; 6-minute walk distance.

Results:

For the two AS groups, there were no significant differences in demographics or in LV volumes, mass, ejection fraction and scar burden before or after AVR. Both AS groups showed significantly lower cardiac PCr/ATP and stress MBF than healthy volunteers, but not compared to T2DM controls.

Pre-AVR cardiac PCr/ATP, global stress MBF and PDSR assessments were significantly lower in patients with AS and T2DM than patients with AS without T2DM. Post-AVR, patients with

AS without T2DM showed significant improvements in cardiac PCr/ATP, stress MBF, GLS and 6-minute walk distance, whereas those with AS and T2DM did not.

Conclusions:

Severe AS-associated abnormalities in myocardial PCr/ATP and stress MBF are exacerbated by T2DM comorbidity. AVR reverses myocardial abnormalities and limitations in exercise capacity in patients with severe AS alone, but this recovery is undermined by T2DM comorbidity.

5.2 Introduction

Aortic stenosis (AS) is the most frequent degenerative valvular heart disease in the developed world[290-292]. With an ageing population in most societies, the burden of AS on health systems is expected to continue to increase[293]. In parallel, driven by the obesity epidemic, the prevalence of type 2 diabetes (T2DM) is increasing across all age groups. AS and T2DM are therefore increasingly frequent comorbidities[166] with 22 to 36% of severe symptomatic AS patients having coexisting T2DM[167-173,174]. The comorbidity with T2DM influences the prognosis of AS with increased morbidity and mortality following aortic valve replacement (AVR) even after adjustment for comorbidities such as vascular disease or renal dysfunction[130,175-178]. Although distinct pathological entities, AS and T2DM share common features of altered myocardial energy metabolism, left ventricular concentric remodeling and coronary microvascular dysfunction[75,170,179,180]. The mechanism underlying the poor prognosis of patients with AS and T2DM comorbidity are incompletely understood. One potential explanation is the collective impact of the two conditions on cardiac metabolism, structure and perfusion.

Compromised cardiac energy production is an important contributor to most forms of heart disease including T2DM[249,294]. The relative concentration of phosphocreatine to ATP (PCr/ATP) is a sensitive indicator of the energetic state of the myocardium and can be assessed non-invasively using ^{31}phosphorus magnetic resonance spectroscopy (^{31}P-MRS)[246]. Using ^{31}P-MRS, reductions in myocardial energetics has also been demonstrated in patients with severe AS prior to AVR which then reverse upon relief of pressure overload and reverse re-modelling 6 months after AVR[252].

Cardiovascular magnetic resonance imaging (CMR) is the reference standard for the assessment of the cardiac alterations in AS including left ventricular volume, mass, function and perfusion changes[75,167,170]. In addition, there is a growing evidence base to indicate tissue characterization using CMR provides prognostic information, both in asymptomatic AS patients and those undergoing intervention[167,172,295]. With CMR extracellular volume (ECV)-based measures utilize extracellular gadolinium-based contrast agents to calculate the relative (extracellular volume fraction [ECV%]) or absolute (indexed extracellular volume [iECV]) ECV of the myocardium[296].

In this study, using ^{31}P-MRS and CMR we aimed to better understand the combined impact of severe AS and T2DM on the heart in patients undergoing AVR (either by surgical or

transcatheter approach) for severe symptomatic AS and how these myocardial alterations change following AVR. Advanced CMR assessments were supported by 6 minute walk tests, and clinical outcome analysis. Our hypothesis was that the comorbid disease burden associated with T2DM would attenuate myocardial recovery after AVR in patients with AS.

5.3 Methods

Study Design and Oversight

This single-centre, longitudinal prospective cohort study complied with the Declaration of Helsinki and was approved by the National Research Ethics Committee (Ref:18/YH/0168). The study was co-funded by the Wellcome Trust (Grant 207726/Z/17/Z) and Diabetes UK (18/0005870).

Participants

Adult patients with severe AS who had been referred for surgical or transcatheter AVR were eligible for inclusion. The diagnosis of severe AS was based on peak aortic forward flow velocity of greater than 4m/s on valve clinic echocardiography according to current cardiovascular society guidelines[292,297]. Ninety-five participants, 65 with severe AS in isolation and 30 with combined severe AS and T2DM awaiting AVR were prospectively recruited. Data collection was completed between April 2019 and April 2022. Patients with AS and T2DM had an established T2DM diagnosis according to World Health Organization criteria and they were free of known diabetes complications[298]. Fifteen normal body weight and 15 overweight healthy volunteers were recruited to serve as healthy control cohorts. As control cohorts for T2DM alone, with no concomitant AS, 15 normal weight and 15 overweight T2DM patients with no known cardiovascular disease were recruited. All participants for all study cohorts provided written informed consent.

Potentially suitable patients with severe AS were pre-screened from AVR waiting lists (by surgical or transcatheter approach) at the Leeds Teaching Hospitals NHS Trust, United Kingdom. These surgical and transcatheter AVR lists were reviewed once weekly for new additions. Hospital electronic health care records were screened to assess potential eligibility.

Potentially eligible patients with AS were invited for a research visit by postal mail (Figure-1, CONSORT diagram).

T2DM controls and non-diabetic controls were contemporary participants and were recruited from primary care general practices in Yorkshire, United Kingdom. Electronic health care records were screened to assess potential eligibility by primary care physicians. Potentially eligible T2DM controls and healthy controls were then sent study information by postal mail and invited to contact research investigators to discuss study participation.

Patients with AS underwent ^{31}P-MRS and CMR within 1-month prior to AVR. The surviving participants were then invited for a repeat scan 6-months post-AVR. Patients were followed for a median of 13-months post-AVR for clinical outcomes via hospital electronic health care records. T2DM controls underwent identical assessment at baseline and 6-months later; normal-weight and overweight healthy controls were assessed once.

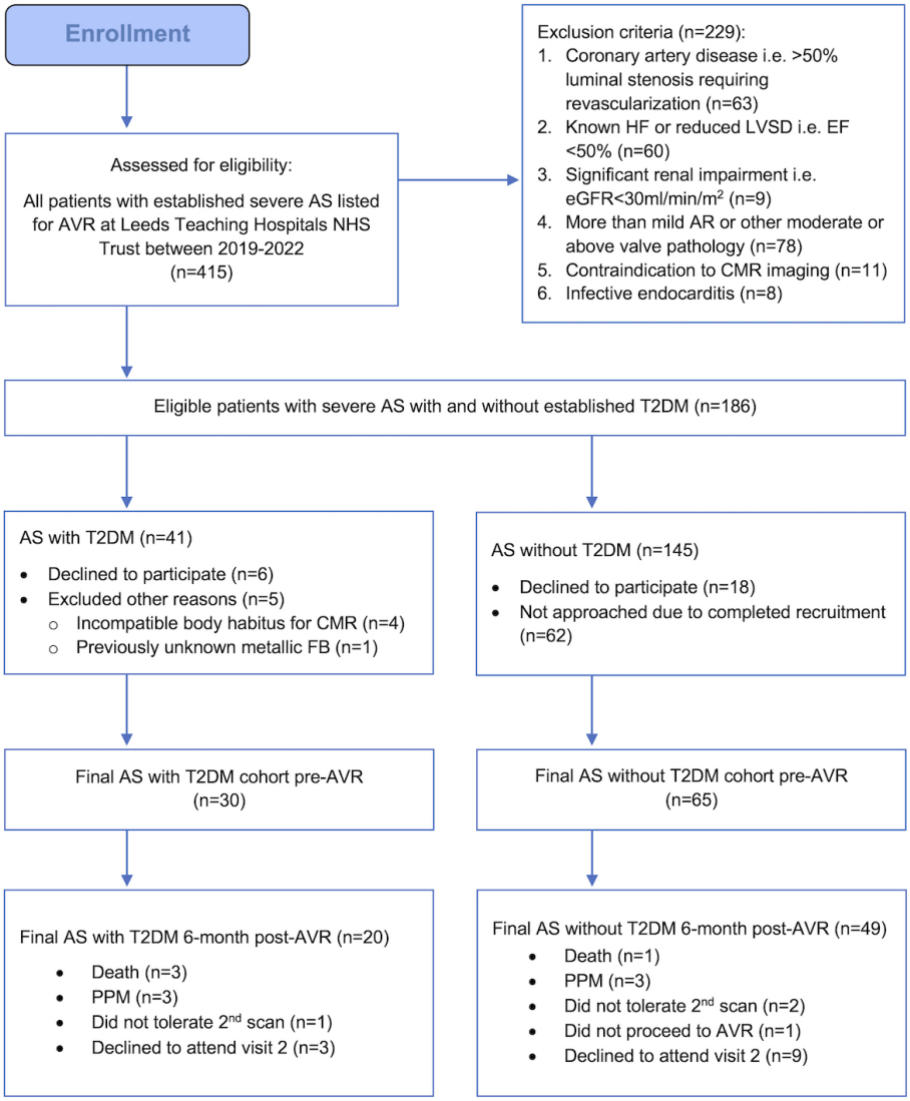

Figure 5.1: Consort diagram

Exclusion criteria

Participants were excluded if they had known previous myocardial infarction, previous CABG, angioplasty, flow-limiting coronary artery disease (CAD), chronic obstructive lung disease, asthma, tobacco smoking, more than mild bystander valve disease, significant kidney dysfunction [estimated glomerular filtration rate (eGFR)<30mL/min/1.73m^2], permanent atrial fibrillation, known heart failure or reduced left ventricular ejection fraction (<50%), cardiomyopathy (based on infiltrative diseases [e.g., amyloidosis], accumulation diseases [e.g., haemochromatosis, Fabry disease], hypertrophic cardiomyopathy), or any

contraindication to CMR scanning. As the research protocol included a 6-minute walk test, potential participants with mechanical or permanent mobility issues were also excluded. All patients listed for AVR had flow-limiting CAD excluded by invasive angiography and prior myocardial infarction excluded by late gadolinium enhancement imaging.
Exclusion criteria for T2DM controls and healthy controls were known CAD, cardiac surgery, tobacco smoking, amyloidosis, permanent atrial fibrillation, more than mild valvular heart disease, kidney dysfunction (eGFR]<30mL/min/1.73m^2), and contraindications to CMR.

Anthropometric measurements

Height and weight were recorded, and body mass index (BMI) was calculated. The blood pressure was recorded whilst seated over 10-minutes. A 12-lead electrocardiogram was recorded. A fasting blood sample was taken for assessments of full blood count, eGFR, lipid profile, glycated hemoglobin (HbA1c), insulin, free fatty acid, beta hydroxybutyrate, and N-terminal pro hormone B-type natriuretic peptide (NT-proBNP).

^{31}Phosphorus-magnetic resonance spectroscopy

^{31}P-MRS was performed to assess myocardial energetics status from a voxel placed in the mid-ventricular septum, with subjects lying supine and a ^{31}P transmitter/receiver cardiac coil (Rapid Biomedical GmbH, Rimpar, Germany) placed over the heart on a 3.0 Tesla MR system (Prisma, Siemens, Erlangen, Germany) as previously described[39]. ^{31}P-MRS is not licensed for scanning patients with a pacemaker, consequently patients who required a pacemaker implantation post-AVR underwent repeat CMR but not repeat ^{31}P-MRS.

Cardiovascular magnetic resonance

The CMR protocol consisted of cine imaging using a steady state free precession sequence, native pre- and post-contrast T1 mapping, stress and rest perfusion and late gadolinium enhancement imaging.
Native T1 maps were acquired in 3 short-axis slices, using a breath-held modified look-locker inversion recovery acquisition as previously described[299]. Post-contrast T1 mapping was performed using the same approach 15-minutes after last contrast injection.

Perfusion imaging used free-breathing, motion-corrected automated in-line perfusion mapping. Adenosine was infused at a rate of 140μg/kg/min, for a minimum of 3 minutes according to hemodynamic and symptomatic response as previously described[299]. Two trained cardiologists with advanced life support training monitored the patients during adenosine stress imaging.

Late gadolinium enhancement was performed using a phase-sensitive inversion recovery sequence >8-minutes after contrast administration.

Additional ^{31}P-MRS and CMR quantitative analyses methodology details appear in supplementary material.

Quantitative analysis of ^{31}P-MRS and CMR data

All ^{31}P-MRS analysis was performed off-line blinded to participant details by NJ using software within Matlab version R2012a (Mathworks, Natick, Massachusetts) as previously described[39]. The anonymisation codes were only unlocked once all data analysis was completed[39].

All CMR image analysis was performed by NJ and scan contours were subsequently reviewed by EL, also blinded to participant details, using cvi42 software (Circle Cardiovascular Imaging, Calgary, Canada). Images for biventricular volumes, function and LV maximal wall thickness were analysed as previously described[39].

Left atrial (LA) volume and ejection fraction (EF) were calculated using the biplane area-length method in the horizontal and vertical long axes as previously described[276]. Strain measurements were performed using cvi42 Tissue Tracking from the short axis images, and the long axis views. Peak early diastolic strain rate was measured[276].

Myocardial perfusion image reconstruction and processing was implemented using the Gadgetron software framework[241]. Rest/stress MBF were measured for each of the 16 segments using the AHA classification. T1 maps and ECV were analysed using cvi42 software as previously described[39]. Indexed ECV [iECV] Extracellular volume (ECV)-based measures utilize extracellular gadolinium-based contrast agents to calculate the relative (extracellular volume fraction [ECV%]) or absolute (indexed extracellular volume [iECV]) ECV of the myocardium[296].

The LV short axis stack of late gadolinium hyperenhancement imaging images was first assessed visually for presence of late gadolinium hyperenhancement, followed by quantification when late gadolinium hyperenhancement was present as previously

described(20). Late gadolinium hyperenhancement was defined as areas of signal intensity ≥5 standard deviations from normal myocardium and was expressed as the percentage of LV mass, quantified in a blinded fashion.

Six-minute walk test

The participants were instructed to walk along a 30-meter corridor and cover the maximum achievable distance in 6-minutes under the supervision of study investigators with medical training and with experience in conducting the test[300]. At the end of 6-minutes, participants were asked to stop, and the distance walked was measured in meters.

Surgical risk scores and frailty scores

Both Euro Score II and the Society of Thoracic Surgeons risk scores were recorded[301]. As validated measures of frailty and comorbidity, both the Rockwood Frailty Score and the Charlson comorbidity index were recorded[302].

Clinical outcomes

The study was not designed to assess the clinical outcome differences between the AS patients with and without T2DM, nevertheless patients were followed for a median of 13-months post-AVR for clinical outcomes via Leeds Teaching Hospitals electronic health care records. Clinical event rate of cardiovascular mortality after AVR, and separately event rates for composite of all-cause mortality, myocardial infarction, infective endocarditis, and heart failure hospitalization were assessed. For the composite clinical event outcomes all time-to-event analyses were based on the first relevant unrefuted event: that is, an event of a particular type included in the analysis if it has been confirmed on the health care notes.

Sample size

A priori sample size calculation was performed based on the pilot data of myocardial energetics and stress myocardial blood flow (MBF) obtained from 10 severe AS patients (5 with and 5 without T2DM). This showed mean PCr/ATP in the group with T2DM comorbidity 1.33±0.25 versus 1.71±0.28 in the isolated AS group. Assuming two-tailed paired t-test analysis (α=0.05 and β=0.90), calculations suggested that 9 patients in each group would be needed. A second a priori sample size calculation was performed for comparisons of stress MBF between the two groups (T2DM comorbidity: 1.28±0.66 versus isolated AS: 1.89±0.68ml/min/g). Based on this pilot data assuming two-tailed paired t-test analysis (α=0.05 and β=0.90), calculations suggested that 25 patients in each group would be needed. A third priori sample size calculation was performed to detect a modest 13% improvement in PCr/ATP ratio in the AS patients with T2DM after AVR. Based on pilot data assuming two-tailed paired t-test analysis (α=0.05 and β=0.8), 11 AS patients with T2DM would be needed to complete the study. These targets were exceeded in our study.

Statistical analysis

Statistical analysis was performed using GraphPad Prism software (version 9.0.0). All data were checked for normality using the Shapiro-Wilks test and presented as mean or median with 95% confidence intervals as appropriate. Categorical data are presented as numbers and percentages and compared with Pearson's chi-square test. Comparisons between the 3 groups were performed by 1-way ANOVA with post hoc Bonferroni corrections. Differences in non-parametric variables were assessed using a Kruskal-Wallis test. Student t-test was used for comparison of normally distributed datasets and Mann-Whitney U test was used for non-parametric tests where data were obtained for only two groups. Comparisons between pre- and post-AVR measurements in patients with AS were performed with ANOVA with post hoc Bonferroni corrections. $P \leq 0.05$ was used as a threshold of significance.

A 2-sided log-rank test was used to calculate average event rate ratios and confidence intervals over a median period of 13-months. Kaplan-Meier plots were constructed for time-to-event analyses.

5.4 Results

Participant demographics and clinical characteristics:

Demographics, clinical, and biochemical data at baseline are shown in Table-1.
Between May 2019, and April 2022, 95 participants with severe AS (30 with and 65 without T2DM comorbidity) and 15 healthy controls were recruited.

Baseline

Age and sex distributions were comparable between the groups (Table-1).
The median surgical risk scores were similar between the AS patients with and without T2DM and patients were matched in AS severity. While frailty scores were similar, the Charlson index was higher in T2DM comorbidity group. Between the two AS groups, blood pressure measurements and heart rates were similar, but the BMI was higher in the T2DM comorbidity group in line with expectations. Resting heart rates were higher in both AS groups than healthy controls.
AS patients with T2DM were receiving statin treatment at higher rates and reflecting this, they showed lower total and LDL cholesterol levels. The fasting glucose, HbA1c and circulating ketone levels were higher in AS patients with T2DM. While none of the AS patients were in the anemic range, the haemoglobin levels were lower in AS patients with T2DM.
Pre-operative 6-minute walk distance and plasma NT-proBNP levels did not differ significantly between the AS groups.

Table 5.1: Clinical Characteristics and biochemistry

Variable	Healthy Volunteers n=15	Aortic stenosis without T2DM n=65	Aortic stenosis with T2DM n=30	P value
Age, y	71(69,74)	71(69,74)	70(67,74)	0.93
Female, n (%)	5(33)	27(42)	8(27)	0.14
BMI, kg/m²	26(24,27)*	27(26,28)€	31(29,33)	**<0.0001**
Heart rate, bpm	62(56,67)†	72(69,75)	69(63,74)	**0.01**
Systolic BP, mmHg	136(129,143)	132(128,137)	131(123,139)	0.44
Diastolic BP, mmHg	76(73,79)	77(75,79)	73(70,77)	0.14
Creatinine, umol/L	73(70,77)	77(73,81)	81(74,87)	0.22
Haemoglobin, g/L	149(145,152)*	143(139,147)	136(131,142)	**0.004**
Haematocrit, L/L	0.45(0.44,0.47)*	0.44(0.43,0.46)	0.42(0.41,0.43)	**0.008**
Total cholesterol, mmol/L	5.3(4.8,5.7)*	5.6(4.4,6.7)€	4.2(3.9,4.6)	**0.001**
HDL, mmol/L	1.7(1.6,1.9)*	1.6(1.5,1.7)€	1.3(1.1,1.4)	**0.0002**
LDL, mmol/L	2.9(2.6,3.3)*	2.9(2.6,3.2)€	2.2(1.9,2.5)	**0.007**
TG, mmol/L	1.3(1.0,1.5)	1.4(1.2,1.5)	1.9(1.4,2.4)	0.1
HbA1c, mmol/mol	37(36,39)*	38(37,38)€	56(50,61)	**<0.0001**
Glucose, mmol/L	5(4,5)*	5(4,5)€	8(7,10)	**<0.0001**
Insulin, pmol/L	29[15-58]*	38[24-65]€	86[47-145]	**0.0002**
HOMA IR, Molar Units	0.79[0.41-1.39]*	1.31[0.6-2.17]€	3.28[1.77-6.16]	**0.0003**
FFA, mmol/L	0.48(0.44,0.51)	0.53(0.46,0.6)	0.51(0.42,0.59)	0.84
D-3-Hydroxybutyrate, mmol/L	-	0.14(0.09,0.18)	0.17(0.10,0.24)	**0.02**
NT- proBNP, ng/L	42[35-66] *	377[181-2039]†	404[201-1019]	**<0.0001**
Medications				
ACEi	-	5(8)	13(43)	**0.0001**
ARB	-	11(17)	3(11)	0.46
Beta blocker	-	17(27)	14(46)	0.09
CCB	-	16(25)	11(36)	0.15
Loop diuretic	-	10(16)	10(33)	0.28
Statin	-	26(41)	25(83)	**0.0001**
ASA	-	18(28)	11(37)	0.5
DOAC	-	12(19)	3(10)	0.14
Metformin	-	-	16(59)	-
Sulfonylurea	-	-	6(22)	-
DPP4i	-	-	3(15)	-
GLP-1RA	-	-	0(0)	-
SGLT2i	-	-	3(11)	-
AS Clinical Details				
TTE Vmax, m/s	-	4.5(4.4,4.7)	4.5(4.3,4.7)	0.95
Duration severe AS, (months)	-	8(7,10)	10(6,14)	0.5
Bicuspid AV, n (%)		17(27)	4(13)	0.2
STS Score		0.88[0.66-1.35]	0.97[0.7-1.2]	0.8
Euro Score II	-	0.89[0.72-1.22]	1.03[0.7-1.3]	0.24
Rockwood Score	-	2.1(1.9,2.4)	2.2(2.0,2.3)	0.81
Charlson Comorbidity Index		3.7(3.4,4.0)	4.5(4.1,4.9)	**0.002**
NYHA Class, (%)				
I		10(16)	4(13)	0.92
II		41(64)	18(60)	0.67
III		10(16)	8(27)	0.06
IV		0(0)	0(0)	-
6 min walk test, m	-	396(365,436)	360(306,415)	0.14
Cardiovascular Past Medical History				
Stroke TIA, n(%)	-	4(6)	2(1)	0.90
PAF, n(%)	-	7(11)	3(10)	0.70
Hyperlipidemia, n (%)	-	17(27)	12(40)	0.75

€ signifies p<0.05 between Aortic Stenosis patients with and without type 2 diabetes mellitus,

* signifies p<0.05 between T2DM and AS group and HV, † signifies p≤0.05 between Iso-AS and HV.

AV indicates aortic valve; AS, aortic stenosis; T2DM, type 2 diabetes mellitus; BMI, body mass index; bpm, beats per minute; HDL, high density lipoprotein; LDL, low density lipoprotein; TG, triglycerides; FFA, free fatty acids; ACEI, angiotensin converting enzyme inhibitor; ARB, angiotensin receptor blocker; CCB, calcium channel blocker; ASA, aspirin; DOAC, direct oral anticoagulant; DPP4i, dipeptidyl peptidase-4 inhibitor; GLP-1RA, glucagon-like peptide-1 receptor agonist; SGLT2i, sodium glucose co-transporter-2 inhibitor; V max, peak aortic forward flow velocity; TTE, trans-thoracic echocardiogram; CMR, cardiac magnetic resonance; TIA, transient ischemic attack; HTN, hypertension; PAF, paroxysmal atrial fibrillation;

6months after AVR

At 6-months post-AVR AS patients without T2DM demonstrated improved physical performance after AVR with a longer 6-minute walk distance compared to baseline (396(365,436) to 434(398,472) m, p=0.02). An improvement in exercise tolerance was not observed in AS patients with T2DM (360(306,415) to 331(267,393) m, p=0.45).

Similarly, at 6-months post-AVR AS patients without T2DM displayed a statistically significant reduction in plasma NT-proBNP levels (377(181-2039) to 302(210-652) ng/L, p=0.04). Despite numerical reduction in median NT-proBNP level, this change in T2DM comorbidity group did not reach statistical significance (404(221-1019) to 333(121-809) ng/L, p=0.76) (Table-5.3).

Cardiac geometry and function

Baseline

Baseline CMR results are shown in Table-2.

At baseline all groups were comparable in terms of LV volumes, stroke volume index and ejection fraction. Diastolic function measured by peak longitudinal diastolic strain rate was significantly reduced in AS patients with T2DM compared to AS patients without T2DM (Figure-3A). There was no significant reduction in peak longitudinal diastolic strain rate in AS patients without T2DM compared to healthy controls pre-AVR.

The LV wall thickness, mass, and concentricity index (LV mass: LV end diastolic volume ratio) were all higher in both AS groups compared to the healthy controls. There was no difference in LV mass, mass index or wall thickness between AS patients with and without T2DM (Table-2).

The RV ejection fraction was reduced in both AS groups compared to healthy controls.

Table 5.2: Baseline CMR and 31P-MRS findings

	Healthy Volunteers n=15	Aortic stenosis without T2DM n=65	Aortic stenosis with T2DM n=30	*P value	**P value
LV end-diastolic volume indexed to BSA, mL/m²	78(69,87)	80(74,86)	92(80,105)	0.14	0.17
LV end-systolic volume indexed to BSA, ml/m²	28(24,31)	32(26,37)	34(27,41)	0.28	0.34
LV mass, g	102(87,117)*	146(136,157)†	170(148,193)	**0.0001**	0.44
LV mass index, g/m²	55(47,62)	76(71,80)	80(72,89)	**0.0003**	**0.99**
LV mass to LV end-diastolic volume, g/mL	0.66(0.58,0.73)*	0.99(0.92,1.05)†	0.98(0.89,1.1)	**<0.0001**	0.99
LV stroke volume, ml	95(82,109)	94(89,100)	103(95,111)	0.18	0.22
Svi, ml/m²	52(48,54)	49(47,51)	50(46,53)	0.78	
LV ejection fraction, %	65(63,66)	64(61,67)	61(57,65)	0.41	0.31
LV maximal wall thickness, mm	10(9,11)*	14(13,14)†	14(13,15)	**<0.0001**	0.99
RV end-diastolic volume indexed to BSA, mL/m²	83(76,90)	79(74,84)	78(71,85)	0.41	0.99
RV end-systolic volume indexed to BSA, ml/m²	32(28,37)	37(33,40)	36(30,42)	0.62	0.99
RV stroke volume, ml	97(86,107)†	82(77,87)	86(78,95)	**0.02**	0.83
RV ejection fraction, %	62(58,65)*	55(52,57)†	55(51,59)	**0.04**	0.99
LA biplane end-systolic volumes, mL	72(60,85)	95(81,108)	101(85,118)	0.13	0.99
Biplane LA EF, %	59(51,66)*	45(41,50)	40(33,46)	**0.004**	0.26
Peak longitudinal diastolic strain rate, s^{-1}	0.79(0.68,0.9)	0.83(0.74,0.92)	0.66(0.57,0.75)	**0.01**	**0.01**
Mean native T1, (ms)	1209(1163,1255)	1231(1209,1254)	1260(1231,1289)	0.13	0.38
Extra cellular volume, (%)	25(24,26)	26(25,27)	27(25,29)	0.14	0.35
Indexed extra cellular volume, ml/m²	13.9(11.1,16.6) *	17.9(16.4,19.4)	19.2(16,22)	**0.03**	0.99
LGE, (%)	-	3.2(2.5,3.9)	3.8(2.6,5)	-	0.34
PCr/ATP ratio	2.17(1.87,2.46)*	1.74(1.62,1.86)†	1.44(1.32,1.56)	**<0.0001**	**0.002**
Increase in RPP, %	25(17,30)	23(17,28)	25(17,32)	0.59	0.61
Stress MBF, ml/min/g	2.14(1.69,2.58)*	1.67(1.5,1.84)	1.25(1.22,1.38)	**<0.0001**	**0.001**
Rest MBF, ml/min/g	0.67(0.58,0.73)	0.73(0.68,0.78)	0.68(0.59,0.75)	0.35	0.93
MPR	3.8(2.3,5.3)*	2.4(2.2,2.7)†	1.8(1.6,2.0)	**<0.0001**	**0.02**

*P signifies ANOVA comparisons across the 3 study groups, **P signifies comparisons between severe aortic stenosis patients with and without type 2 diabetes mellitus with Bonferroni corrections

* signifies p<0.05 between aortic stenosis and type 2 diabetes mellitus group and healthy volunteers; † signifies p≤0.05 between isolated aortic stenosis patients and healthy volunteers.

Values are means with 95% confidence intervals or percentages.

BSA indicates body surface area; LV, Left ventricle; RV, right ventricle; LV, left ventricular; LA, left atrial; LA EF, left atrial ejection fraction; PCr, phosphocreatine; ATP, adenosine tri-phosphate; RPP, rate pressure product; Svi, stroke volume indexed to body surface area; MBF, myocardial blood flow; MPR, myocardial perfusion reserve.

Six months after AVR

Six months after AVR, both AS groups displayed significant reductions in LV end diastolic volumes. Peak diastolic strain rate showed no improvements after AVR in AS patients with T2DM (Figure-3A).

While no significant reduction in maximal LV wall thickness was detected in either AS group, there was an overall significant regression in LV mass after AVR in AS patients without T2DM (146(136,157) to 125(115,135) g, p=0.001) and in LV mass index (76(71,80) to 61(56,67) g/m^2, p=0.002).

The numeric reductions in LV mass after AVR did not reach statistical significance in AS patients with T2DM comorbidity (170(148,193) to 138(117,158) g, p=0.44), or in LV mass index (80(72,89) to 67(59,74) g/m^2, p=0.19) (Table-3).

Myocardial fibrosis and scar burden

Baseline

Comparing AS patients with and without T2DM, there was no significant difference in native T1 mapping, extra-cellular volume (ECV) fraction measurements, the indexed-ECV (total ECV of the myocardium indexed to body surface area) or in myocardial scar burden on LGE suggesting no detectable differences in CMR markers of myocardial fibrosis.

Six months after AVR

Neither AS group demonstrated a significant change in ECV fraction, indexed-ECV or myocardial scar burden. Following AVR there was a statistically significant reduction in native pre-contrast T1 mapping measurements in AS patients without T2DM (1231(1209,1254) to 1198(1172,1224) ms, p<0.0001). A trend in the same direction was observed in AS patients with T2DM comorbidity native pre-contrast T1 mapping measurements (1260(1231,1289) to 1207(1148,1266) ms, p=0.05) (Table-3).

Myocardial energetics

Baseline

Baseline ^{31}P-MRS results are shown in Table-2.

There was a stepwise decline in PCr/ATP ratio with the highest values in the healthy controls and the smallest in AS patients with T2DM (Healthy controls: 2.17(1.87,2.46) versus AS patients without T2DM:1.74(1.62,1.86) versus AS patients with T2DM:1.44(1.32,1.56), p<0.0001). While both AS groups demonstrated significantly lower values compared to healthy controls, the difference in energetics between the two AS groups was also statistically significant (Figure-3B).

Six months after AVR

While the AS patients without T2DM showed significant improvements in myocardial energetics post-AVR (1.74(1.62,1.86) to 2.11(1.79,2.43), p=0.0014), AS patients with T2DM comorbidity showed no improvements (1.44(1.32,1.56) to 1.30(1.07,1.53), p=0.47) (Table-3). (Figure-3B).

Myocardial perfusion

Baseline

Changes in rate pressure product (RPP) from rest to stress, rest and stress MBF and myocardial perfusion reserve (MPR) measurements are summarized in Table-2. Participants from all groups demonstrated a similar increase in RPP during adenosine stress.

Rest MBF values were comparable across the groups. However, in a similar pattern to energetics, there was a stepwise decline in global stress MBF with the highest values in the healthy controls and the lowest in AS patients with T2DM (Healthy controls: 2.14(1.69,2.58) versus AS patients without T2DM: 1.67(1.5,1.84) versus AS patients with T2DM: 1.25(1.22,1.38), p<0.0001). While both AS groups demonstrated significant reductions compared to healthy controls, the difference in stress MBF between the two AS groups was also significant (Figure-3C). MPR was significantly reduced in AS group with T2DM compared to the AS patients without T2DM and the healthy controls.

Six months after AVR

No significant change in rest MBF was seen. Post AVR both AS groups demonstrated significant improvements in stress MBF (Figure-3C) and MPR. Despite the improvements post-AVR, AS patients without T2DM continued to display significantly higher stress MBF than the AS patients with T2DM comorbidity (AS patients without T2DM: 1.80(1.59,2.01) versus AS patients with T2DM: 1.48(1.29,1.66) ml/min/g, p= 0.03). (Table-3).

Table 5.3: Longitudinal changes in CMR and 31P-MRS parameters, findings at baseline and 6 months post aortic valve replacement

	Aortic stenosis without T2DM		**Aortic stenosis with T2DM**	
Variable	**Pre-AVR**	**Post-AVR**	**Pre-AVR**	**Post-AVR**
NT- proBNP, ng/L	377 (181-2039)	302(210-652)	404(201-1019)	333(121-809)
6 min walk test, m	360 (306,415)	434(398,472)	396(365,426)	331(267,393**)**
LV EDVi, mL/m²	80(74,86)	73(68,78)	92(80,105)	74(66,83)
LV ESVi, ml/m²	32(26,37)	27(23,30)	34(27,41)	32(25,39)
LV mass, g	146(136,157)	125[115,135]	170(148,193)	138[117,158]
LV mass to LV end-diastolic volume, g/mL	0.99(0.92,1.05)	0.88(0.83,0.93)	0.98(0.89,1.1)	0.93(0.85,0.99)
LV mass index, g/m²	76(71,80)	61(56,67)	80(72,89)	67(59,74)
LV maximal wall thickness, mm	14(13,14)	13(12,14)	14(13,15)	14(13,14)
SVI, ml/m²	49(47,51)	47(44,50)	50(46,53)	42[38,46]
LV EF, %	64(61,67)	64(60,67)	61(57,65)	59(53,64)
RV EF, %	55(52,57)	55(52,57)	55(51,59)	55[49,61]
LA biplane ESV, mL	95(81,108)	97(80,114)	101(85,118)	96[76,115]
Biplane LA EF, %	45(41,50)	44(37,51)	40(33,46)	37(29,45)
Peak longitudinal diastolic strain rate, s^{-1}	0.83(0.74,0.92)	0.82(0.68,0.97)	0.66(0.57,0.75)	0.68(0.59,0.76)
Mean native T1, (ms)	1231(1209,1254)	1198(1172,1224)	1260(1231,1289)	1207(1148,1266]
ECV, (%)	26(25,27)	26(25,27)	27(25,29)	28(26,30)
Indexed ECV, ml/m²	17.9(16.4,19.4)	16.7(15.3, 18.2)	19.2(16.9,22.8)	18.7(16.2, 21.2)

Scar percentage on LGE, (%)	3.22(2.54,3.9)	3.6(2.1,4.9)	3.8(2.6,5)	4.7(2.5,6.9)
PCr/ATP ratio	1.74(1.62,1.86)	2.11(1.79,2.43)	1.44(1.32,1.56)	1.30(1.07,1.53)
Stress MBF, ml/min/g	1.67(1.51,1.84)	1.80(1.59,2.01)	1.25(1.12,1.34)	1.48(1.29,1.66)
Rest MBF, ml/min/g	0.73(0.68,0.78)	0.64(0.59,0.70)	0.68(0.6,0.75)	0.65(0.57,0.73)
MPR	2.43(2.2,2.7)	2.70(2.5,3.0)	1.83(1.60,2.04)	2.30(1.9,2.8)

Values are means with 95% confidence intervals or percentages.

BSA indicates body surface area; LV, Left ventricle; RV, right ventricle; T2DM, type 2 diabetes mellitus; Iso-AS, isolated aortic stenosis; ECV, extracellular volume; iECV, indexed extracellular volume; LV, left ventricular; LA, left atrial; LA EF, left atrial ejection fraction; PCr, phosphocreatine; ATP, adenosine tri-phosphate; RPP, rate pressure product; Svi, stroke volume indexed to body surface area; MBF, myocardial blood flow; MPR, myocardial perfusion reserve.

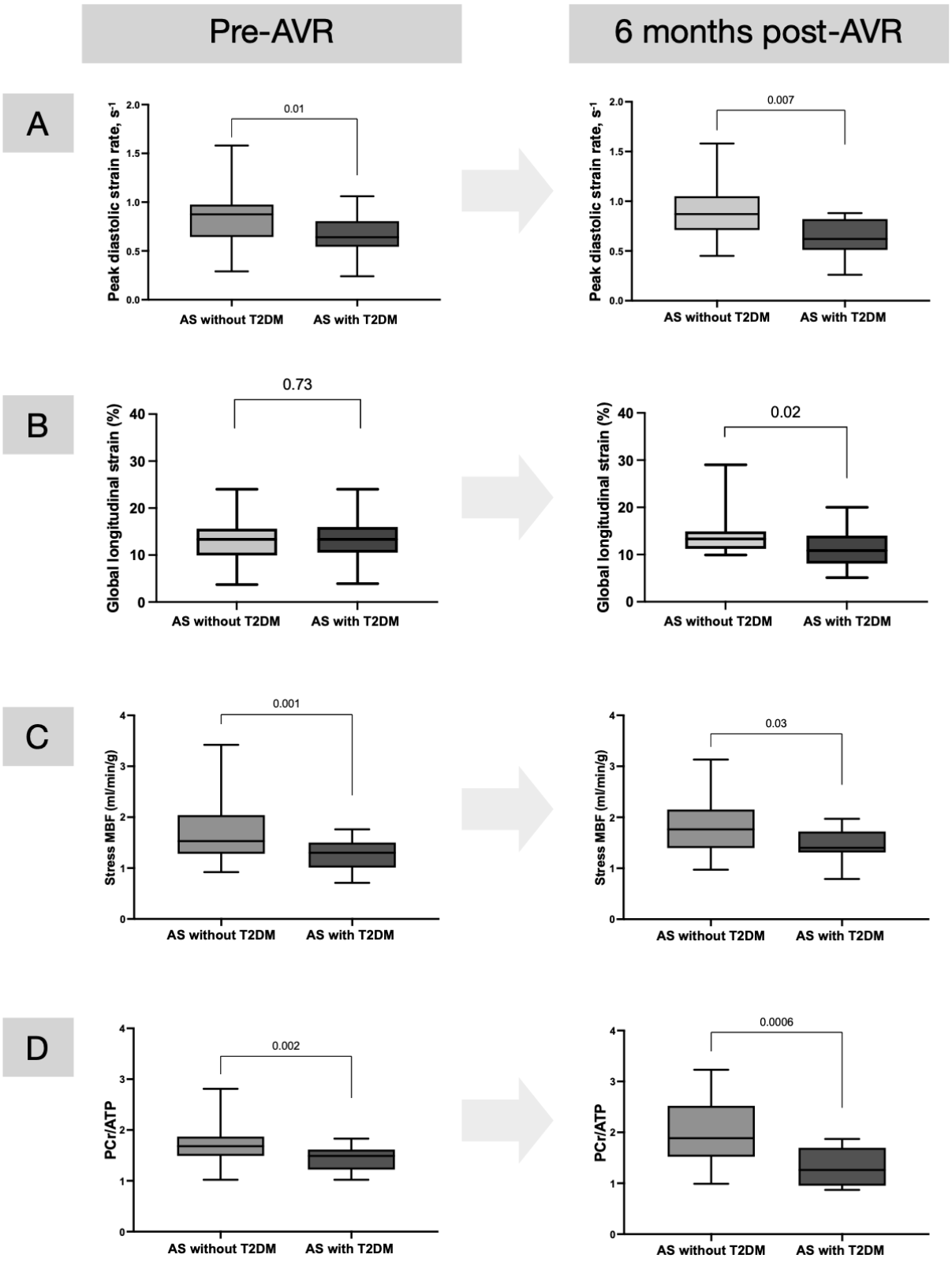

Figure 5.3: Differences in (A) peak diastolic strain rate (-%), (B) myocardial energetics and (C) stress myocardial blood flow between the isolated aortic stenosis (AS) with and without type

2 diabetes mellitus (T2DM) within 1 month before and 6 months after aortic valve replacement (AVR).

Clinical outcomes

Incidence of clinical outcomes following aortic valve intervention in the AS groups are shown in Table 4.

This preliminary study was not designed to detect clinical outcome differences between the AS patients with and without T2DM. However, participants were followed up for a median of 13-months (IQR:10-26months) after surgical or transcatheter AVR. There was a total of 7 clinical events in the study group. There was numerically a higher incidence of cardiovascular mortality in T2DM comorbidity group than the AS group without T2DM (Hazard ratio 7.6; 95% CI: 0.9-64, p=0.04). Cumulative incidence of the clinical events following AVR (a composite of all-cause death, heart failure hospitalization, infective endocarditis, myocardial infarction [embolic event 1-week post-AVR]) was significantly lower in AS group without T2DM (Hazard ratio: 7.3; 95% CI: 1.2-45, p=0.03, fig 4).

Table 5.4: Clinical events following aortic valve replacement

Clinical Outcomes	**Aortic stenosis without T2DM** (n=65)	**Aortic stenosis with T2DM** (n=30)
Cardiovascular death, n (%)	1 (2)	3 (11)
HF Hospitalization, n (%)	0 (0)	1 (4)
Infective endocarditis, n (%)	0 (0)	1 (4)
Myocardial infarction, n (%)	0 (0)	1 (4)

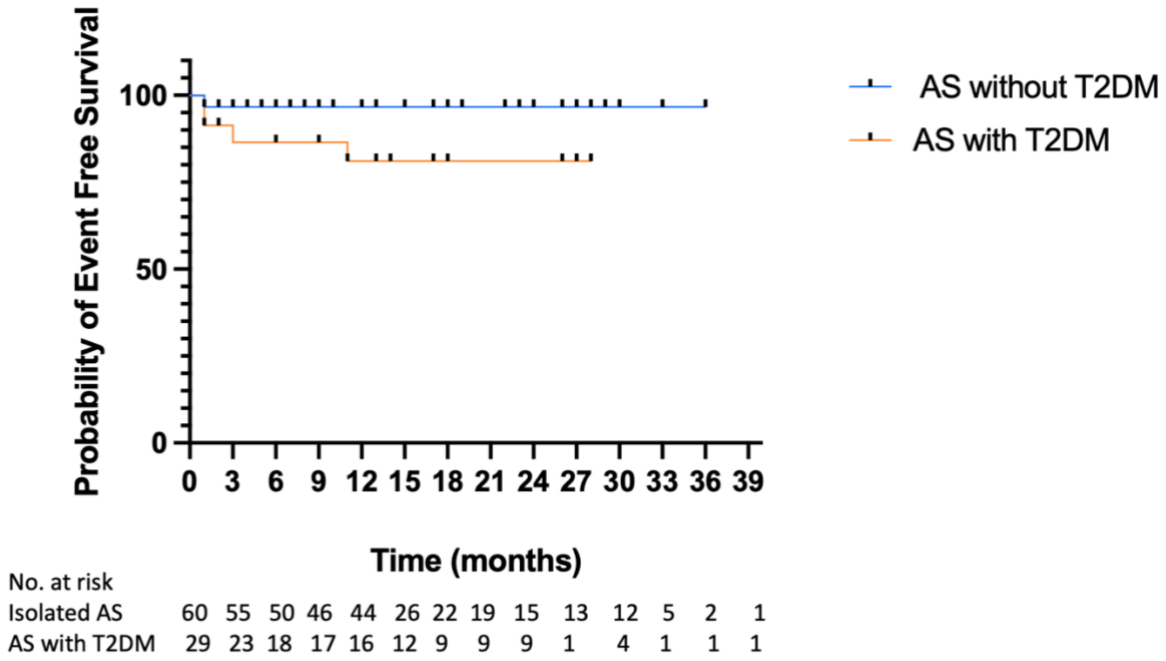

Figure 5.4: Kaplan-Meier curve showing probability of event free survival of composite clinical endpoints of all-cause death, heart failure hospitalization, infective endocarditis, myocardial infarction, p=0.03.

5.5 Discussion

In this prospective longitudinal study of severe symptomatic AS patients undergoing AVR by surgical or transcatheter approach, comorbidity with T2DM was associated with residual myocardial abnormalities and continued limitations in exercise capacity after AVR. Specifically, patients with T2DM comorbidity showed no improvements in myocardial energetics or diastolic function after AVR, and exercise capacity did not improve in this group. Moreover, despite significant improvements in myocardial perfusion after AVR, stress MBF remained significantly lower in patients with T2DM comorbidity compared to AS patients with no T2DM.

Our findings indicate that effectiveness of AVR was attenuated in reversing myocardial alterations and improving clinical outcomes by comorbid T2DM even in patients with no other significant comorbidities such as renal dysfunction or concomitant coronary artery disease which are also common in patients with AS. By contrast AVR was highly effective in AS patients

with no T2DM comorbidity, with both perfusion and energetics returning to the normal range and exercise tolerance improving. With a relatively small number of events and a short duration of follow-up, our finding that the AS patients with T2DM experienced higher clinical event rates should not be overstated.

In line with our findings, prior studies tracking changes in perfusion in AS patients showed that AVR is associated with restoration of myocardial perfusion with improved microcirculatory function resulting from the relief of mechanical obstruction and left ventricular mass regression in isolated AS patients without accompanying significant epicardial coronary artery stenosis[252,303]. However, here we also show that combined effects of T2DM and AS on MBF result in a greater reduction in stress perfusion indices before AVR.

Myocardial energetic compromise, indicated by a decreased PCr/ATP ratio, is a predictor of mortality[287], linked to contractile dysfunction[287,304], and is a well-recognized complication of T2DM[179,180] and severe AS[75,303]. Moreover, previous studies showed that after AVR, there is restoration of myocardial energetics which is in line with our findings in AS patients with no T2DM with 21% relative increase in mean PCr/ATP ratio from pre-AVR measurements[75,303]. However, here we show, even after AVR, AS patients with T2DM comorbidity display no improvements in energetics.

Clinical perspectives

In a recent editorial, Otto et al likened treatment of AS by only surgical or transcatheter AVR, to treating coronary artery disease only with coronary revascularization, underscoring the importance of primary and secondary prevention with lifestyle behaviors and medications, rather than just mechanical intervention to relieve obstruction with end-stage disease[305]. Our findings support this assertion and suggest that a more patient-centered approach to the treatment of AS may be needed which sufficiently embraces the complexities imposed by cardiometabolic comorbidities in patients with AS. AS patients with T2DM comorbidity may require more intensive lifestyle and diabetes control strategies during earlier stages of valvular dysfunction to protect the myocardium from an eventual double insult from the adverse effects of concomitant T2DM and AS. Sufficiently powered future clinical trials are needed to test if such prevention strategies yield reductions in clinical outcomes and improve myocardial recovery after AVR in severe AS patients with these comorbidities.

Limitations

This study had several limitations. A small sample recruited at a single site increases the risk of bias and type I error, while the study may be underpowered to identify subtle correlations with clinical outcomes. Due to the cross-sectional nature of the study causality of the observed differences cannot be inferred. This preliminary study was not designed to detect clinical outcome differences between the AS patients with and without T2DM, but it was powered to detect differences in imaging assessed surrogate markers. Despite this, a higher clinical event rate was detected during the initial 13-month follow-up period post-AVR. A larger study with a longer follow-up duration will be required to confirm the significance of the observed clinical outcome differences. As such, this study should be considered preliminary and exploratory but does support a need for future work. The complexity of the imaging protocol may limit its widespread use, but if feasible larger multicenter studies with extended follow-up, may have the potential to track perfusion and energetics changes and evaluate their influence on clinical outcomes after AVR.

5.6 Conclusion

Our findings suggest that combined myocardial alterations with antagonistic reductions in myocardial energetics, perfusion and subclinical LV systolic performance may explain the increased clinical risk seen in patients with combined severe AS and DM. Given the combined insult on the myocardium, increased rates of clinical events and poorer functional recovery, further work is needed to assess if earlier valve replacement or medical therapy targeted at reversing microvascular or metabolic dysfunction has prognostic benefit in this large subset of patients.

Chapter 6

The Mitochondrial Bioenergetic Phenotype in Type 2 Diabetes

6.1 Abstract

Background:

High resolution respirometry (HRR) techniques is the reference technique for ex-vivo assessment of mitochondrial respiratory function. Previous studies in humans with type 2 diabetes mellitus (T2DM) using HRR have shown deficiency in mitochondrial respiration at complex II and III in the electron transport chain. In a population, where potentially confounding significant coronary artery disease was excluded at baseline, we sought to test the hypothesis that the presence of T2DM in subjects with severe AS would be associated with impaired mitochondrial oxidative capacity.

Methods:

This was a single centre, prospective cohort study in which sixty-seven participants, (23 with and 44 without T2DM) awaiting aortic valve intervention were prospectively recruited. Thirty-five patients with severe AS (15 with and 20 without T2DM) donated intraoperative biopsies to measure mitochondrial oxidative capacity. Discrepancy between the number of participants recruited and samples obtained can be seen due to the impact of the COVID-19 pandemic on staff access to research laboratories.

Myocardial tissue was excised from the right atrial appendage, transported on ice in a biopsy preservation solution within 10 minutes of excision for high resolution respirometry (HRR) analysis and gene testing using real time quantitative polymerase chain reaction (qPCR).

Results:

Patients with and without T2DM were matched for age, sex, systolic and diastolic blood pressure, and measures of AS severity. Patients with T2DM displayed significantly increased BMI and divergent fasting lipid parameters reflective of increased statin use. HbA1c, serum insulin and fasting glucose were expectantly higher in subjects with T2DM with increased HOMA-IR levels confirming increased insulin resistance.

There was no significant absolute difference in maximal, non-physiological, mitochondrial respiration with uncoupling with CCCP (AS without T2DM: 34(28,39) versus AS with T2DM: 29(23,35) pmol/[s*mg], p=0.52, fig 2). Isolated activity at complex II with ROT also did not show any significant absolute difference in mitochondrial respiration (AS without T2DM: 12.7(10,15) versus AS with T2DM: 11.9(9,15) pmol/[s*mg], p=0.63). There was a significant negative correlation between subject HbA1c level and both maximal un-coupled mitochondrial respiration (r=-0.386, p=0.03, fig 4), and mitochondrial respiration isolated at complex II (r=-0.418, p=0.02, fig 5). Decreased complex II activity was also seen to correlate with serum fasting glucose levels in the presence of LCFA (p=0.03).

Conclusion:

These findings suggest even in the absence of coronary artery disease, worsening T2DM control is associated with reduced mitochondrial oxidative capacity with impaired ETC activity at complex II. These findings support previous work done in the field and may go some way to explain to explain the energetic impairment and adverse prognostic association seen in subjects with combined severe AS and T2DM.

6.2 Introduction

Mitochondrial oxidative phosphorylation

Mitochondria are the 'work horses' of cells generating ATP via oxidative phosphorylation (oxphos), this is achieved via a series of complexes which are present in the inner mitochondrial membrane (table 1).

Table 6.1: Respiratory chain complexes

Complex I	**NADH dehydrogenase**
Complex II	**Succinate dehydrogenase**
Complex III	**Cytochrome C reductase**
Complex IV	**Cytochrome C oxidase**
Complex V	**ATP synthase**

Complex I which is the first enzyme of the respiratory chain oxidises NADH, which is generated via the tricarboxylic acid (TCA) cycle in the mitochondrial matrix, and then uses the two electrons to reduce ubiquinone to ubiquinol (Co-enzyme Q). Ubiquinol is then re-oxidised by cytochrome bc1 complex (III) and transports electrons to reduce molecular oxygen to water at complex V. The redox energy released by this process drives the transfer of protons from the mitochondrial matrix to the periplasmic space which then generates the proton motive forces across the inner mitochondrial membrane at complex I, III IV. Complex V then uses this force to produce ATP from ADP and inorganic phosphates[77,306,307] (Fig 1).

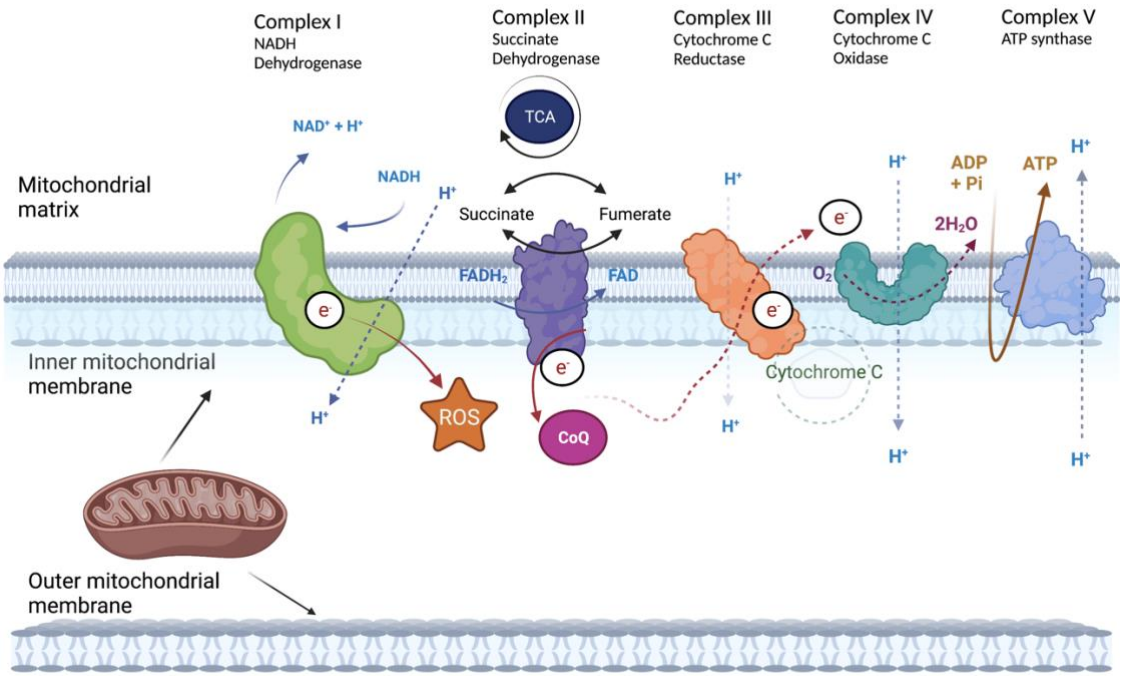

Figure 6.1: Schematic representation of the mitochondrial electron transport chain. Adapted from Zhao et al. Mitochondrial electron transport chain, ROS generation and uncoupling. International Journal of Molecular Medicine; 2019. ADP represent adenosine diphosphate, ATP; adenosine triphosphate, CoQ; Co enzyme Q.

High resolution respirometry

High resolution respirometry (HRR) allows for a reproducible, ex-vivo assessment of myocardial mitochondrial oxidative phosphorylation (oxphos), and thus compliments non-invasive measures of myocardial energetics such as ^{31}P-MRS.

The non-coupled state of maximum respiration is experimentally induced via use of uncouplers to collapse the proton gradient across the inner mitochondrial membrane and measure the capacity of the electron transport chain (ETC). Substrate control with electron entry isolated at complex I (pyruvate and malate) or complex II (succinate and rotenone) restricts capacity allowing for specific assessment of different ETC complexes.

A closed chamber with polarographic oxygen sensers monitors the O_2 and CO_2 concentrations in incubation medium over time, allowing for calculation of the oxygen consumption rate (OCR), used as a direct correlate of mitochondrial respiration[308,309].

Oxygen flux represents basal or substrate saturated respiration before adding ADP, ADP stimulated coupled respiration with octanoyl, glutamate and succinate (state III) and maximal non-physiological uncoupled respiration after adding the uncoupling agent CCCP.
HRR is a well-established technique for assessment of mitochondrial function and has been used previously to investigate the energetic impairment in heart failure and diabetes[44,310].

Impaired mitochondrial function in diabetes

Impaired myocardial energy metabolism is a well-established feature of the T2DM phenotype[39,180,247,311]. The mitochondria can be seen as a central confluence upon which many of the dysregulated metabolic pathways seen in T2DM converge, and thus have garnered increasing interest in understanding the aetiology of diabetic cardiomyopathy. Mitochondrial dysfunction has been closely linked to insulin resistance[312-314] and studies utilising skeletal muscle biopsies show reduced maximal ADP stimulated respiration (state 3) and ETC function in subjects with T2DM[315], a deficiency that has interestingly been shown to reverse with exercsise[313].
Work by Montaigne and colleagues in 2014 using HRR analysis of right atrial myocardial samples in patients with T2DM undergoing coronary artery bypass grafting (CABG) demonstrated increased myocardial oxidative stress, with impaired ETC complex II and III activity compared to non-diabetic controls, independent of obesity[44]. However, the authors recognised the potential confounding factor of ischemia in this group of T2DM patients with significant concomitant coronary artery disease[44]. Given the nature of human myocardial sample acquisition, establishing robust control groups remains challenging, in this study we aimed to assess the impact of diabetes on myocardial mitochondrial function in subjects with severe AS, in the absence of significant coronary artery disease or LV systolic dysfunction.

6.3 Methods

Study Design and Oversight

This was a single centre prospective cohort study which complied with the declaration of Helsinki and was approved by the National Research Ethics Committee (Ref:18/YH/0168).

The study was co-funded by the Wellcome Trust (Grant 207726/Z/17/Z) and Diabetes UK (18/0005870).

Participants

Participants enrolled in the DAS study (Ref:18/YH/0168) in the surgical cohorts were consented for excision of myocardial tissue during aortic valve replacement. All patients had a diagnosis of severe AS based on peak aortic forward flow velocity of greater than 4 m/s on valve clinic echocardiography. Sixty-seven participants, (23 with and 44 without T2DM) awaiting aortic valve intervention were prospectively recruited. Thirty-five patients with severe AS (15 with and 20 without T2DM) donated intraoperative biopsies to measure mitochondrial oxidative capacity. Data collection was completed between April 2019 and April 2022. Discrepancy between number of subjects recruited and tissue samples donated can be seen predominantly due to the impact of the COVID-19 pandemic, limiting research staff access to cardiac theatres between April 2020 – September 2020. AS patients with T2DM comorbidity had an established T2DM diagnosis according to World Health Organization criteria and they were free of known diabetes complications[298]. Significant coronary artery disease, defined as luminal stenosis >50%, was excluded with x-ray coronary angiography in all subjects prior to enrollment.

Exclusion criteria

Participants were excluded if they had known previous myocardial infarction, flow-limiting coronary artery disease, known LV systolic dysfunction (LVEF <50%), more than mild bystander valve disease, significant renal impairment [estimated glomerular filtration rate (eGFR)<30mL/min/1.73m^2], permanent atrial fibrillation, or any contraindication to CMR scanning. All patients listed for AVR had flow-limiting coronary atheroma excluded by invasive angiography and prior myocardial infarction excluded by late gadolinium enhancement imaging.

Myocardial Tissue Samples

Myocardial tissue was excised from the right atrial appendage by the cardiothoracic surgeon performing surgical AVR immediately preceding central venous cannulation and prior to cardioplegia. Samples were immediately immersed in a biopsy preservation solution (BIOPS) and transported on ice to the laboratory within 10-minutes of excision.

High Resolution Respirometry

Myocardial tissue was removed using anatomical forceps under microscopic guidance. Tissue was placed into relaxing and biopsy preservation solution for high-resolution respirometry (BIOPS[316]). Tissue was permeabilized with freshly prepared saponin (50 µg·mL^{-1}) and washed in mitochondrial respiration medium, MiR05[317].

Functional studies were performed using high-resolution respirometry Oxygraph-2k (O2k, Oroboros Instruments, Innsbruck, Austria) with a polarographic oxygen electrode and two 2 mL chambers containing MiR05.

Oxygen concentration and flux were simultaneously recorded and analysed by Dat lab software (Datlab Version 6.1, Oroboros Instruments, Innsbruck, Austria). Reagents were added through a small capillary tube in the chamber using Hamilton syringes (Oroboros Instruments, Innsbruck, Austria). Mitochondrial substrate or inhibitors were added into respiration medium in a step-by-step manner to determine flux through the mitochondrial complexes of AS patients with and without diabetes. Complex I fatty acid utilization was measured using palmitoyl-carnitine (0.4 mM) in conjunction with malate (0.5 mM). Complex I-linked substrate state was induced in mitochondrial preparations by addition of NADH-generating substrates glutamate (10 mM) and pyruvate (5 mM). ADP (2.5 mM) was added to trigger oxidative phosphorylation limited by β-oxidation. Cytochrome *c* (10 µM) was used to test the integrity of the outer membrane. Maximisation of electron flux through complex I and complex II was achieved through addition of succinate (10 mM). Maximal respiration was determined by uncoupling the mitochondrial with CCCP (5 µM). Rotenone (0.5 µM) was added to inhibit complex I, resulting in a rate of oxidative phosphorylation limited by complex II. Antimycin A (12.5 µM) was used to inhibit complex 5 to determine background respiration.

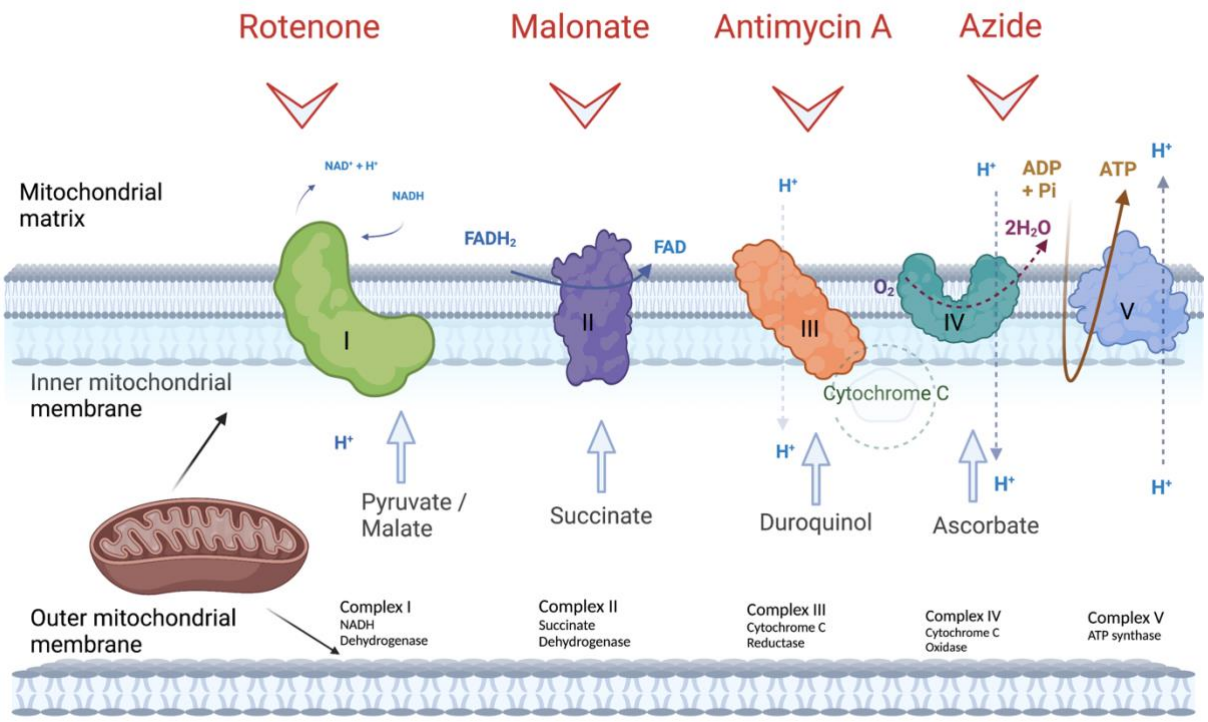

Figure 6.2: Schematic representation of the mitochondrial substrates and inhibitors used during high resolution respirometry and their respective actions on the mitochondrial complexes involved in oxidative phosphorylation. Adapted from; Chen, YR and Zweier, Jl. Cardiac mitochondria and reactive oxygen species generation. Circulation Research; 2014

Gene Testing

Myocardial expression of the following genes (Table 1) was measured using real time quantitative polymerase chain reaction (qPCR). Whereby detection of the PCR product was monitored by measuring the real time increase in fluorescence. The threshold cycle (CT) of each target product was determined, the CT is the number of PCR cycles required for the fluorescence signal to exceed the detection threshold value.

Table 1: Myocardial gene expression measured using real time quantitative polymerase chain reaction (qPCR) and their respective functions.

Gene Tested	Function
ACADL	Oxidation of short chain fatty acids
CPT1	Mitochondrial enzyme, catalyses transfer of acyl group of LCFA-CoA from co-enzyme A to l-carnitine
CD36	Scavenger receptor for LCFA uptake
GLUT-4	Insulin mediated glucose uptake
PDK4	Inhibits flux of glucose metabolite intermediates into the citric acid cycle

Statistical Analysis

Statistical analysis was performed using GraphPad Prism software (version 9.0.0). All data were checked for normality using the Shapiro-Wilks test and presented as mean or median with 95% confidence intervals as appropriate. Categorical data are presented as numbers and percentages and compared with Pearson's chi-square test. Differences in non-parametric variables were assessed using a Kruskal-Wallis test. Student t-test was used for comparison of normally distributed datasets and Mann-Whitney U test was used for non-parametric tests where data were obtained for only two groups. Correlations analyses were performed using Pearson correlation calculation for parametric data and Spearman calculation for non-parametric data. $P \leq 0.05$ was used as a threshold of significance.

6.4 Results

Participant demographics and clinical characteristics:

Demographics, clinical, and biochemical data at baseline prior to AVR are shown in Table-2. Subjects with and without T2DM were well matched for age, sex and hemodynamic parameters at rest. BMI was significantly higher in the T2DM cohort, with lower serum total cholesterol (TC) and low-density lipoprotein (LDL) levels reflective of increased guideline directed statin therapy in this group. HbA1c, serum insulin and fasting glucose were expectantly higher in subjects with T2DM with increased HOMA-IR levels confirming persisting increased insulin resistance.

There was no significant difference in markers of AS severity (peak aortic forward flow velocity or plasma NT-pro-BNP level), renal function, plasma FFA or ketone levels. No significant difference was seen in LV mass, however LVEF was significantly reduced in subjects with T2DM, albeit with both groups still within normal range.

Table 6.2: Demographics and clinical characteristics

Variable	**AS without T2DM N=20**	**AS with T2DM N= 15**	**P value**
Age, y	68(65-70)	67(63,71)	0.68
Female, n (%)	9(45)	6(40)	
BMI, kg/m²	28(27,29)	31(29,34)	**0.006**
Heart rate, bpm	73(69,77)	70(63,77)	0.28
Systolic BP, mmHg	132(127,136)	130(119,140)	0.46
Diastolic BP, mmHg	78(76,80)	76(71,81)	0.38
Creatinine, umol/L	77(72,82)	81(71,90)	0.65

Haemoglobin, g/L	148(144,151)	139(132,145)	**0.02**
Total cholesterol, mmol/L	5.8(4.3,7.3)	4.3(3.8,3.7)	**0.01**
HDL, mmol/L	1.5(1.4,1.7)	1.2(1.0,1.4)	**0.002**
LDL, mmol/L	3.0(2.6,3.3)	2.2(1.9,2.6)	**0.02**
TG, mmol/L	1.3(1.2,1.5)	2.1(1.3,2.8)	0.07
HbA1c, mmol/mol	37(36,38)	57(49,64)	**<0.0001**
Glucose, mmol/L	5.2(4.9,5.4)	8.2(6.6,9.7)	**<0.0001**
Insulin, pmol/L	61(43,80)	126(63,188)	**0.0006**
HOMA IR, Molar Units	2.0(1.3,2.6)	5.5(2.5,8.6)	**0.0004**
FFA, mmol/L	0.51(0.43,0.59)	0.48(0.37,0.58)	0.71
D-3-Hydroxybutyrate, mmol/L	0.14(0.09,0.18)	0.14(0.09,0.20)	0.05
NT- proBNP, ng/L	301[131-1317]	265[174-504]	0.85
TTE Vmax, m/s	4.5(4.3,4.6)	4.4(4.3,4.6)	0.94
Rockwood Score	1.98(1.8,2.2)	2.1(2.0,2.2)	0.47
Charlson Comorbidity Index	3.2(2.9,3.5)	4.0(3.6,4.3)	**0.006**
LV mass, g	150(137,163)	169(140,197)	0.16
LV mass index, g/m²	76(70,81)	80(69,90)	0.49
LV ejection fraction, %	65(62,69)	61(56,66)	**0.04**

Myocardial mitochondrial function

There was no significant difference in maximal, non-physiological, mitochondrial respiration with uncoupling with CCCP (AS without T2DM: 34(28,39) versus AS with T2DM: 29(23,35) pmol/[s*mg], p=0.52, fig 3). Isolated activity at complex II with ROT also failed to show any significant absolute difference in mitochondrial respiration (AS without T2DM: 12.7(10,15) versus AS with T2DM: 11.9(9,15) pmol/[s*mg], p=0.63, fig 4).

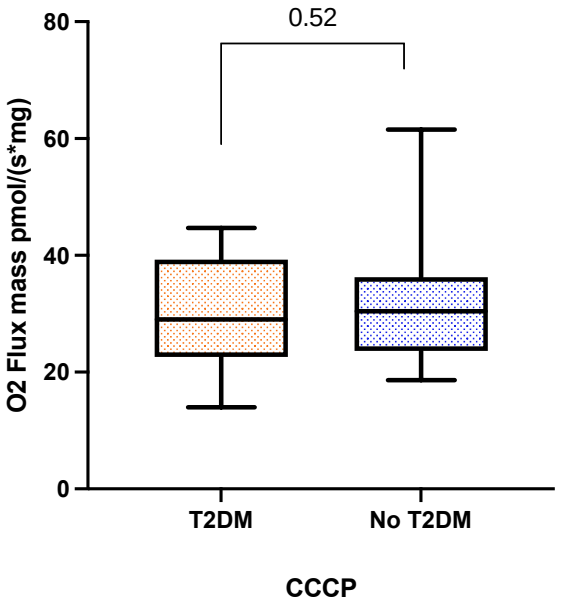

Figure 6.3: Difference in maximal mitochondrial respiration with CCCP un-coupling between groups with and without T2DM.

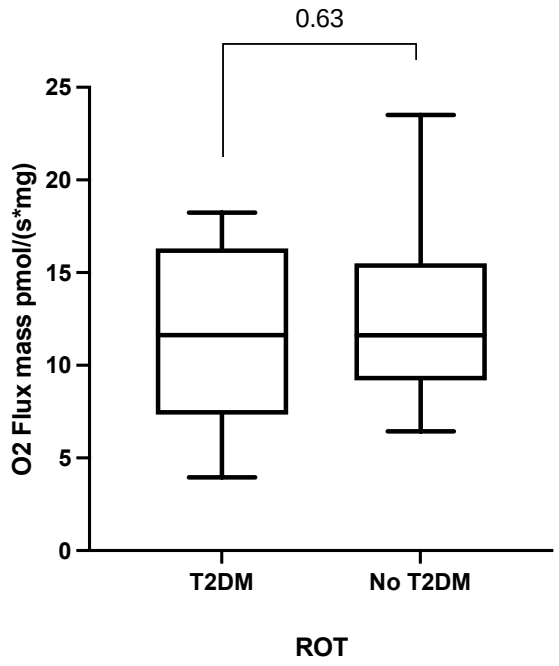

Figure 6.4: Difference in maximal mitochondrial respiration isolated at complex II with rotenone in patients with and without T2DM.

Correlations

With the LCFA palmitate as fuel source, there was a significant negative correlation between subject HbA1c level and both maximal un-coupled mitochondrial respiration (r=-0.386, p=0.03, fig 5), and mitochondrial respiration isolated at complex II (r=-0.418, p=0.02, fig 6). Decreased complex II activity was also seen to correlate with serum fasting glucose levels in the presence of LCFA (p=0.03). Of note significant correlation was not observed when the medium chain FA (MCFA) octanoyl was used as substrate.

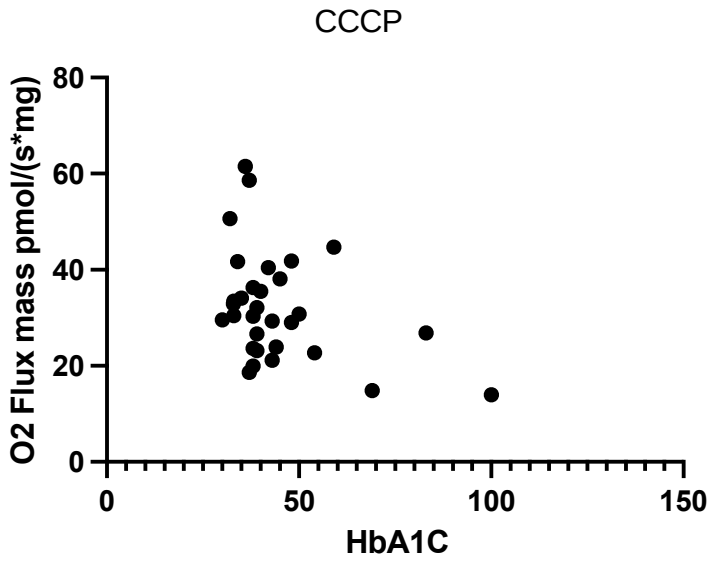

Figure 6.5: Correlation between serum HbA1c level and maximal un-coupled mitochondrial respiration with CCCP.

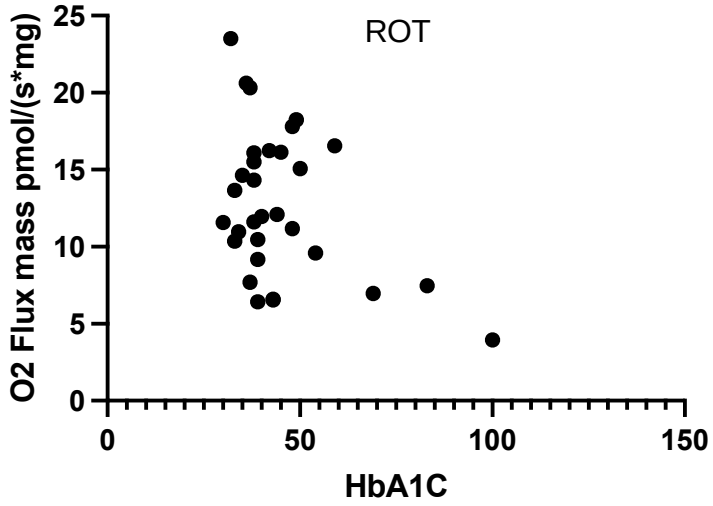

Figure 6.6: Correlation between serum HbA1c level and mitochondrial respiration isolated at complex II with ROT.

No significant correlation was observed between HOMA-IR and mitochondrial respiration with ROT or CCCP. There was significant positive correlation between serum LDL level and complex II activity, when activated by succinate (p=0.03).

Gene expression

There was a trend towards increased expression of ACADL with increased HbA1c level which did not reach significance (p=0.17), however increased ACADL expression was observed with increasing serum fasting glucose (p=0.017), (fig 7).

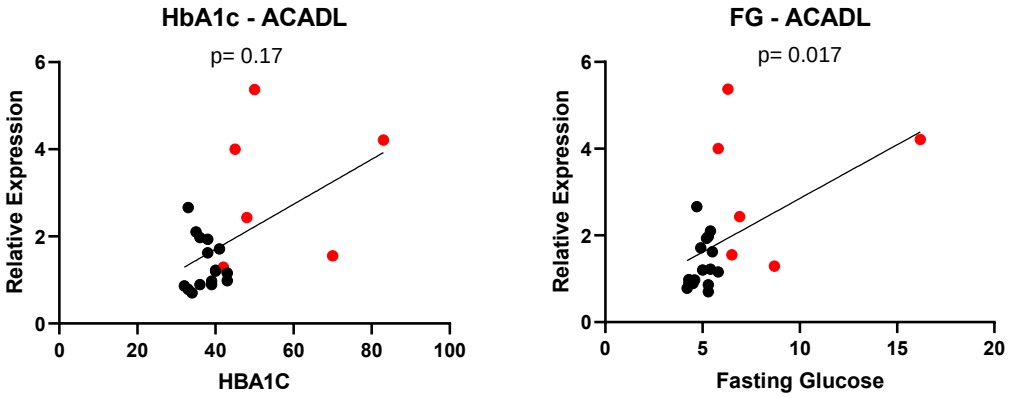

Figure 7: Correlation between relative expression of ACADL and serum HbA1c and fasting glucose, (individuals with diagnosis of T2DM can be seen in red).

Increased HbA1c level was also seen to confer reduced expression of CD36, (p=0.02). No significant difference was observed between individuals with and without T2DM and expression of CPT1a or PDK4.

6.5 Discussion

To our knowledge this is the first study using HRR to assess myocardial mitochondrial function in patients with T2DM where significant coronary artery disease was specifically excluded at baseline. Our results suggest worsening T2DM control, with increasing serum HbA1c and fasting glucose levels, to be associated with reduced mitochondrial ETC activity at complex II. Interestingly no correlation was observed between mitochondrial function and insulin resistance (HOMA-IR). These findings support recent work by Zweck and colleagues, in heart

transplant recipients, which showed both overt T2DM and impaired fasting glucose to be associated with impaired mitochondrial respiration at complex II with succinate but not medium chain fatty acid substrate in isolation[318]. Similar results were also shown in previous work by Montaigne et al, in patients with T2DM and coronary artery disease, and suggests chronic hyperglycaemia rather than insulin resistance leads to mitochondrial dysfunction in diabetes[44]. In rodent models hyperglycaemia has been shown to lead to dynamin related protein 1(DrP-1) induced mitochondrial fission and apoptosis [319], and post translational modifications of proteins involved in mitochondrial dynamics have been observed in high glucose conditions, with resultant mitochondrial dysfunction and fragmentation[320,321].

Myocardial mitochondrial dysfunction in T2DM with early respirometry techniques was first described in 2009[322]. However, teasing out the specific underlying mechanism has proved challenging, especially in the context of confounding ischaemic heart disease and the presence of obesity in the majority of individuals with T2DM. Work by Montaigne et al showed mitochondrial dysfunction at complex II and III in the ETC to be independent of BMI status, with increased fragmentation of the mitochondrial network and reduced expression of the mitofusion protein 1(MFN1)[44]. Our results support the assertion of impairment in complex II activity in T2DM leading to reduced mitochondrial function, interestingly these findings were only seen with palmitate substrate as fuel source, suggesting there may be less efficient utilisation of long chain fatty acid in diabetes, leading to substrate oxidation and phosphorylation uncoupling. Decreased mitochondrial oxphos in subjects with overt left ventricular systolic dysfunction has been shown in the context of medium chain fatty acid oxidation[310], therefore the mitochondrial dysfunction seen in T2DM may represent an early stage of metabolic adaptation in which an inherent lipotoxic environment and preferential long chain fatty acid substrate use becomes maladaptive, leading to sequential mitochondrial fragmentation, fission and dysfunction. Our findings of progressive decline in maximal uncoupled oxphos with worsening diabetic control, increased acyl-CoA dehydrogenase long chain (ACADL) gene expression in a state of hyperglycaemia and preferential use of long chain fatty acid in a high LDL environment may also support this theory. Further work is needed to assess if targeted interventions aimed at reducing the chronic hyperglycaemic state yield any improvements in mitochondrial function.

Limitations

This work can be seen to have several important limitations, significant discrepancy between number of recruits and samples obtained may introduce unforeseen selection bias and resultant underpowering of the sample size. This may account for the lack of a significant absolute difference in mitochondrial function between subjects with and without T2DM, despite non-T2DM cohort showing numerically higher respiration and previous studies suggesting significant reduction in T2DM[44,318]. Although patients were matched for age, blood pressure and AS severity, with significant coronary artery disease excluded in all patients, the role of additional confounding factors, particularly obesity must be considered. Equally the cohort with isolated severe AS cannot be seen as a truly normal control group and represents a cohort with significant, potentially confounding metabolic disturbances[323].

6.6 Conclusion

In this study using high resolution respirometry to assess myocardial mitochondrial function in patients with severe AS with and without T2D, worsening diabetic control and chronic hyperglycaemia was associated with impaired maximal uncoupled and complex II mitochondrial respiration in the presence of palmitate These findings may go some way to explain the impairment in myocardial energetics seen in diabetes and the adverse prognostic association seen in patients with combined severe AS and T2DM

Chapter 7

Type 2 diabetes is associated with sarcopenic obesity in subjects with severe aortic stenosis and with residual impairment in post operative exercise capacity following aortic valve replacement

7.1 Abstract

Background and aims:

Due to the obesity epidemic type 2 diabetes mellitus (T2DM) and severe aortic stenosis (AS) are increasingly frequent co-morbidities and the presence of T2DM has been shown to adversely impact on post-procedural morbidity and mortality in patients undergoing both surgical and transcatheter aortic valve replacement. T2DM is a major cause of functional decline amongst older adults, with insulin playing a key role in skeletal muscle signalling pathways and muscle growth. Low skeletal muscle mass has previously been shown to be predictive of mortality, prolonged hospital stay and functional decline in patients undergoing trans-catheter aortic valve replacement for severe AS. In this single centre prospective longitudinal study, we sought to test the hypothesis that the presence of DM co-morbidity is severe AS patients would increase sarcopenia, impair functional exercise capacity, and attenuate recovery following aortic valve replacement.

Methods:

Ninety-five participants, 65 with severe AS in isolation (Iso-AS) and 30 with combined severe AS and T2DM (AS-DM) awaiting aortic valve intervention were prospectively recruited. 15 age matched healthy volunteers served as a control group. Subjects underwent MR imaging to allow quantitative assessment of thigh skeletal muscle mass and 6-minute walk test evaluation of functional exercise capacity within 1-month prior to and 6-months post aortic valve replacement. Patients were followed up for a median of 13 months for survival outcomes and length of hospital stay via electronic records.

Results:

Groups were matched in age, sex distributions, median surgical risk scores, clinical frailty scores and AS severity. Pre-AVR both AS groups with and without DM co-morbidity displayed significantly reduced skeletal muscle mass indexed to BMI (p=0.0004) compared to healthy controls. Whilst no significant difference in skeletal muscle mass or 6-minute walk test between AS groups was observed at baseline, at 6-months post AVR, patients with DM comorbidity showed significantly reduced skeletal muscle mass (Iso-AS: 103[97,110] cm/m^2

vs AS-DM: 95[87,103] cm/m^2, p=0.02) and did not show significant improvement in 6-minute walk test distance compared to subjects with isolated AS (Iso-AS:396[365,436] to 434[398,472]m, p=0.02, AS-DM: 360[306,415] to 331[267,393]m, p=0.45).
Whilst skeletal muscle mass at baseline was not predictive of all-cause mortality, negative correlation was observed with post operative length of hospital stay (r=-0.72, p=0.001).

Conclusions:

Following aortic valve replacement patients with comorbid type 2 diabetes display increased sarcopenia and impairment of functional exercise capacity, the impact of sarcopenia may go some way to explain the increased morbidity seen in AS patients with DM following AVR.

7.2 Introduction

Aortic stenosis (AS) is the most common degenerative valve disease in the developed world, with a prevalence of 12% in patients over 75 years[127,324] . With ageing demographics, the burden of AS on global health systems is expected to continue to increase[126]. In parallel, sarcopenia, a syndrome of progressive and generalised loss of skeletal muscle mass and strength, is highly prevalent in geriatric populations[325,326]. Low skeletal muscle mass has been shown to impact on post-operative outcomes in a variety of conditions and to be predictive of mortality, prolonged hospital stay and functional decline in patients undergoing trans-catheter aortic valve replacement (TAVR) for severe AS[327-330]. Therefore, identification of additional prognostic markers for AS patients at increased risk of sarcopenia may offer the opportunity for targeted risk factor modulation.

Due to the obesity epidemic type 2 diabetes mellitus (T2DM) and severe AS are increasingly frequent co-morbidities and the presence of T2DM has been shown to adversely impact on post-procedural morbidity and mortality in patients undergoing both surgical and transcatheter aortic valve replacement, however the reasons behind this are not fully understood [331-334]. T2DM is a major cause of functional decline amongst older adults, with insulin playing a key role in skeletal muscle signalling pathways and muscle growth [335-337].

The development of insulin resistance leads to decreased skeletal muscle mass in T2DM patients, with worsened glycaemic control linked to increased rates of sarcopenia[338,339]. In addition, the use of insulin sensitisers has been shown to attenuate muscle loss amongst T2DM patients[340].

An expanding body of evidence advocates increased utilisation of cardiac magnetic resonance imaging (MRI) in patient with severe AS to allow for more refined risk stratification [135,139,141,170,341]. Single slice MRI of the thigh muscle cross sectional area (CSA) has been shown to correlate closely with whole body skeletal muscle mass (SMM) and sarcopenia in both normal weight individuals and those with sarcopenia in the presence of elevated body mass index (BMI) the so called sarcopenic obesity syndrome inherent to T2DM [342,343]. Therefore, the additional assessment of baseline SMM in patients undergoing cardiac MRI prior to aortic valve replacement (AVR) may allow for quick effective identification of patients with sarcopenia who are at increased risk of post operative morbidity and prolonged hospital stay, without the use of ionising radiation.

In this single centre prospective longitudinal study we sought to test the hypothesis that the presence of T2DM co-morbidity is severe AS patients would increase sarcopenia, impair functional exercise capacity and attenuate recovery following AVR. MRI assessments were supported by 6-minute walk tests, biochemical and clinical outcome analysis.

7.3 Methods

Study Design and Oversight

This single-centre, longitudinal prospective cohort study complied with the Declaration of Helsinki and was approved by the National Research Ethics Committee (Ref:18/YH/0168). The study was co-funded by the Wellcome Trust (Grant 207726/Z/17/Z) and Diabetes UK (18/0005870). This was a sub-study as part of the DAS study described fully in chapter 5.

Participants

Adult patients with severe AS who had been referred for surgical or transcatheter AVR were eligible for inclusion. Eligibility criteria, recruitment pathway and CONSORT diagram, methodological details with the exception of leg muscle imaging are provided earlier in Chapter 5.

Magnetic resonance imaging

All scans were performed on a Siemens 3T Magnetom Prisma system (Erlangen, Germany). Both thigh muscles were scanned in the supine position using built-in posterior and anterior coils. Thigh imaging was performed after participants had been supine for more than 15 min to minimise the impact of fluid shifts. Coil position was standardised with the iso-centre over the mid-thigh, 20cm below the femoral head, for all participants. Three slices (proximal, mid and distal thigh) were obtained (slice thickness 10mm, TR 665ms, TE 11ms, FA 160 °, matrix 348x512, figure 1) with an acquisition time of 2 minutes.

Figure 1: Segmentation method of MRI muscle CSAs at the A: (proximal), B: (medial), and C: (distal) ends of the left thigh.

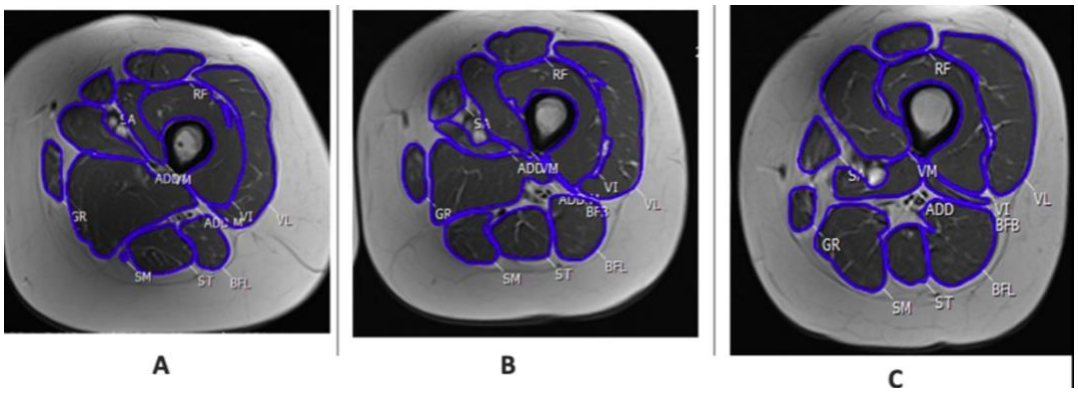

The muscles selected for segmentation were the anterior muscles compartment, four heads of the QUAD (the rectus femoris (RF), vastus lateralis (VL), vastus intermedius (VI), and vastus medialis (VM)),and the sartorius (SA)). The four muscles composing the posterior compartment, hamstrings muscles (biceps femoris short head (BFB), biceps femoris long head (BFL), semitendinosus (ST) and semimembranosus (SM)). And medial muscles compartment, adductors (adductor longus, magnus and pectineus together (add m, add L) and gracilis (GR).

Quantitative analysis of MRI data

All MR image analysis was performed blinded to participant details by AA with contours subsequently reviewed by NJ and EL, also blinded to participant details, using cvi42 software (Circle Cardiovascular Imaging, Calgary, Canada). The CSA of the thigh muscles in all slices were measured by manual tracing just inside the muscle fascial lines to exclude non-muscular elements (figure 2) [342,344].

Total muscle CSA (cm^2) was calculated by addition of muscle CSA across the three slices and then indexed to height, body surface area (BSA) and BMI as previously described [345,346]. Skeletal muscle volume (cm^3) was calculated by multiplying tissue CSA and slice thickness (10mm), volume units were then converted to mass (kg) by multiplying by an assumed constant density for adipose tissue free skeletal muscle (1.04 kg/L) [347].

Six-minute walk test

The participants were instructed to walk along a 30-meter corridor and cover the maximum achievable distance in 6-minutes under the supervision of study investigators with medical training and with experience in conducting the test. At the end of 6-minutes, participants were asked to stop, and the distance walked was measured in meters[226].

Surgical risk scores and frailty scores

Both Euro Score II and the Society of Thoracic Surgeons risk scores were recorded[301]. As validated measures of frailty and comorbidity, both the Rockwood Frailty Score and the Charlson comorbidity index were recorded[348].

Clinical outcomes

The study was not designed to assess the clinical outcome differences between the AS patients with and without T2DM, nevertheless patients were followed for a median of 13-months post-AVR for clinical outcomes via Leeds Teaching Hospitals electronic health care records. Clinical event rate of cardiovascular mortality after AVR, and separately event rates for composite of all-cause mortality and length of hospital stay were calculated.

Statistical analysis

Statistical analysis was performed using GraphPad Prism software (version 9.0.0). All data were checked for normality using the Shapiro-Wilks test and presented as mean or median with 95% confidence intervals as appropriate. Categorical data are presented as numbers and percentages and compared with Pearson's chi-square test. Comparisons between the 3 groups were performed by 1-way ANOVA with post hoc Bonferroni corrections. Differences in non-parametric variables were assessed using a Kruskal-Wallis test. Student t-test was used for comparison of normally distributed datasets and Mann-Whitney U test was used for non-parametric tests where data were obtained for only two groups. Comparisons between pre- and post-AVR measurements in patients with AS were performed with ANOVA with post hoc Bonferroni corrections. $P \leq 0.05$ was used as a threshold of significance.

A 2-sided log-rank test was used to calculate average event rate ratios and confidence intervals over a median period of 13-months. Kaplan-Meier plots were constructed for time-to-event analyses.

7.4 Results

Participant demographics and clinical characteristics:

Demographics, clinical, and biochemical data at baseline are shown in Table-1.
Between May 2019, and April 2022, 95 participants with severe AS (30 with and 65 without T2DM comorbidity) and 15 healthy controls were recruited.

Baseline

Age and sex distributions were comparable between the groups (Table-1).
The median surgical risk scores were similar between the AS patients with and without T2DM and patients were matched in AS severity. While frailty scores were similar, the Charlson index was higher in T2DM comorbidity group. Between the two AS groups, blood pressure measurements and heart rates were similar, but the BMI was higher in the T2DM comorbidity group in line with expectations. Resting heart rates were higher in both AS groups than healthy controls.
AS patients with T2DM were receiving statin treatment at higher rates and reflecting this, they showed lower total and LDL cholesterol levels. The fasting glucose, HbA1c and circulating ketone levels were higher in AS patients with T2DM. While none of the AS patients were in the anemic range, the haemoglobin levels were lower in AS patients with T2DM. Plasma NT-proBNP levels did not differ significantly between the AS groups.

Six months after AVR

6-months post-AVR AS patients without T2DM displayed a statistically significant reduction in plasma NT-proBNP levels (377(181-2039) to 302(210-652) ng/L, p=0.04). Despite numerical reduction in median NT-proBNP level, this change in T2DM comorbidity group did not reach statistical significance (404(221-1019) to 333(121-809) ng/L, p=0.76).

Table 1: Clinical Characteristics and biochemistry

Variable	HV n=10	AS without T2DM n=65	T2DM and AS n=30	P value
Age, y	69(65,73)	71(69,74)	70(67,74)	0.76
Female, n (%)	4(40)	27(42)	8(27)	0.22
Height,m	1.71(1.66,1.75)	1.69(1.67,1.71)	1.71(1.67,1.75)	0.77
BMI, kg/m²	26(24,27)*	27(26,28)€	31(29,33)	**0.007**
Heart rate, bpm	62(56,67)†	72(69,75)	69(63,74)	**0.009**
Systolic BP, mmHg	136(129,143)	132(128,137)	131(129,134)	0.43
Diastolic BP, mmHg	76(73,79)	77(75,79)	73(69,77)	0.14
Creatinine, umol/L	73(70,77)	77(73,81)	82(75,89)	0.13
Haemoglobin, g/L	149(145,152)*	143(139,147)	138(132,143)	**0.01**
Haematocrit, L/L	0.45(0.44,0.47)*	0.44(0.43,0.46)	0.42(0.41,0.44)	**0.02**
Total cholesterol, mmol/L	5.3(4.8,5.7)*	5.6(4.4,6.7)€	4.2(3.9,4.5)	**0.0008**
HDL, mmol/L	1.7(1.6,1.9)*	1.6(1.5,1.7)€	1.3(1.4,1.5)	**0.0003**
LDL, mmol/L	2.9(2.6,3.3)*	2.9(2.6,3.2)€	2.3(1.9,2.5)	**0.01**
TG, mmol/L	1.3(1.0,1.5)	1.4(1.2,1.5)	1.8(1.3,2.3)	0.24
HbA1c, mmol/mol	37(36,39)*	38(37,38)€	56(50,61)	**<0.0001**
Glucose, mmol/L	5(4,5)*	5(4,5)€	9(7,10)	**<0.0001**
Insulin, pmol/L	29[15-58]*	38[24-65]€	86[47-145]	**0.0002**
HOMA IR, Molar Units	0.79[0.41-1.39]*	1.31[0.6-2.17]€	3.28[1.77-6.16]	**0.0003**
FFA, mmol/L	0.48(0.44,0.51)	0.53(0.46,0.6)	0.51(0.42,0.59)	0.84
D-3-Hydroxybutyrate, mmol/L	-	0.14(0.09,0.18)	0.17(0.10,0.24)	**0.02**
NT- proBNP, ng/L	42[35-66] *	377[181-2039]†	404[224-1066]	**<0.0001**
Medications				
ACEi	-	5(8)	11(41)	**0.0002**
ARB	-	11(17)	3(11)	0.46
Beta blocker	-	17(27)	12(44)	0.09
CCB	-	16(25)	11(41)	0.13
Loop diuretic	-	10(16)	7(26)	0.25
Statin	-	26(41)	22(81)	**0.0003**
ASA	-	18(28)	10(37)	0.4
DOAC	-	12(19)	2(7)	0.17
Metformin	-	-	16(59)	-
Sulfonylurea	-	-	6(22)	-
DPP4i	-	-	3(15)	-
GLP-1RA	-	-	0(0)	-
SGLT2i	-	-	3(11)	-
AS Clinical Details				
TTE Vmax, m/s	-	4.5(4.4,4.7)	4.6(4.4,4.7)	0.92
Duration severe AS, (months)	-	8(7,10)	10(6,14)	0.5
Bicuspid AV, n (%)		17(27)	3(11)	0.1
STS Score		0.88[0.66-1.35]	0.97[0.69-1.16]	0.9
Euro Score II	-	0.89[0.72-1.22]	1.03[0.9-1.3]	0.16
Rockwood Score	-	2.1(1.9,2.4)	2.2(2.0,2.3)	0.81
Charlson Comorbidity Index		3.7(3.4,4.0)	4.5(4.1,4.9)	**0.002**
NYHA Class, (%)				
I		10(16)	4(15)	0.92
II		41(64)	16(59)	0.67
III		10(16)	6(22)	0.07
IV		0(0)	0(0)	-
6 min walk test, m	-	396(365,436)	360(306,415)	0.14

SAVR, n (%)		46(73)	22(71)	0.87
TAVI, n (%)		17(27)	9(29)	0.75
Length of hospital stay, (days)		7(6,8)	8(6,10)	0.77
Cardiovascular Past Medical History				
Stroke TIA, n(%)	-	4(6)	2(7)	0.9
PAF, n(%)	-	7(11)	2(7)	0.64
Hyperlipidemia, n (%)	-	17(27)	11(41)	0.73

€ signifies p<0.05 between T2DM and AS group and Iso-AS, * signifies p<0.05 between T2DM and AS group and HV, † signifies p≤0.05 between Iso-AS and HV.

AV indicates aortic valve; AS, aortic stenosis; T2DM, type 2 diabetes mellitus; BMI, body mass index; bpm, beats per minute; HDL, high density lipoprotein; LDL, low density lipoprotein; TG, triglycerides; FFA, free fatty acids; ACEI, angiotensin converting enzyme inhibitor; ARB, angiotensin receptor blocker; CCB, calcium channel blocker; ASA, aspirin; DOAC, direct oral anticoagulant; DPP4i, dipeptidyl peptidase-4 inhibitor; GLP-1RA, glucagon-like peptide-1 receptor agonist; SGLT2i, sodium glucose co-transporter-2 inhibitor; V max, peak aortic forward flow velocity; TTE, trans-thoracic echocardiogram; CMR, cardiac magnetic resonance; TIA, transient ischemic attack; HTN, hypertension; PAF, paroxysmal atrial fibrillation;

Skeletal muscle:

Baseline

Baseline MRI results are shown in table-2.

There was no significant difference in un-indexed skeletal muscle CSA or mass between the groups, however both AS groups with and without T2DM co-morbidity displayed significantly reduced skeletal muscle mass indexed to BMI (p=0.0004). At baseline T2DM participants did not show significantly lower SMM versus isolated AS patients. Expectantly, male participants showed significantly increased SM CSA (male: 12[11,12]m/kg/m^2, female:8[8,9]m/kg/m^2, p=0.0001).

Six months after AVR

Longitudinal changes in skeletal muscle measurements are shown in table-3.

6-months post AVR AS patients with T2DM co-morbidity showed significantly reduced skeletal muscle CSA versus patients with isolated AS. This was apparent when SM CSA was indexed to both height (Iso-AS: 103[97,110] cm/m^2 vs AS-DM: 95[87,103] cm/m^2, p=0.02) and BMI (Iso-AS: 11[10,12]m/kg/m^2 vs AS-DM: 9[8,10] m/kg/m^2, p=0.03), figure-3.

6-minute walk test

Baseline

Pre-operative 6-minute walk test distance did not differ significantly between AS groups with and without T2DM (Iso-AS: 396[365,436]m vs AS-DM: 360[306,415]m, p=0.14).

Six months after AVR

At 6-months post-AVR AS patients without T2DM demonstrated improved physical performance after AVR with a longer 6-minute walk distance compared to baseline (396(365,436) to 434(398,472) m, p=0.02). An improvement in exercise tolerance was not observed in AS patients with T2DM (360(306,415) to 331(267,393) m, p=0.45).

Table 2: Baseline differences in skeletal muscle

Variable	HV n=10	AS without T2DM n=65	T2DM and AS n=30	P value
Thigh SM CSA, cm^2	343(285,402)	297(276,318)	303(277,329)	0.23
Thigh SMM, Kg	3.6(3,4.2)	3.0(2.8,3.3)	3.2(2.9,3.4)	0.26
Thigh SM CSA/height, cm/m^2	200(170,230)	175(163,186)	178(165,190)	0.18
Thigh SM CSA / BMI, $cm/kg/m^2$	13(11,16)	11(10,12)	10(9,11)*	**0.01**
SMM, indexed to height, Kg/m^2	1.2(1.1,1.4)	1.1(0.9,1.3)	1.0(0.9,1.1)	0.18
SMM, indexed to BMI	0.14(0.12,0.16)	011(0.10,0.12)†	0.10(0.08,0.11)*	**0.0004**

BMI indicates body mass index; CSA, cross-sectional area; SMM, skeletal muscle mass;
€ signifies p<0.05 between T2DM and AS group and Iso-AS, * signifies p<0.05 between T2DM and AS group and HV, † signifies p≤0.05 between Iso-AS and HV.

Table 3: Longitudinal changes in skeletal muscle and clinical parameters following AVR

	Aortic stenosis without T2DM		Aortic stenosis with T2DM	
Variable	**Pre-AVR**	**Post-AVR**	**Pre-AVR**	**Post-AVR**
NT- proBNP, ng/L	377 (181-2039)	302(210-652)	404(201-1019)	333(121-809)
6 min walk test, m	360 (306,415)	434(398,472)	396(365,426)	331(267,393**)**
Thigh SM CSA, cm²	297(276,318)	298(275,321)	303(277,329)	275(243,307)
Thigh SM CSA / BMI, cm/kg/m²	11(10,12)	11(10,12)	10(9,11)	9(8,10)
Thigh SMM, Kg	3.0(2.8,3.3)	3.0(2.7,3.3)	3.2(2.9,3.4)	2.9(2.5,3.2)
SMM, indexed to height, Kg/m²	1.1(0.9,1.3)	1.1(1.0,1.1)	1.0(0.9,1.1)	0.9(0.7,1.0)
SMM, indexed to BMI	0.11(0.10,0.12)	0.11(0.10,0.12)	0.10(9,11)	0.09(0.08,0.10)

Values are means with 95% confidence intervals or percentages. BMI indicates body mass index; CSA, cross-sectional area; SMM, skeletal muscle mass;

Figure 3: Baseline differences in skeletal muscle cross sectional area indexed to body mass index between healthy volunteers, isolated aortic stenosis and combined aortic stenosis and type two diabetes.

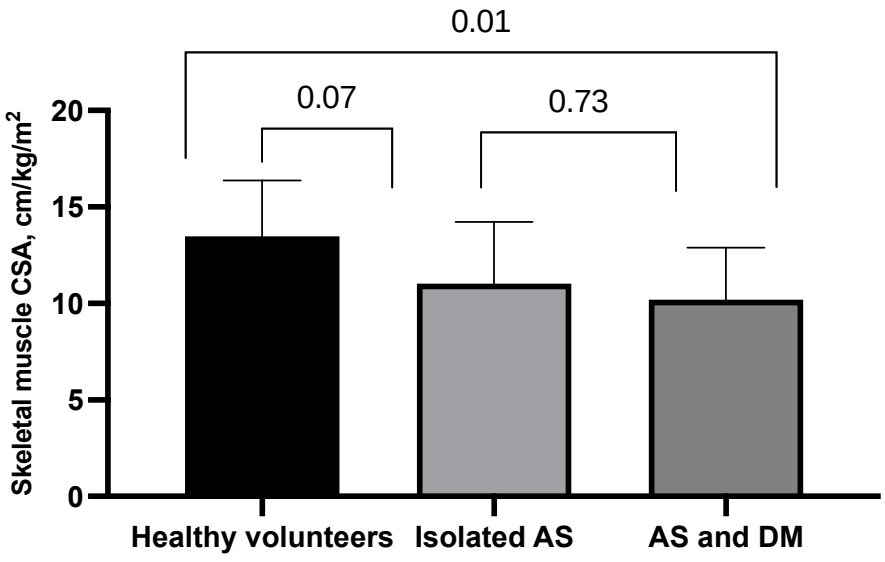

Clinical outcomes

Length of hospital stay did not differ significantly between the AS groups with and without T2DM (Iso-AS: 7[6,8] days vs AS-DM:8[6,10] days, p=0.77).

This preliminary study was not designed to detect clinical outcome differences between the AS patients with and without T2DM. However, participants were followed up for a median of 13-months (IQR:10-26months) after surgical or transcatheter AVR. There was numerically a higher incidence of cardiovascular mortality in T2DM comorbidity group than the AS group without T2DM (Hazard ratio 7.6; 95% CI: 0.9-64, p=0.04).

Correlations

No association was seen between SMM and all-cause mortality, regardless of indexing metric, however a negative correlation was observed between SMM and length of hospital stay (r=-0.72, p=0.001). In addition, a positive correlation was seen between SMM and 6-minute walk test distance (r=0.78, p=0.002).

Whilst no significant correlation was observed between SMM and HbA1c (p=0.06) or fasting glucose (p=0.24) a modest negative correlation was seen between insulin resistance measured by HOMA-IR and SMM (r=-0.23, p=0.04).

Multiple regression analysis

The correlation between insulin resistance (HOMA-IR) and SMM was also seen when adjusting for the variables of age and sex (β-0.002, SE 0.0009, p=0.04). Older age was associated with lower SM CSA (p=0.001), however CFS did not show significant relationship with SMM (p=0.32).

7.5 Discussion

In this prospective longitudinal study of severe symptomatic AS patients undergoing AVR by surgical or transcatheter approach, comorbidity with T2DM was associated with sarcopenia and residual impairment in functional exercise capacity at 6-months post AVR compared to

patients without T2DM. Of note both AS groups with and without T2DM co-morbidity displayed relative sarcopenia at baseline compared to age matched healthy controls, but whilst AVR appeared highly effective at improving exercise capacity in isolated AS patients, this was not seen in those with co-morbid T2DM. A negative correlation was observed between insulin resistance, as measured by HOMA-IR, and skeletal muscle mass, suggesting that the post operative recovery of skeletal muscle mass and function may be jeopardised by increasing insulin resistance in patients with T2DM co-morbidity.

Diabetes and sarcopenia

Normal ageing is associated with significant changes in body composition with reduction in skeletal muscle mass of up to 40% between the ages 20-70 years[349]. However, the additional presence of insulin resistance in ageing populations hastens skeletal muscle loss and functional decline. Sarcopenic obesity, the presence of relative sarcopenia in individuals with increased adiposity, represents a confluence of ageing demographics and the obesity epidemic[350]. The prevalence of sarcopenic obesity is as high as 20% in individuals over the age of 80 years and results in a vicious cycle of loss of muscle mass, mobility, and increased insulin resistance[350,351]. With increasing use of transcatheter AVR in elderly populations, the impact of sarcopenic obesity on post operative functional recovery may be increasingly significant.

Whilst several neurohormonal, immunological, nutritional and exercise related factors contribute to age related decline in lean muscle mass, there are intrinsic metabolic derangements inherent to the DM phenotype that exacerbate muscle loss. Firstly, DM is characterised by decreased mitochondrial oxidative capacity in both cardiac and skeletal myocytes [36,38,352]. Insulin and mitochondria are interdependent, through the inhibitory effects of insulin on FOXO1, with insulin signalling therefore crucial to maintaining the integrity of the mitochondrial electron transport chain (ETC)[353]. Additionally, chronic exposure to reactive oxygen species (ROS) in DM may alter mitochondrial function and lead to insulin resistance[353]. Lower mitochondrial capacity has been shown to be closely linked to exercise impairment [354]. It is also seen that the response to oxidative stress is impaired in aged mitochondria, compounding the impact of co-morbid DM in elderly populations [355]. Secondly, intramyocellular lipid accumulation which contributes to skeletal muscle ageing, is exacerbated in DM with increased circulating free fatty acids and impaired beta-oxidation[356].

Thirdly, a synergistic relationship between myocellular lipid accumulation and proinflammatory pathways has been observed[356].

Clinical perspective

Our results highlight several clinically relevant new findings, firstly severe AS patients with DM comorbidity display significantly impaired recovery of functional exercise capacity at 6 months following AVR, therefore residual sarcopenic obesity and functional limitation may account for some of the worsened morbidity seen in DM patients following aortic valve intervention[331,332,334]. Secondly, although caution must be exercised over inferences regarding causality, our results suggest a link between increasing sarcopenia and insulin resistance in AS patients, suggesting a potential role for targeted medical therapy and lifestyle intervention in DM patients prior to cardiac surgery. However further larger studies are needed to fully assess if targeted interventions have prognostic benefit in this group. Thirdly, with increasingly refined risk stratification in patients with severe AS to evaluate those that may benefit from earlier intervention, assessment of sarcopenia using MRI or 6-minute walk test, or the presence of diabetes co-morbidity may be incorporated into traditional surgical risk and frailty scoring systems. Interestingly in our cohort Rockwood score was not seen to correlate significantly with skeletal muscle mass, suggesting use of additional imaging or functional assessments of frailty may be beneficial in AS patients.

Limitations

This work had several limitations. A small sample recruited at a single site increases the risk of bias and type I error, while the study may be underpowered to identify subtle correlations with clinical outcomes. Due to the cross-sectional nature of the study causality of the observed differences cannot be inferred.

Sarcopenia is a complex process defined by both skeletal muscle loss and functional impairment. Whilst 6-minute walk test was used for assessment of functional exercise capacity in this cohort, the influence of additional confounding factors, such as cardiovascular function, on 6-minute walk test distance must be considered.

The cost and complexity of analysis may limit the wider application of MR imaging to assess SM mass in AS patients pre-operatively.

Chapter 8

General Conclusions

To the best of my knowledge, this work has shown for the first time that co-morbid T2DM is associated with exacerbated reductions in myocardial PCr/ATP ratio inherent to severe aortic stenosis and hypertrophic cardiomyopathy and leads to a worsening of coronary microvascular function with reductions in global stress myocardial blood flow. Detrimental impacts were also seen in myocardial scar burden in patients with HCM and T2DM, and an additive worsening of systolic and diastolic left ventricular contractile function. These findings may go some way to explain the increased morbidity and mortality in subjects with co-morbid HCM and T2DM[195]. These results also demonstrate deleterious, residual myocardial alterations in patients with severe AS and T2DM, which persist at least six months following aortic valve replacement and may account for the increased post procedural cardiovascular mortality observed in this cohort[178]. Overall, however, as these studies are observational, it is not possible to fully determine whether the observed associations between high-energy phosphate metabolism, perfusion and cardiac structural and functional changes are causal.

The findings in this work relied heavily upon use of cardiac ^{31}P-MRS, despite its longstanding use within the field of cardiac metabolic research, its wider clinical application is yet to be established. This work demonstrates a modified, shortened, free-breathing supine ^{31}P-MRS protocol which it is hoped may allow for the increased use of the technique in a wider patient group.

Ultimately this work demonstrates the potential power of both CMR and cardiac ^{31}P-MRS as tools to identify sub-clinical structural, functional, and metabolic derangements that may allow for more refined identification of high-risk patients with cardiometabolic co-morbidities.

However, the answers provided by this thesis must be seen to provoke several further questions, larger multi-centre studies are needed to fully establish both the causality of the associations described, and if targeted therapeutic interventions, aimed at reversing the energetic impairment or improving myocardial perfusion, yield any tangible benefit in-terms of patient outcomes. It also remains to be shown that the adoption of advanced MR imaging biomarkers into traditional risk scoring systems for HCM and AS, will allow identification of individuals at increased risk of adverse events.

It is hoped that the results of this work may represent an early step towards a more holistic approach towards the treatment of AS and HCM, one that fully recognises the importance of cardiometabolic co-morbidity.

Bibliography

References

1. Rubler S, Dlugash J, Yuceoglu YZ, Kumral T, Branwood AW, Grishman A. New type of cardiomyopathy associated with diabetic glomerulosclerosis. *Am J Cardiol.* 1972;30(6):595-602.
2. Kannel WB, Hjortland M, Castelli WP. Role of diabetes in congestive heart failure: the Framingham study. *Am J Cardiol.* 1974;34(1):29-34.
3. Rydén L, Grant PJ, Anker SD, et al. ESC Guidelines on diabetes, pre-diabetes, and cardiovascular diseases developed in collaboration with the EASD: the Task Force on diabetes, pre-diabetes, and cardiovascular diseases of the European Society of Cardiology (ESC) and developed in collaboration with the European Association for the Study of Diabetes (EASD). *Eur Heart J.* 2013;34(39):3035-3087.
4. Jia G, Hill MA, Sowers JR. Diabetic Cardiomyopathy. *Circulation Research.* 2018;122(4):624-638.
5. Dillmann WH. Diabetic Cardiomyopathy. *Circulation Research.* 2019;124(8):1160-1162.
6. Maack C, Lehrke M, Backs J, et al. Heart failure and diabetes: metabolic alterations and therapeutic interventions: a state-of-the-art review from the Translational Research Committee of the Heart Failure Association-European Society of Cardiology. *Eur Heart J.* 2018;39(48):4243-4254.
7. Bertoni AG, Hundley WG, Massing MW, Bonds DE, Burke GL, Goff DC, Jr. Heart failure prevalence, incidence, and mortality in the elderly with diabetes. *Diabetes Care.* 2004;27(3):699-703.
8. Thrainsdottir IS, Aspelund T, Thorgeirsson G, et al. The association between glucose abnormalities and heart failure in the population-based Reykjavik study. *Diabetes Care.* 2005;28(3):612-616.
9. Yap J, Tay WT, Teng THK, et al. Association of Diabetes Mellitus on Cardiac Remodeling, Quality of Life, and Clinical Outcomes in Heart Failure With Reduced and Preserved Ejection Fraction. *Journal of the American Heart Association.* 2019;8(17):e013114.
10. Devereux RB, Roman MJ, Liu JE, et al. An appraisal of echocardiography as an epidemiological tool. The Strong Heart Study. *Ann Epidemiol.* 2003;13(4):238-244.
11. Bluemke DA, Kronmal RA, Lima JA, et al. The relationship of left ventricular mass and geometry to incident cardiovascular events: the MESA (Multi-Ethnic Study of Atherosclerosis) study. *J Am Coll Cardiol.* 2008;52(25):2148-2155.
12. Levy D, Garrison RJ, Savage DD, Kannel WB, Castelli WP. Prognostic implications of echocardiographically determined left ventricular mass in the Framingham Heart Study. *N Engl J Med.* 1990;322(22):1561-1566.
13. Salvador DB, Gamba MR, Gonzalez-Jaramillo N, et al. Diabetes and Myocardial Fibrosis: A Systematic Review and Meta-Analysis. *JACC: Cardiovascular Imaging.* 2022;15(5):796-808.

14. Gulati A, Jabbour A, Ismail TF, et al. Association of fibrosis with mortality and sudden cardiac death in patients with nonischemic dilated cardiomyopathy. *Jama.* 2013;309(9):896-908.
15. Boucher J, Kleinridders A, Kahn CR. Insulin receptor signaling in normal and insulin-resistant states. *Cold Spring Harb Perspect Biol.* 2014;6(1).
16. Bertero E, Maack C. Metabolic remodelling in heart failure. *Nature Reviews Cardiology.* 2018;15(8):457-470.
17. Faselis C, Katsimardou A, Imprialos K, Deligkaris P, Kallistratos M, Dimitriadis K. Microvascular Complications of Type 2 Diabetes Mellitus. *Curr Vasc Pharmacol.* 2020;18(2):117-124.
18. Jia G, DeMarco VG, Sowers JR. Insulin resistance and hyperinsulinaemia in diabetic cardiomyopathy. *Nature Reviews Endocrinology.* 2016;12(3):144-153.
19. Rosenkranz AC, Hood SG, Woods RL, Dusting GJ, Ritchie RH. B-type natriuretic peptide prevents acute hypertrophic responses in the diabetic rat heart: importance of cyclic GMP. *Diabetes.* 2003;52(9):2389-2395.
20. Wang J, Song Y, Wang Q, Kralik PM, Epstein PN. Causes and characteristics of diabetic cardiomyopathy. *Rev Diabet Stud.* 2006;3(3):108-117.
21. Passino C, Barison A, Vergaro G, et al. Markers of fibrosis, inflammation, and remodeling pathways in heart failure. *Clin Chim Acta.* 2015;443:29-38.
22. Shome JS, Perera D, Plein S, Chiribiri A. Current perspectives in coronary microvascular dysfunction. *Microcirculation.* 2017;24(1):e12340.
23. Xu YZ, Zhang X, Wang L, et al. An increased circulating angiotensin II concentration is associated with hypoadiponectinemia and postprandial hyperglycemia in men with nonalcoholic fatty liver disease. *Intern Med.* 2013;52(8):855-861.
24. Ashrafian H, Neubauer S. Metabolomic profiling of cardiac substrate utilization: fanning the flames of systems biology? *Circulation.* 2009;119(13):1700-1702.
25. Lopaschuk GD, Ussher JR, Folmes CD, Jaswal JS, Stanley WC. Myocardial fatty acid metabolism in health and disease. *Physiol Rev.* 2010;90(1):207-258.
26. Neubauer S. The failing heart--an engine out of fuel. *N Engl J Med.* 2007;356(11):1140-1151.
27. Carley AN, Taegtmeyer H, Lewandowski ED. Matrix revisited: mechanisms linking energy substrate metabolism to the function of the heart. *Circ Res.* 2014;114(4):717-729.
28. Mootha VK, Arai AE, Balaban RS. Maximum oxidative phosphorylation capacity of the mammalian heart. *Am J Physiol.* 1997;272(2 Pt 2):H769-775.
29. Oriaku G, Xiang B, Dai G, et al. Effects of retrograde cardioplegia on myocardial perfusion and energy metabolism in immature porcine myocardium. *J Thorac Cardiovasc Surg.* 2000;119(6):1102-1109.
30. Glatz JFC, Bonen A, Ouwens DM, Luiken JJFP. Regulation of Sarcolemmal Transport of Substrates in the Healthy and Diseased Heart. *Cardiovascular Drugs and Therapy.* 2006;20(6):471-476.
31. Lopaschuk GD, Ussher JR. Evolving Concepts of Myocardial Energy Metabolism. *Circulation Research.* 2016;119(11):1173-1176.
32. Stanley WC, Recchia FA, Lopaschuk GD. Myocardial Substrate Metabolism in the Normal and Failing Heart. *Physiological Reviews.* 2005;85(3):1093-1129.
33. Murashige D, Jang C, Neinast M, et al. Comprehensive quantification of fuel use by the failing and nonfailing human heart. *Science.* 2020;370(6514):364-368.
34. Bessman SP, Geiger PJ. Transport of energy in muscle: the phosphorylcreatine shuttle. *Science.* 1981;211(4481):448-452.

35. Ingwall JS. *ATP and the Heart.* Vol 11: Springer Science & Business Media; 2002.
36. Levelt E, Rodgers CT, Clarke WT, et al. Cardiac energetics, oxygenation, and perfusion during increased workload in patients with type 2 diabetes mellitus. *Eur Heart J.* 2016;37(46):3461-3469.
37. Dassanayaka S, Readnower RD, Salabei JK, et al. High glucose induces mitochondrial dysfunction independently of protein O-GlcNAcylation. *Biochem J.* 2015;467(1):115-126.
38. Scheuermann-Freestone M, Madsen PL, Manners D, et al. Abnormal cardiac and skeletal muscle energy metabolism in patients with type 2 diabetes. *Circulation.* 2003;107(24):3040-3046.
39. Thirunavukarasu S, Jex N, Chowdhary A, et al. Empagliflozin Treatment Is Associated With Improvements in Cardiac Energetics and Function and Reductions in Myocardial Cellular Volume in Patients With Type 2 Diabetes. *Diabetes.* 2021;70(12):2810-2822.
40. Taegtmeyer H, McNulty P, Young ME. Adaptation and maladaptation of the heart in diabetes: Part I: general concepts. *Circulation.* 2002;105(14):1727-1733.
41. Rodrigues B, Cam MC, McNeill JH. Metabolic disturbances in diabetic cardiomyopathy. *Molecular and Cellular Biochemistry.* 1998;180(1):53-57.
42. Kruljac I, Ćaćić M, Ćaćić P, et al. Diabetic ketosis during hyperglycemic crisis is associated with decreased all-cause mortality in patients with type 2 diabetes mellitus. *Endocrine.* 2017;55(1):139-143.
43. Teshima Y, Takahashi N, Nishio S, et al. Production of reactive oxygen species in the diabetic heart. Roles of mitochondria and NADPH oxidase. *Circ J.* 2014;78(2):300-306.
44. Montaigne D, Marechal X, Coisne A, et al. Myocardial contractile dysfunction is associated with impaired mitochondrial function and dynamics in type 2 diabetic but not in obese patients. *Circulation.* 2014;130(7):554-564.
45. Levelt E, Gulsin G, Neubauer S, McCann GP. MECHANISMS IN ENDOCRINOLOGY: Diabetic cardiomyopathy: pathophysiology and potential metabolic interventions state of the art review. *Eur J Endocrinol.* 2018;178(4):R127-r139.
46. Himms-Hagen J, Harper ME. Physiological role of UCP3 may be export of fatty acids from mitochondria when fatty acid oxidation predominates: an hypothesis. *Exp Biol Med (Maywood).* 2001;226(2):78-84.
47. Schaffer JE. Lipotoxicity: Many Roads to Cell Dysfunction and Cell Death: Introduction to a Thematic Review Series. *J Lipid Res.* 2016;57(8):1327-1328.
48. Jia G, Habibi J, DeMarco VG, et al. Endothelial Mineralocorticoid Receptor Deletion Prevents Diet-Induced Cardiac Diastolic Dysfunction in Females. *Hypertension.* 2015;66(6):1159-1167.
49. Pal PB, Sonowal H, Shukla K, Srivastava SK, Ramana KV. Aldose Reductase Mediates NLRP3 Inflammasome-Initiated Innate Immune Response in Hyperglycemia-Induced Thp1 Monocytes and Male Mice. *Endocrinology.* 2017;158(10):3661-3675.
50. Liu W, Chen P, Deng J, Lv J, Liu J. Resveratrol and polydatin as modulators of Ca(2+) mobilization in the cardiovascular system. *Ann N Y Acad Sci.* 2017;1403(1):82-91.
51. Belke DD, Swanson EA, Dillmann WH. Decreased sarcoplasmic reticulum activity and contractility in diabetic db/db mouse heart. *Diabetes.* 2004;53(12):3201-3208.
52. Bisognano JD, Weinberger HD, Bohlmeyer TJ, et al. Myocardial-directed overexpression of the human beta(1)-adrenergic receptor in transgenic mice. *J Mol Cell Cardiol.* 2000;32(5):817-830.

53. Murthy VL, Naya M, Foster CR, et al. Association between coronary vascular dysfunction and cardiac mortality in patients with and without diabetes mellitus. *Circulation.* 2012;126(15):1858-1868.
54. Vincent MA, Clerk LH, Lindner JR, et al. Microvascular recruitment is an early insulin effect that regulates skeletal muscle glucose uptake in vivo. *Diabetes.* 2004;53(6):1418-1423.
55. Widyantoro B, Emoto N, Nakayama K, et al. Endothelial cell–derived endothelin-1 promotes cardiac fibrosis in diabetic hearts through stimulation of endothelial-to-mesenchymal transition. *Circulation.* 2010;121(22):2407-2418.
56. Kenchaiah S, Evans JC, Levy D, et al. Obesity and the risk of heart failure. *N Engl J Med.* 2002;347(5):305-313.
57. Després JP. The insulin resistance-dyslipidemic syndrome of visceral obesity: effect on patients' risk. *Obes Res.* 1998;6 Suppl 1:8s-17s.
58. Okura T, Nakata Y, Yamabuki K, Tanaka K. Regional body composition changes exhibit opposing effects on coronary heart disease risk factors. *Arterioscler Thromb Vasc Biol.* 2004;24(5):923-929.
59. Van Gaal LF, Mertens IL, De Block CE. Mechanisms linking obesity with cardiovascular disease. *Nature.* 2006;444(7121):875-880.
60. Fantuzzi G, Mazzone T. Adipose tissue and atherosclerosis: exploring the connection. *Arterioscler Thromb Vasc Biol.* 2007;27(5):996-1003.
61. Pou KM, Massaro JM, Hoffmann U, et al. Visceral and Subcutaneous Adipose Tissue Volumes Are Cross-Sectionally Related to Markers of Inflammation and Oxidative Stress: The Framingham Heart Study. *Circulation.* 2007;116(11):1234-1241.
62. Després J-P. The Insulin Resistance—Dyslipidemic Syndrome of Visceral Obesity: Effect on Patients' Risk. *Obesity Research.* 1998;6(S1):8S-17S.
63. Schmidt MI, Duncan BB, Sharrett AR, et al. Markers of inflammation and prediction of diabetes mellitus in adults (Atherosclerosis Risk in Communities study): a cohort study. *The Lancet.* 1999;353(9165):1649-1652.
64. Antonopoulos AS, Antoniades C. Cardiac Magnetic Resonance Imaging of Epicardial and Intramyocardial Adiposity as an Early Sign of Myocardial Disease. *Circulation: Cardiovascular Imaging.* 2018;11(8):e008083.
65. Mazurek T, Zhang L, Zalewski A, et al. Human epicardial adipose tissue is a source of inflammatory mediators. *Circulation.* 2003;108(20):2460-2466.
66. Venteclef N, Guglielmi V, Balse E, et al. Human epicardial adipose tissue induces fibrosis of the atrial myocardium through the secretion of adipo-fibrokines. *Eur Heart J.* 2015;36(13):795-805a.
67. Greulich S, Maxhera B, Vandenplas G, et al. Secretory products from epicardial adipose tissue of patients with type 2 diabetes mellitus induce cardiomyocyte dysfunction. *Circulation.* 2012;126(19):2324-2334.
68. Ingwall JS, Weiss RG. Is the failing heart energy starved? On using chemical energy to support cardiac function. *Circ Res.* 2004;95(2):135-145.
69. Ingwall JS. Energy metabolism in heart failure and remodelling. *Cardiovasc Res.* 2009;81(3):412-419.
70. Krajčová A, Urban T, Megvinet D, et al. High resolution respirometry to assess function of mitochondria in native homogenates of human heart muscle. *PLoS One.* 2020;15(1):e0226142.
71. Hudsmith LE, Neubauer S. Detection of myocardial disorders by magnetic resonance spectroscopy. *Nat Clin Pract Cardiovasc Med.* 2008;5 Suppl 2:S49-56.

72. Tyler DJ, Emmanuel Y, Cochlin LE, et al. Reproducibility of 31P cardiac magnetic resonance spectroscopy at 3 T. *NMR Biomed.* 2009;22(4):405-413.
73. Dass S, Cochlin LE, Suttie JJ, et al. Exacerbation of cardiac energetic impairment during exercise in hypertrophic cardiomyopathy: a potential mechanism for diastolic dysfunction. *European Heart Journal.* 2015;36(24):1547-1554.
74. Dass S, Holloway C, Suttie J, et al. Patients with Dilated Cardiomyopathy (DCM) have appropriate myocardial oxygenation response to vasodilator stress. *Journal of Cardiovascular Magnetic Resonance.* 2013;15(1):O68.
75. Mahmod M, Francis JM, Pal N, et al. Myocardial perfusion and oxygenation are impaired during stress in severe aortic stenosis and correlate with impaired energetics and subclinical left ventricular dysfunction. *J Cardiovasc Magn Reson.* 2014;16(1):29.
76. Nakamura M, Sadoshima J. Mechanisms of physiological and pathological cardiac hypertrophy. *Nature Reviews Cardiology.* 2018;15(7):387-407.
77. Miyazono Y, Hirashima S, Ishihara N, Kusukawa J, Nakamura K-i, Ohta K. Uncoupled mitochondria quickly shorten along their long axis to form indented spheroids, instead of rings, in a fission-independent manner. *Scientific Reports.* 2018;8(1):350.
78. Shimizu I, Minamino T. Physiological and pathological cardiac hypertrophy. *J Mol Cell Cardiol.* 2016;97:245-262.
79. Saltiel AR, Kahn CR. Insulin signalling and the regulation of glucose and lipid metabolism. *Nature.* 2001;414(6865):799-806.
80. Maillet M, van Berlo JH, Molkentin JD. Molecular basis of physiological heart growth: fundamental concepts and new players. *Nat Rev Mol Cell Biol.* 2013;14(1):38-48.
81. DeBosch B, Treskov I, Lupu TS, et al. Akt1 is required for physiological cardiac growth. *Circulation.* 2006;113(17):2097-2104.
82. Truebestein L, Hornegger H, Anrather D, et al. Structure of autoinhibited Akt1 reveals mechanism of PIP(3)-mediated activation. *Proc Natl Acad Sci U S A.* 2021;118(33).
83. Takimoto E, Koitabashi N, Hsu S, et al. Regulator of G protein signaling 2 mediates cardiac compensation to pressure overload and antihypertrophic effects of PDE5 inhibition in mice. *J Clin Invest.* 2009;119(2):408-420.
84. Rainer PP, Kass DA. Old dog, new tricks: novel cardiac targets and stress regulation by protein kinase G. *Cardiovasc Res.* 2016;111(2):154-162.
85. Carnicer R, Crabtree MJ, Sivakumaran V, Casadei B, Kass DA. Nitric oxide synthases in heart failure. *Antioxidants & redox signaling.* 2013;18(9):1078-1099.
86. Kukreja RC, Salloum FN, Das A. Cyclic guanosine monophosphate signaling and phosphodiesterase-5 inhibitors in cardioprotection. *Journal of the American College of Cardiology.* 2012;59(22):1921-1927.
87. Saxton RA, Sabatini DM. mTOR Signaling in Growth, Metabolism, and Disease. *Cell.* 2017;168(6):960-976.
88. Zhang D, Contu R, Latronico MV, et al. MTORC1 regulates cardiac function and myocyte survival through 4E-BP1 inhibition in mice. *J Clin Invest.* 2010;120(8):2805-2816.
89. Sadoshima J, Izumo S. Rapamycin selectively inhibits angiotensin II-induced increase in protein synthesis in cardiac myocytes in vitro. Potential role of 70-kD S6 kinase in angiotensin II-induced cardiac hypertrophy. *Circ Res.* 1995;77(6):1040-1052.
90. Shioi T, McMullen JR, Tarnavski O, et al. Rapamycin attenuates load-induced cardiac hypertrophy in mice. *Circulation.* 2003;107(12):1664-1670.

91. Kushwaha SS, Raichlin E, Sheinin Y, et al. Sirolimus affects cardiomyocytes to reduce left ventricular mass in heart transplant recipients. *Eur Heart J.* 2008;29(22):2742-2750.
92. Holtwick R, van Eickels M, Skryabin BV, et al. Pressure-independent cardiac hypertrophy in mice with cardiomyocyte-restricted inactivation of the atrial natriuretic peptide receptor guanylyl cyclase-A. *J Clin Invest.* 2003;111(9):1399-1407.
93. Kerkelä R, Ulvila J, Magga J. Natriuretic Peptides in the Regulation of Cardiovascular Physiology and Metabolic Events. *J Am Heart Assoc.* 2015;4(10):e002423.
94. Oka T, Akazawa H, Naito AT, Komuro I. Angiogenesis and cardiac hypertrophy: maintenance of cardiac function and causative roles in heart failure. *Circ Res.* 2014;114(3):565-571.
95. Carmeliet P, Ng YS, Nuyens D, et al. Impaired myocardial angiogenesis and ischemic cardiomyopathy in mice lacking the vascular endothelial growth factor isoforms VEGF164 and VEGF188. *Nat Med.* 1999;5(5):495-502.
96. Moslehi JJ. Cardiovascular Toxic Effects of Targeted Cancer Therapies. *N Engl J Med.* 2016;375(15):1457-1467.
97. Patten IS, Rana S, Shahul S, et al. Cardiac angiogenic imbalance leads to peripartum cardiomyopathy. *Nature.* 2012;485(7398):333-338.
98. Semenza GL. Hypoxia-inducible factor 1 and cardiovascular disease. *Annu Rev Physiol.* 2014;76:39-56.
99. Shiojima I, Sato K, Izumiya Y, et al. Disruption of coordinated cardiac hypertrophy and angiogenesis contributes to the transition to heart failure. *J Clin Invest.* 2005;115(8):2108-2118.
100. Izumiya Y, Shiojima I, Sato K, Sawyer DB, Colucci WS, Walsh K. Vascular endothelial growth factor blockade promotes the transition from compensatory cardiac hypertrophy to failure in response to pressure overload. *Hypertension.* 2006;47(5):887-893.
101. van Rooij E, Liu N, Olson EN. MicroRNAs flex their muscles. *Trends in Genetics.* 2008;24(4):159-166.
102. Huang Z-P, Chen J, Seok HY, et al. MicroRNA-22 Regulates Cardiac Hypertrophy and Remodeling in Response to Stress. *Circulation Research.* 2013;112(9):1234-1243.
103. Rupert CE, Coulombe KL. The roles of neuregulin-1 in cardiac development, homeostasis, and disease. *Biomark Insights.* 2015;10(Suppl 1):1-9.
104. Odiete O, Hill MF, Sawyer DB. Neuregulin in cardiovascular development and disease. *Circ Res.* 2012;111(10):1376-1385.
105. Waring CD, Vicinanza C, Papalamprou A, et al. The adult heart responds to increased workload with physiologic hypertrophy, cardiac stem cell activation, and new myocyte formation. *Eur Heart J.* 2014;35(39):2722-2731.
106. Fukazawa R, Miller TA, Kuramochi Y, et al. Neuregulin-1 protects ventricular myocytes from anthracycline-induced apoptosis via erbB4-dependent activation of PI3-kinase/Akt. *J Mol Cell Cardiol.* 2003;35(12):1473-1479.
107. Bersell K, Arab S, Haring B, Kühn B. Neuregulin1/ErbB4 signaling induces cardiomyocyte proliferation and repair of heart injury. *Cell.* 2009;138(2):257-270.
108. D'Uva G, Aharonov A, Lauriola M, et al. ERBB2 triggers mammalian heart regeneration by promoting cardiomyocyte dedifferentiation and proliferation. *Nat Cell Biol.* 2015;17(5):627-638.
109. Turkbey EB, McClelland RL, Kronmal RA, et al. The impact of obesity on the left ventricle: the Multi-Ethnic Study of Atherosclerosis (MESA). *JACC: Cardiovascular Imaging.* 2010;3(3):266-274.

110. Taegtmeyer H, Sen S, Vela D. Return to the fetal gene program: a suggested metabolic link to gene expression in the heart. *Ann N Y Acad Sci.* 2010;1188:191-198.
111. Schiattarella GG, Hill JA. Inhibition of hypertrophy is a good therapeutic strategy in ventricular pressure overload. *Circulation.* 2015;131(16):1435-1447.
112. Perrino C, Naga Prasad SV, Mao L, et al. Intermittent pressure overload triggers hypertrophy-independent cardiac dysfunction and vascular rarefaction. *J Clin Invest.* 2006;116(6):1547-1560.
113. Anderson ME, Brown JH, Bers DM. CaMKII in myocardial hypertrophy and heart failure. *J Mol Cell Cardiol.* 2011;51(4):468-473.
114. Schulman H, Anderson ME. Ca/Calmodulin-dependent Protein Kinase II in Heart Failure. *Drug Discov Today Dis Mech.* 2010;7(2):e117-e122.
115. Zhang CL, McKinsey TA, Chang S, Antos CL, Hill JA, Olson EN. Class II histone deacetylases act as signal-responsive repressors of cardiac hypertrophy. *Cell.* 2002;110(4):479-488.
116. Gallo P, Latronico MVG, Gallo P, et al. Inhibition of class I histone deacetylase with an apicidin derivative prevents cardiac hypertrophy and failure. *Cardiovascular Research.* 2008;80(3):416-424.
117. Sato PY, Chuprun JK, Schwartz M, Koch WJ. The evolving impact of g protein-coupled receptor kinases in cardiac health and disease. *Physiol Rev.* 2015;95(2):377-404.
118. Woodall MC, Ciccarelli M, Woodall BP, Koch WJ. G protein-coupled receptor kinase 2: a link between myocardial contractile function and cardiac metabolism. *Circ Res.* 2014;114(10):1661-1670.
119. Schumacher SM, Koch WJ. Noncanonical Roles of G Protein-coupled Receptor Kinases in Cardiovascular Signaling. *J Cardiovasc Pharmacol.* 2017;70(3):129-141.
120. Marian AJ, Braunwald E. Hypertrophic Cardiomyopathy: Genetics, Pathogenesis, Clinical Manifestations, Diagnosis, and Therapy. *Circ Res.* 2017;121(7):749-770.
121. Thienpont B, Aronsen JM, Robinson EL, et al. The H3K9 dimethyltransferases EHMT1/2 protect against pathological cardiac hypertrophy. *J Clin Invest.* 2017;127(1):335-348.
122. Papait R, Cattaneo P, Kunderfranco P, et al. Genome-wide analysis of histone marks identifying an epigenetic signature of promoters and enhancers underlying cardiac hypertrophy. *Proc Natl Acad Sci U S A.* 2013;110(50):20164-20169.
123. Jung WI, Sieverding L, Breuer J, et al. Detection of phosphomonoester signals in proton-decoupled 31P NMR spectra of the myocardium of patients with myocardial hypertrophy. *J Magn Reson.* 1998;133(1):232-235.
124. Doenst T, Pytel G, Schrepper A, et al. Decreased rates of substrate oxidation ex vivo predict the onset of heart failure and contractile dysfunction in rats with pressure overload. *Cardiovasc Res.* 2010;86(3):461-470.
125. Huss JM, Imahashi K, Dufour CR, et al. The nuclear receptor ERRalpha is required for the bioenergetic and functional adaptation to cardiac pressure overload. *Cell Metab.* 2007;6(1):25-37.
126. d'Arcy JL, Coffey S, Loudon MA, et al. Large-scale community echocardiographic screening reveals a major burden of undiagnosed valvular heart disease in older people: the OxVALVE Population Cohort Study. *Eur Heart J.* 2016;37(47):3515-3522.
127. Baumgartner H, Falk V, Bax JJ, et al. 2017 ESC/EACTS Guidelines for the management of valvular heart disease. *Eur Heart J.* 2017;38(36):2739-2791.
128. Taniguchi T, Morimoto T, Shiomi H, et al. Initial surgical versus conservative strategies in patients with asymptomatic severe aortic stenosis. *Journal of the American College of Cardiology.* 2015;66(25):2827-2838.

129. Lancellotti P, Magne J, Dulgheru R, et al. Outcomes of Patients With Asymptomatic Aortic Stenosis Followed Up in Heart Valve Clinics. *JAMA Cardiology.* 2018;3(11):1060-1068.
130. Malaisrie SC, McDonald E, Kruse J, et al. Mortality while waiting for aortic valve replacement. *Ann Thorac Surg.* 2014;98(5):1564-1570; discussion 1570-1561.
131. Pellikka PA, Sarano ME, Nishimura RA, et al. Outcome of 622 Adults With Asymptomatic, Hemodynamically Significant Aortic Stenosis During Prolonged Follow-Up. *Circulation.* 2005;111(24):3290-3295.
132. Grothues F, Smith GC, Moon JC, et al. Comparison of interstudy reproducibility of cardiovascular magnetic resonance with two-dimensional echocardiography in normal subjects and in patients with heart failure or left ventricular hypertrophy. *Am J Cardiol.* 2002;90(1):29-34.
133. Bohbot Y, Renard C, Manrique A, et al. Usefulness of Cardiac Magnetic Resonance Imaging in Aortic Stenosis. *Circulation: Cardiovascular Imaging.* 2020;13(5):e010356.
134. Debry N, Maréchaux S, Rusinaru D, et al. Prognostic significance of left ventricular concentric remodelling in patients with aortic stenosis. *Arch Cardiovasc Dis.* 2017;110(1):26-34.
135. Dweck MR, Joshi S, Murigu T, et al. Left ventricular remodeling and hypertrophy in patients with aortic stenosis: insights from cardiovascular magnetic resonance. *Journal of Cardiovascular Magnetic Resonance.* 2012;14(1):50.
136. Kwiecinski J, Chin CWL, Everett RJ, et al. Adverse prognosis associated with asymmetric myocardial thickening in aortic stenosis. *Eur Heart J Cardiovasc Imaging.* 2018;19(3):347-356.
137. Dobson LE, Fairbairn TA, Musa TA, et al. Sex-related differences in left ventricular remodeling in severe aortic stenosis and reverse remodeling after aortic valve replacement: A cardiovascular magnetic resonance study. *Am Heart J.* 2016;175:101-111.
138. Carroll JD, Carroll EP, Feldman T, et al. Sex-associated differences in left ventricular function in aortic stenosis of the elderly. *Circulation.* 1992;86(4):1099-1107.
139. Azevedo CF, Nigri M, Higuchi ML, et al. Prognostic significance of myocardial fibrosis quantification by histopathology and magnetic resonance imaging in patients with severe aortic valve disease. *J Am Coll Cardiol.* 2010;56(4):278-287.
140. Chin CW, Messika-Zeitoun D, Shah AS, et al. A clinical risk score of myocardial fibrosis predicts adverse outcomes in aortic stenosis. *Eur Heart J.* 2016;37(8):713-723.
141. Dweck MR, Joshi S, Murigu T, et al. Midwall fibrosis is an independent predictor of mortality in patients with aortic stenosis. *J Am Coll Cardiol.* 2011;58(12):1271-1279.
142. Treibel TA, López B, González A, et al. Reappraising myocardial fibrosis in severe aortic stenosis: an invasive and non-invasive study in 133 patients. *Eur Heart J.* 2018;39(8):699-709.
143. Cheitlin MD, Robinowitz M, McAllister H, Hoffman JI, Bharati S, Lev M. The distribution of fibrosis in the left ventricle in congenital aortic stenosis and coarctation of the aorta. *Circulation.* 1980;62(4):823-830.
144. Pellman J, Zhang J, Sheikh F. Myocyte-fibroblast communication in cardiac fibrosis and arrhythmias: Mechanisms and model systems. *J Mol Cell Cardiol.* 2016;94:22-31.
145. O'Brien KD, Shavelle DM, Caulfield MT, et al. Association of angiotensin-converting enzyme with low-density lipoprotein in aortic valvular lesions and in human plasma. *Circulation.* 2002;106(17):2224-2230.
146. Rajamannan NM, Evans FJ, Aikawa E, et al. Calcific aortic valve disease: not simply a degenerative process: A review and agenda for research from the National Heart and

Lung and Blood Institute Aortic Stenosis Working Group. Executive summary: Calcific aortic valve disease-2011 update. *Circulation.* 2011;124(16):1783-1791.
147. Mohler ER, 3rd, Gannon F, Reynolds C, Zimmerman R, Keane MG, Kaplan FS. Bone formation and inflammation in cardiac valves. *Circulation.* 2001;103(11):1522-1528.
148. Rajamannan NM. Low-density lipoprotein and aortic stenosis. *Heart.* 2008;94(9):1111-1112.
149. Pawade TA, Newby DE, Dweck MR. Calcification in Aortic Stenosis. *Journal of the American College of Cardiology.* 2015;66(5):561-577.
150. Thanassoulis G, Massaro JM, Cury R, et al. Associations of long-term and early adult atherosclerosis risk factors with aortic and mitral valve calcium. *Journal of the American College of Cardiology.* 2010;55(22):2491-2498.
151. Tzolos E, Dweck MR. Threshold effect for lipoprotein(a) in aortic stenosis. *Heart.* 2021;107(17):1367-1368.
152. Cowell SJ, Newby DE, Prescott RJ, et al. A Randomized Trial of Intensive Lipid-Lowering Therapy in Calcific Aortic Stenosis. *New England Journal of Medicine.* 2005;352(23):2389-2397.
153. Chan KL, Teo K, Dumesnil JG, Ni A, Tam J. Effect of Lipid lowering with rosuvastatin on progression of aortic stenosis: results of the aortic stenosis progression observation: measuring effects of rosuvastatin (ASTRONOMER) trial. *Circulation.* 2010;121(2):306-314.
154. El Accaoui RN, Gould ST, Hajj GP, et al. Aortic valve sclerosis in mice deficient in endothelial nitric oxide synthase. *American Journal of Physiology-Heart and Circulatory Physiology.* 2014;306(9):H1302-H1313.
155. Simões e Silva AC, Silveira KD, Ferreira AJ, Teixeira MM. ACE2, angiotensin-(1-7) and Mas receptor axis in inflammation and fibrosis. *Br J Pharmacol.* 2013;169(3):477-492.
156. Peltonen T, Näpänkangas J, Ohtonen P, et al. (Pro)renin receptors and angiotensin converting enzyme 2/angiotensin-(1-7)/Mas receptor axis in human aortic valve stenosis. *Atherosclerosis.* 2011;216(1):35-43.
157. Capoulade R, Clavel MA, Mathieu P, et al. Impact of hypertension and renin–angiotensin system inhibitors in aortic stenosis. *European journal of clinical investigation.* 2013;43(12):1262-1272.
158. Bull S, Loudon M, Francis JM, et al. A prospective, double-blind, randomized controlled trial of the angiotensin-converting enzyme inhibitor Ramipril In Aortic Stenosis (RIAS trial). *Eur Heart J Cardiovasc Imaging.* 2015;16(8):834-841.
159. Aikawa E, Otto CM. Look more closely at the valve: imaging calcific aortic valve disease. In. Vol 125: Am Heart Assoc; 2012:9-11.
160. Garg V, Muth AN, Ransom JF, et al. Mutations in NOTCH1 cause aortic valve disease. *Nature.* 2005;437(7056):270-274.
161. Nkomo VT, Gardin JM, Skelton TN, Gottdiener JS, Scott CG, Enriquez-Sarano M. Burden of valvular heart diseases: a population-based study. *The Lancet.*368(9540):1005-1011.
162. Mahmod M, Bull S, Suttie JJ, et al. Myocardial steatosis and left ventricular contractile dysfunction in patients with severe aortic stenosis. *Circ Cardiovasc Imaging.* 2013;6(5):808-816.
163. Heather LC, Howell NJ, Emmanuel Y, et al. Changes in Cardiac Substrate Transporters and Metabolic Proteins Mirror the Metabolic Shift in Patients with Aortic Stenosis. *PLoS One.* 2011;6(10):e26326.
164. Tran DH, Wang ZV. Glucose Metabolism in Cardiac Hypertrophy and Heart Failure. *Journal of the American Heart Association.* 2019;8(12):e012673.

165. Luptak I, Yan J, Cui L, Jain M, Liao R, Tian R. Long-Term Effects of Increased Glucose Entry on Mouse Hearts During Normal Aging and Ischemic Stress. *Circulation.* 2007;116(8):901-909.
166. Larsson SC, Wallin A, Håkansson N, Stackelberg O, Bäck M, Wolk A. Type 1 and type 2 diabetes mellitus and incidence of seven cardiovascular diseases. *International Journal of Cardiology.* 2018;262:66-70.
167. Musa TA, Treibel TA, Vassiliou VS, et al. Myocardial Scar and Mortality in Severe Aortic Stenosis. *Circulation.* 2018;138(18):1935-1947.
168. Makkar RR, Thourani VH, Mack MJ, et al. Five-Year Outcomes of Transcatheter or Surgical Aortic-Valve Replacement. *New England Journal of Medicine.* 2020;382(9):799-809.
169. Abramowitz Y, Jilaihawi H, Chakravarty T, et al. Impact of Diabetes Mellitus on Outcomes After Transcatheter Aortic Valve Implantation. *American Journal of Cardiology.* 2016;117(10):1636-1642.
170. Singh A, Greenwood JP, Berry C, et al. Comparison of exercise testing and CMR measured myocardial perfusion reserve for predicting outcome in asymptomatic aortic stenosis: the PRognostic Importance of MIcrovascular Dysfunction in Aortic Stenosis (PRIMID AS) Study. *European Heart Journal.* 2017;38(16):1222-1229.
171. Bull S, Loudon M, Francis JM, et al. A prospective, double-blind, randomized controlled trial of the angiotensin-converting enzyme inhibitor Ramipril In Aortic Stenosis (RIAS trial). *European Heart Journal - Cardiovascular Imaging.* 2015;16(8):834-841.
172. Treibel TA, Kozor R, Schofield R, et al. Reverse Myocardial Remodeling Following Valve Replacement in Patients With Aortic Stenosis. *Journal of the American College of Cardiology.* 2018;71(8):860-871.
173. Culler SD, Cohen DJ, Brown PP, et al. *The Annals of Thoracic Surgery.* 2018;105(4):1137-1143.
174. López-de-Andrés A, Perez-Farinos NA-O, de Miguel-Díez J, et al. Impact of type 2 diabetes mellitus in the utilization and in-hospital outcomes of surgical aortic valve replacement in Spain (2001-2015). (1475-2840 (Electronic)).
175. Halkos ME, Kilgo P, Lattouf OM, et al. The Effect of Diabetes Mellitus on In-Hospital and Long-Term Outcomes After Heart Valve Operations. *The Annals of Thoracic Surgery.* 2010;90(1):124-130.
176. Auensen A, Hussain AI, Bendz B, et al. Morbidity outcomes after surgical aortic valve replacement. *Open Heart.* 2017;4(1):e000588.
177. Dimagli A, Sinha S, Caputo M, Angelini GD, Benedetto U. Trend in morbidity and mortality in surgical aortic valve replacement: a retrospective, observational, single-centre study. *Interact Cardiovasc Thorac Surg.* 2020;31(6):796-802.
178. Anwaruddin S, Desai ND, Vemulapalli S, et al. Evaluating Out-of-Hospital 30-Day Mortality After Transfemoral Transcatheter Aortic Valve Replacement: An STS/ACC TVT Analysis. *JACC Cardiovasc Interv.* 2021;14(3):261-274.
179. Levelt E, Rodgers CT, Clarke WT, et al. Cardiac energetics, oxygenation, and perfusion during increased workload in patients with type 2 diabetes mellitus. *European Heart Journal.* 2016;37(46):3461-3469.
180. Levelt E, Mahmod M, Piechnik SK, et al. Relationship Between Left Ventricular Structural and Metabolic Remodeling in Type 2 Diabetes. *Diabetes.* 2016;65(1):44-52.
181. Raher MJ, Thibault HB, Buys ES, et al. A short duration of high-fat diet induces insulin resistance and predisposes to adverse left ventricular remodeling after pressure

overload. *American Journal of Physiology-Heart and Circulatory Physiology.* 2008;295(6):H2495-H2502.
182. Watkins H, Ashrafian H, Redwood C. Inherited cardiomyopathies. *N Engl J Med.* 2011;364(17):1643-1656.
183. Towbin JA, Bowles NE. The failing heart. *Nature.* 2002;415(6868):227-233.
184. Crilley JG, Boehm EA, Blair E, et al. Hypertrophic cardiomyopathy due to sarcomeric gene mutations is characterized by impaired energy metabolism irrespective of the degree of hypertrophy. *J Am Coll Cardiol.* 2003;41(10):1776-1782.
185. Jung WI, Hoess T, Bunse M, et al. Differences in cardiac energetics between patients with familial and nonfamilial hypertrophic cardiomyopathy. *Circulation.* 2000;101(12):E121.
186. Shivu GN, Abozguia K, Phan TT, Ahmed I, Henning A, Frenneaux M. (31)P magnetic resonance spectroscopy to measure in vivo cardiac energetics in normal myocardium and hypertrophic cardiomyopathy: Experiences at 3T. *Eur J Radiol.* 2008.
187. Neubauer S, Krahe T, Schindler R, et al. 31P magnetic resonance spectroscopy in dilated cardiomyopathy and coronary artery disease. Altered cardiac high-energy phosphate metabolism in heart failure. *Circulation.* 1992;86(6):1810-1818.
188. Neubauer S, Horn M, Pabst T, et al. Contributions of 31P-magnetic resonance spectroscopy to the understanding of dilated heart muscle disease. *Eur Heart J.* 1995;16 Suppl O:115-118.
189. Neubauer S, Horn M, Cramer M, et al. Myocardial phosphocreatine-to-ATP ratio is a predictor of mortality in patients with dilated cardiomyopathy. *Circulation.* 1997;96(7):2190-2196.
190. Ho CY, Seidman CE. A contemporary approach to hypertrophic cardiomyopathy. *Circulation.* 2006;113(24):e858-862.
191. Maron BJ, Gardin JM, Flack JM, Gidding SS, Kurosaki TT, Bild DE. Prevalence of hypertrophic cardiomyopathy in a general population of young adults. Echocardiographic analysis of 4111 subjects in the CARDIA Study. Coronary Artery Risk Development in (Young) Adults. *Circulation.* 1995;92(4):785-789.
192. McKenna WJ, Mogensen J, Elliott PM. Role of genotyping in risk factor assessment for sudden death in hypertrophic cardiomyopathy. *J Am Coll Cardiol.* 2002;39(12):2049-2051.
193. Neubauer S, Kolm P, Ho CY, et al. Distinct Subgroups in Hypertrophic Cardiomyopathy in the NHLBI HCM Registry. *Journal of the American College of Cardiology.* 2019;74(19):2333-2345.
194. Ho CY, Charron P, Richard P, Girolami F, Van Spaendonck-Zwarts KY, Pinto Y. Genetic advances in sarcomeric cardiomyopathies: state of the art. *Cardiovascular Research.* 2015;105(4):397-408.
195. Liu Q, Li D, Berger AE, Johns RA, Gao L. Survival and prognostic factors in hypertrophic cardiomyopathy: a meta-analysis. *Scientific Reports.* 2017;7(1):11957.
196. Elliott PM, Anastasakis A, Borger MA, et al. 2014 ESC Guidelines on diagnosis and management of hypertrophic cardiomyopathy: the Task Force for the Diagnosis and Management of Hypertrophic Cardiomyopathy of the European Society of Cardiology (ESC). *Eur Heart J.* 2014;35(39):2733-2779.
197. Maron BJ, Spirito P, Shen W-K, et al. Implantable Cardioverter-Defibrillators and Prevention of Sudden Cardiac Death in Hypertrophic Cardiomyopathy. *JAMA.* 2007;298(4):405-412.

198. Elliott K, Watkins H, Redwood CS. Altered regulatory properties of human cardiac troponin I mutants that cause hypertrophic cardiomyopathy. *J Biol Chem.* 2000;275(29):22069-22074.
199. Bottinelli R, Coviello DA, Redwood CS, et al. A mutant tropomyosin that causes hypertrophic cardiomyopathy is expressed in vivo and associated with an increased calcium sensitivity. *Circ Res.* 1998;82(1):106-115.
200. Lowey S. Functional consequences of mutations in the myosin heavy chain at sites implicated in familial hypertrophic cardiomyopathy. *Trends Cardiovasc Med.* 2002;12(8):348-354.
201. Nollet EE, Westenbrink BD, Boer RAd, Kuster DWD, Velden Jvd. Unraveling the Genotype‐Phenotype Relationship in Hypertrophic Cardiomyopathy: Obesity‐Related Cardiac Defects as a Major Disease Modifier. *Journal of the American Heart Association.* 2020;9(22):e018641.
202. Marcus ML, Harrison DG, Chilian WM, et al. Alterations in the coronary circulation in hypertrophied ventricles. *Circulation.* 1987;75(1 Pt 2):I19-25.
203. Olivotto I, Girolami F, Sciagrà R, et al. Microvascular function is selectively impaired in patients with hypertrophic cardiomyopathy and sarcomere myofilament gene mutations. *J Am Coll Cardiol.* 2011;58(8):839-848.
204. Blair E, Redwood C, Ashrafian H, et al. Mutations in the gamma(2) subunit of AMP-activated protein kinase cause familial hypertrophic cardiomyopathy: evidence for the central role of energy compromise in disease pathogenesis. *Hum Mol Genet.* 2001;10(11):1215-1220.
205. Ferrantini C, Belus A, Piroddi N, Scellini B, Tesi C, Poggesi C. Mechanical and energetic consequences of HCM-causing mutations. *J Cardiovasc Transl Res.* 2009;2(4):441-451.
206. Fraysse B, Weinberger F, Bardswell SC, et al. Increased myofilament Ca2+ sensitivity and diastolic dysfunction as early consequences of Mybpc3 mutation in heterozygous knock-in mice. *J Mol Cell Cardiol.* 2012;52(6):1299-1307.
207. Javadpour MM, Tardiff JC, Pinz I, Ingwall JS. Decreased energetics in murine hearts bearing the R92Q mutation in cardiac troponin T. *J Clin Invest.* 2003;112(5):768-775.
208. Petersen SE, Jerosch-Herold M, Hudsmith LE, et al. Evidence for Microvascular Dysfunction in Hypertrophic Cardiomyopathy. *Circulation.* 2007;115(18):2418-2425.
209. Spindler M, Saupe KW, Christe ME, et al. Diastolic dysfunction and altered energetics in the alphaMHC403/+ mouse model of familial hypertrophic cardiomyopathy. *J Clin Invest.* 1998;101(8):1775-1783.
210. Ashrafian H, Redwood C, Blair E, Watkins H. Hypertrophic cardiomyopathy:a paradigm for myocardial energy depletion. *Trends Genet.* 2003;19(5):263-268.
211. Redwood CS, Moolman-Smook JC, Watkins H. Properties of mutant contractile proteins that cause hypertrophic cardiomyopathy. *Cardiovasc Res.* 1999;44(1):20-36.
212. Seidman JG, Seidman C. The genetic basis for cardiomyopathy: from mutation identification to mechanistic paradigms. *Cell.* 2001;104(4):557-567.
213. Morimoto S, Nakaura H, Yanaga F, Ohtsuki I. Functional consequences of a carboxyl terminal missense mutation Arg278Cys in human cardiac troponin T. *Biochem Biophys Res Commun.* 1999;261(1):79-82.
214. Sweeney HL, Feng HS, Yang Z, Watkins H. Functional analyses of troponin T mutations that cause hypertrophic cardiomyopathy: insights into disease pathogenesis and troponin function. *Proc Natl Acad Sci U S A.* 1998;95(24):14406-14410.

215. Petersen SE, Jerosch-Herold M, Hudsmith LE, et al. Evidence for microvascular dysfunction in hypertrophic cardiomyopathy: new insights from multiparametric magnetic resonance imaging. *Circulation.* 2007;115(18):2418-2425.
216. Cecchi F, Olivotto I, Gistri R, Lorenzoni R, Chiriatti G, Camici PG. Coronary microvascular dysfunction and prognosis in hypertrophic cardiomyopathy. *N Engl J Med.* 2003;349(11):1027-1035.
217. Camici P, Chiriatti G, Lorenzoni R, et al. Coronary vasodilation is impaired in both hypertrophied and nonhypertrophied myocardium of patients with hypertrophic cardiomyopathy: a study with nitrogen-13 ammonia and positron emission tomography. *J Am Coll Cardiol.* 1991;17(4):879-886.
218. Perrone-Filardi P, Bacharach SL, Dilsizian V, Panza JA, Maurea S, Bonow RO. Regional systolic function, myocardial blood flow and glucose uptake at rest in hypertrophic cardiomyopathy. *Am J Cardiol.* 1993;72(2):199-204.
219. Basso C, Thiene G, Corrado D, Buja G, Melacini P, Nava A. Hypertrophic cardiomyopathy and sudden death in the young: pathologic evidence of myocardial ischemia. *Hum Pathol.* 2000;31(8):988-998.
220. Varnava AM, Elliott PM, Sharma S, McKenna WJ, Davies MJ. Hypertrophic cardiomyopathy: the interrelation of disarray, fibrosis, and small vessel disease. *Heart.* 2000;84(5):476-482.
221. Wasserstrum Y, Barriales-Villa R, Fernández-Fernández X, et al. The impact of diabetes mellitus on the clinical phenotype of hypertrophic cardiomyopathy. *European Heart Journal.* 2018;40(21):1671-1677.
222. Hughes RK, Knott KD, Malcolmson J, et al. Apical Hypertrophic Cardiomyopathy: The Variant Less Known. *Journal of the American Heart Association.* 2020;9(5):e015294.
223. Fumagalli C, Maurizi N, Day SM, et al. Association of Obesity With Adverse Long-term Outcomes in Hypertrophic Cardiomyopathy. *JAMA Cardiology.* 2020;5(1):65-72.
224. Larsen CM, Ball CA, Hebl VB, et al. Effect of Body Mass Index on Exercise Capacity in Patients With Hypertrophic Cardiomyopathy. *Am J Cardiol.* 2018;121(1):100-106.
225. Park J-B, Kim DH, Lee H, et al. Obesity and metabolic health status are determinants for the clinical expression of hypertrophic cardiomyopathy. *European Journal of Preventive Cardiology.* 2020;27(17):1849-1857.
226. Mok M, Nombela-Franco L, Dumont E, et al. Chronic obstructive pulmonary disease in patients undergoing transcatheter aortic valve implantation: insights on clinical outcomes, prognostic markers, and functional status changes. *JACC Cardiovasc Interv.* 2013;6(10):1072-1084.
227. Pennell DJ, Sechtem UP, Higgins CB, et al. Clinical indications for cardiovascular magnetic resonance (CMR): Consensus Panel report. *J Cardiovasc Magn Reson.* 2004;6(4):727-765.
228. Agner BFR, Kühl JT, Linde JJ, et al. Assessment of left atrial volume and function in patients with permanent atrial fibrillation: comparison of cardiac magnetic resonance imaging, 320-slice multi-detector computed tomography, and transthoracic echocardiography. *European Heart Journal - Cardiovascular Imaging.* 2013;15(5):532-540.
229. Kühl JT, Lønborg J, Fuchs A, et al. Assessment of left atrial volume and function: a comparative study between echocardiography, magnetic resonance imaging and multi slice computed tomography. *The International Journal of Cardiovascular Imaging.* 2012;28(5):1061-1071.

230. Qu YY, Paul J, Li H, Ma GS, Buckert D, Rasche V. Left ventricular myocardial strain quantification with two- and three-dimensional cardiovascular magnetic resonance based tissue tracking. *Quant Imaging Med Surg.* 2021;11(4):1421-1436.
231. Simpson RM, Keegan J, Firmin DN. MR assessment of regional myocardial mechanics. *J Magn Reson Imaging.* 2013;37(3):576-599.
232. Barreiro-Pérez M, Curione D, Symons R, Claus P, Voigt JU, Bogaert J. Left ventricular global myocardial strain assessment comparing the reproducibility of four commercially available CMR-feature tracking algorithms. *Eur Radiol.* 2018;28(12):5137-5147.
233. Nagata Y, Takeuchi M, Wu VC, et al. Prognostic value of LV deformation parameters using 2D and 3D speckle-tracking echocardiography in asymptomatic patients with severe aortic stenosis and preserved LV ejection fraction. *JACC Cardiovasc Imaging.* 2015;8(3):235-245.
234. Cerqueira MD, Weissman NJ, Dilsizian V, et al. Standardized myocardial segmentation and nomenclature for tomographic imaging of the heart. A statement for healthcare professionals from the Cardiac Imaging Committee of the Council on Clinical Cardiology of the American Heart Association. *Int J Cardiovasc Imaging.* 2002;18(1):539-542.
235. Liu B, Dardeer AM, Moody WE, et al. Reference ranges for three-dimensional feature tracking cardiac magnetic resonance: comparison with two-dimensional methodology and relevance of age and gender. *Int J Cardiovasc Imaging.* 2018;34(5):761-775.
236. Lim C, Blaszczyk E, Riazy L, et al. Quantification of myocardial strain assessed by cardiovascular magnetic resonance feature tracking in healthy subjects—influence of segmentation and analysis software. *European Radiology.* 2021;31(6):3962-3972.
237. Kellman P, Hernando D, Shah S, et al. Multiecho dixon fat and water separation method for detecting fibrofatty infiltration in the myocardium. *Magn Reson Med.* 2009;61(1):215-221.
238. White SK, Sado DM, Fontana M, et al. T1 mapping for myocardial extracellular volume measurement by CMR: bolus only versus primed infusion technique. *JACC Cardiovasc Imaging.* 2013;6(9):955-962.
239. Jerosch-Herold M, Sheridan DC, Kushner JD, et al. Cardiac magnetic resonance imaging of myocardial contrast uptake and blood flow in patients affected with idiopathic or familial dilated cardiomyopathy. *Am J Physiol Heart Circ Physiol.* 2008;295(3):H1234-h1242.
240. Park YJ, Park S-J, Kim E-K, et al. Semi-quantitative versus quantitative assessments of late gadolinium enhancement extent for predicting spontaneous ventricular tachyarrhythmia events in patients with hypertrophic cardiomyopathy. *Scientific Reports.* 2020;10(1):2920.
241. Kellman P, Hansen MS, Nielles-Vallespin S, et al. Myocardial perfusion cardiovascular magnetic resonance: optimized dual sequence and reconstruction for quantification. *Journal of Cardiovascular Magnetic Resonance.* 2017;19(1):43.
242. Kramer CM, Barkhausen J, Flamm SD, Kim RJ, Nagel E, Society for Cardiovascular Magnetic Resonance Board of Trustees Task Force on Standardized P. Standardized cardiovascular magnetic resonance (CMR) protocols 2013 update. *Journal of cardiovascular magnetic resonance : official journal of the Society for Cardiovascular Magnetic Resonance.* 2013;15(1):91-91.
243. Knott KD, Seraphim A, Augusto JB, et al. The Prognostic Significance of Quantitative Myocardial Perfusion. *Circulation.* 2020;141(16):1282-1291.

244. Kotecha T, Monteagudo JM, Martinez-Naharro A, et al. Quantitative cardiovascular magnetic resonance myocardial perfusion mapping to assess hyperaemic response to adenosine stress. *Eur Heart J Cardiovasc Imaging.* 2021;22(3):273-281.
245. Taegtmeyer H, Hems R, Krebs HA. Utilization of energy-providing substrates in the isolated working rat heart. *Biochemical Journal.* 1980;186(3):701-711.
246. Neubauer S. The Failing Heart — An Engine Out of Fuel. *New England Journal of Medicine.* 2007;356(11):1140-1151.
247. Scheuermann-Freestone M, Madsen PL, Manners D, et al. Abnormal Cardiac and Skeletal Muscle Energy Metabolism in Patients With Type 2 Diabetes. *Circulation.* 2003;107(24):3040-3046.
248. Shivu GN, Phan TT, Abozguia K, et al. Relationship Between Coronary Microvascular Dysfunction and Cardiac Energetics Impairment in Type 1 Diabetes Mellitus. *Circulation.* 2010;121(10):1209-1215.
249. Levelt E, Rodgers CT, Clarke WT, et al. Cardiac energetics, oxygenation, and perfusion during increased workload in patients with type 2 diabetes mellitus. *European heart journal.* 2015.
250. Dass S, Cochlin LE, Suttie JJ, et al. Exacerbation of cardiac energetic impairment during exercise in hypertrophic cardiomyopathy: a potential mechanism for diastolic dysfunction. *European Heart Journal.* 2015.
251. Sairia D, Cameron H, Joseph S, et al. Patients with Dilated Cardiomyopathy (DCM) have appropriate myocardial oxygenation response to vasodilator stress. *Journal of Cardiovascular Magnetic Resonance.* 2013;15.
252. Mahmod M, Francis JM, Pal N, et al. Myocardial perfusion and oxygenation are impaired during stress in severe aortic stenosis and correlate with impaired energetics and subclinical left ventricular dysfunction. *J Cardiovasc Magn Reson.* 2014;16:29.
253. Bottomley PA, Weiss RG, Hardy CJ, Baumgartner WA. Myocardial high-energy phosphate metabolism and allograft rejection in patients with heart transplants. *Radiology.* 1991;181(1):67-75.
254. Tyler DJ, Emmanuel Y, Cochlin LE, et al. Reproducibility of ^{31}P cardiac magnetic resonance spectroscopy at 3T. *NMR Biomed.* 2009;22(4):405-413.
255. Sairia D, Lowri EC, Cameron JH, et al. Development and validation of a short 31P cardiac magnetic resonance spectroscopy protocol. *Journal of Cardiovascular Magnetic Resonance.* 2010(12):123.
256. Blamire AM, Rajagopalan B, Radda GK. Measurement of myocardial pH by saturation transfer in man. *Magnetic Resonance in Medicine.* 1999;41(1):198-203.
257. Sairia Dass, Lowri E Cochlin, Cameron J Holloway, et al. Development and validation of a short 31P cardiac magnetic resonance spectroscopy protocol. *Journal of Cardiovascular Magnetic Resonance* 2010(12):123.
258. Kellman P, Chefd'hotel C, Lorenz CH, Mancini C, Arai AE, McVeigh ER. Fully automatic, retrospective enhancement of real-time acquired cardiac cine MR images using image-based navigators and respiratory motion-corrected averaging. *Magnetic Resonance in Medicine.* 2008;59(4):771-778.
259. Levelt E, Mahmod M, Piechnik SK, et al. Relationship between Left Ventricular Structural and Metabolic Remodelling in Type 2 Diabetes Mellitus. *Diabetes.* 2015.
260. Bland JM, Altman DG. Statistical methods for assessing agreement between two methods of clinical measurement. *Lancet.* 1986;1(8476):307-310.

261. Köstler H, Landschütz W, Koeppe S, et al. Age and gender dependence of human cardiac phosphorus metabolites determined by SLOOP 31P MR spectroscopy. *Magn Reson Med.* 2006;56(4):907-911.
262. Wasserstrum Y, Barriales-Villa R, Fernández-Fernández X, et al. The impact of diabetes mellitus on the clinical phenotype of hypertrophic cardiomyopathy. *European Heart Journal.* 2019;40(21):1671-1677.
263. Timmer SA, Germans T, Götte MJ, et al. Determinants of myocardial energetics and efficiency in symptomatic hypertrophic cardiomyopathy. *Eur J Nucl Med Mol Imaging.* 2010;37(4):779-788.
264. Toepfer CN, Garfinkel AC, Venturini G, et al. Myosin Sequestration Regulates Sarcomere Function, Cardiomyocyte Energetics, and Metabolism, Informing the Pathogenesis of Hypertrophic Cardiomyopathy. *Circulation.* 2020;141(10):828-842.
265. Joy G, Crane J, Lau C, et al. Impact of obesity on myocardial microvasculature assessed using fully-automated inline myocardial perfusion mapping CMR. *European Heart Journal - Cardiovascular Imaging.* 2021;22(Supplement_1).
266. Swoboda PP, McDiarmid AK, Erhayiem B, et al. Diabetes Mellitus, Microalbuminuria, and Subclinical Cardiac Disease: Identification and Monitoring of Individuals at Risk of Heart Failure. *Journal of the American Heart Association: Cardiovascular and Cerebrovascular Disease.* 2017;6(7):e005539.
267. Moon JC, Treibel TA, Schelbert EB. T1 Mapping for Diffuse Myocardial FibrosisA Key Biomarker in Cardiac Disease?∗. *Journal of the American College of Cardiology.* 2013;62(14):1288-1289.
268. O'Hanlon R, Grasso A, Roughton M, et al. Prognostic Significance of Myocardial Fibrosis in Hypertrophic Cardiomyopathy. *Journal of the American College of Cardiology.* 2010;56(11):867-874.
269. Authors/Task Force m, Elliott PM, Anastasakis A, et al. 2014 ESC Guidelines on diagnosis and management of hypertrophic cardiomyopathy: The Task Force for the Diagnosis and Management of Hypertrophic Cardiomyopathy of the European Society of Cardiology (ESC). *European Heart Journal.* 2014;35(39):2733-2779.
270. KG Alberti, Zimmet P. Definition, diagnosis and classification of diabetes mellitus and its complications. Part 1: diagnosis and classification of diabetes mellitus provisional report of a WHO consultation. *Diabet Med.* 1998;15(7):539-553.
271. Thirunavukarasu S, Jex N, Chowdhary A, et al. Empagliflozin Treatment is Associated With Improvements in Cardiac Energetics and Function and Reductions in Myocardial Cellular Volume in Patients With Type 2 Diabetes. *Diabetes.* 2021:db210270.
272. Treibel Thomas A, Kozor R, Menacho K, et al. Left Ventricular Hypertrophy Revisited. *Circulation.* 2017;136(25):2519-2521.
273. Lucian AB Purvis, William T. Clarke, Luca Biasiolli, Robson MD, CT R. Linewidth constraints in Matlab AMARES using per-metabolite T2 and per-voxel ΔB0. *ISMRM.* 2014.
274. Rider OJ, Lewandowski A, Nethononda R, et al. Gender-specific differences in left ventricular remodelling in obesity: insights from cardiovascular magnetic resonance imaging. *Eur Heart J.* 2013;34(4):292-299.
275. Hudsmith LE, Petersen SE, Tyler DJ, et al. Determination of cardiac volumes and mass with FLASH and SSFP cine sequences at 1.5 vs. 3 Tesla: a validation study. *J Magn Reson Imaging.* 2006;24(2):312-318.
276. Gulsin GS, Swarbrick DJ, Hunt WH, et al. Relation of Aortic Stiffness to Left Ventricular Remodeling in Younger Adults With Type 2 Diabetes. *Diabetes.* 2018;67(7):1395.

277. Sado DM, White SK, Piechnik SK, et al. Identification and Assessment of Anderson-Fabry Disease by Cardiovascular Magnetic Resonance Noncontrast Myocardial T1 Mapping. *Circulation: Cardiovascular Imaging.* 2013;6(3):392-398.
278. Karur GR, Robison S, Iwanochko RM, et al. Use of Myocardial T1 Mapping at 3.0 T to Differentiate Anderson-Fabry Disease from Hypertrophic Cardiomyopathy. *Radiology.* 2018;288(2):398-406.
279. Lopes LR, Losi M-A, Sheikh N, et al. Association Between Common Cardiovascular Risk Factors and Clinical Phenotype in Patients with Hypertrophic Cardiomyopathy From the European Society of Cardiology (ESC) EurObservational Research Programme (EORP) Cardiomyopathy/Myocarditis Registry. *European Heart Journal - Quality of Care and Clinical Outcomes.* 2022:qcac006.
280. Office for National Statistics, Population estimates 2020. <https://www.ons.gov.uk/peoplepopulationandcommunity/populationandmigration/populationestimates>, release date 25 June 2021, last accessed 2 March 2022. In.
281. Coats CJ, Gallagher MJ, Foley M, et al. Relation between serum N-terminal pro-brain natriuretic peptide and prognosis in patients with hypertrophic cardiomyopathy. *European Heart Journal.* 2013;34(32):2529-2537.
282. Wang S, Cui H, Ji K, et al. Impact of type 2 diabetes mellitus on mid-term mortality for hypertrophic cardiomyopathy patients who underwent septal myectomy. *Cardiovascular Diabetology.* 2020;19(1):64.
283. Watkins H. Time to Think Differently About Sarcomere-Negative Hypertrophic Cardiomyopathy. *Circulation.* 2021;143(25):2415-2417.
284. Dhandapany Perundurai S, Kang S, Kashyap Deepak K, et al. Adiponectin receptor 1 variants contribute to hypertrophic cardiomyopathy that can be reversed by rapamycin. *Science Advances.*7(2):eabb3991.
285. Gonzalez AB, Young L, Doll JA, Morgan GM, Crawford SE, Plunkett BA. Elevated neonatal insulin-like growth factor I is associated with fetal hypertrophic cardiomyopathy in diabetic women. *American Journal of Obstetrics & Gynecology.* 2014;211(3):290.e291-290.e297.
286. Cecchi F, Olivotto I, Gistri R, Lorenzoni R, Chiriatti G, Camici PG. Coronary Microvascular Dysfunction and Prognosis in Hypertrophic Cardiomyopathy. *New England Journal of Medicine.* 2003;349(11):1027-1035.
287. Neubauer S, Horn M, Cramer M, et al. Myocardial Phosphocreatine-to-ATP Ratio Is a Predictor of Mortality in Patients With Dilated Cardiomyopathy. *Circulation.* 1997;96(7):2190-2196.
288. Tower-Rader A, Mohananey D, To A, Lever HM, Popovic ZB, Desai MY. Prognostic Value of Global Longitudinal Strain in Hypertrophic Cardiomyopathy: A Systematic Review of Existing Literature. *JACC: Cardiovascular Imaging.* 2019;12(10):1930-1942.
289. Ellis J, Valkovič L, Purvis LAB, Clarke WT, Rodgers CT. Reproducibility of human cardiac phosphorus MRS ((31) P-MRS) at 7 T. *NMR in biomedicine.* 2019;32(6):e4095-e4095.
290. Beckmann E, Grau JB, Sainger R, Poggio P, Ferrari G. Insights into the Use of Biomarkers in Calcific Aortic Valve Disease. *The Journal of heart valve disease.* 2010;19(4):441-452.
291. Nishimura Rick A, Otto Catherine M, Bonow Robert O, et al. 2017 AHA/ACC Focused Update of the 2014 AHA/ACC Guideline for the Management of Patients With Valvular Heart Disease. *Journal of the American College of Cardiology.* 2017;70(2):252-289.

292. Vahanian A, Beyersdorf F, Praz F, et al. 2021 ESC/EACTS Guidelines for the management of valvular heart disease: Developed by the Task Force for the management of valvular heart disease of the European Society of Cardiology (ESC) and the European Association for Cardio-Thoracic Surgery (EACTS). *European Heart Journal.* 2022;43(7):561-632.
293. d'Arcy JL, Coffey S, Loudon MA, et al. Large-scale community echocardiographic screening reveals a major burden of undiagnosed valvular heart disease in older people: the OxVALVE Population Cohort Study(). *European heart journal.* 2016;37(47):3515-3522.
294. Neubauer S, Horn M, Pabst T, et al. Contributions of 31P-magnetic resonance spectroscopy to the understanding of dilated heart muscle disease. *European Heart Journal.* 1995;16(suppl O):115-118.
295. Dweck MR, Joshi S, Murigu T, et al. Midwall Fibrosis Is an Independent Predictor of Mortality in Patients With Aortic Stenosis. *Journal of the American College of Cardiology.* 2011;58(12):1271-1279.
296. Chin CWL, Everett RJ, Kwiecinski J, et al. Myocardial Fibrosis and Cardiac Decompensation in Aortic Stenosis. (1876-7591 (Electronic)).
297. Nishimura RA, Otto CM, Bonow RO, et al. 2017 AHA/ACC Focused Update of the 2014 AHA/ACC Guideline for the Management of Patients With Valvular Heart Disease: A Report of the American College of Cardiology/American Heart Association Task Force on Clinical Practice Guidelines. *Circulation.* 2017;135(25):e1159-e1195.
298. Alberti KG, Zimmet PZ. Definition, diagnosis and classification of diabetes mellitus and its complications. Part 1: diagnosis and classification of diabetes mellitus provisional report of a WHO consultation. *Diabet Med.* 1998;15(7):539-553.
299. Chowdhary A, Thirunavukarasu S, Jex N, et al. Coronary microvascular function and visceral adiposity in patients with normal body weight and type 2 diabetes. *Obesity.* 2022;30(5):1079-1090.
300. Mok M, Nombela-Franco L, Urena M, et al. Prognostic Value of Exercise Capacity as Evaluated by the 6-Minute Walk Test in Patients Undergoing Transcatheter Aortic Valve Implantation. *Journal of the American College of Cardiology.* 2013;61(8):897-898.
301. Duchnowski P, Hryniewiecki T, Kuśmierczyk M, Szymanski P. Performance of the EuroSCORE II and the Society of Thoracic Surgeons score in patients undergoing aortic valve replacement for aortic stenosis. *J Thorac Dis.* 2019;11(5):2076-2081.
302. Shimura T, Yamamoto M, Kano S, et al. Impact of the Clinical Frailty Scale on Outcomes After Transcatheter Aortic Valve Replacement. *Circulation.* 2017;135(21):2013-2024.
303. Beyerbacht HP, Lamb HJ, van der Laarse A, et al. Aortic Valve Replacement in Patients with Aortic Valve Stenosis Improves Myocardial Metabolism and Diastolic Function. *Radiology.* 2001;219(3):637-643.
304. Ingwall JS. Energy metabolism in heart failure and remodelling. *Cardiovascular research.* 2009;81(3):412-419.
305. Otto CM, Song J-K. Treatment of Aortic Stenosis With Transcatheter Aortic Valve Implantation. *JAMA.* 2022;327(19):1870-1871.
306. Sharma LK, Lu J, Bai Y. Mitochondrial respiratory complex I: structure, function and implication in human diseases. *Curr Med Chem.* 2009;16(10):1266-1277.
307. Wilson L, Yang Q, Szustakowski JD, Gullicksen PS, Halse R. Pyruvate induces mitochondrial biogenesis by a PGC-1 α-independent mechanism. *American Journal of Physiology - Cell Physiology.* 2007;292(5):C1599.

308. Gnaiger E. Polarographic oxygen sensors, the oxygraph and high-resolution respirometry to assess mitochondrial function. *Drug-induced mitochondrial dysfunction.* 2008;12:327-352.
309. Pesta D, Gnaiger E. High-Resolution Respirometry: OXPHOS Protocols for Human Cells and Permeabilized Fibers from Small Biopsies of Human Muscle. In: Palmeira CM, Moreno AJ, eds. *Mitochondrial Bioenergetics: Methods and Protocols.* Totowa, NJ: Humana Press; 2012:25-58.
310. Stride N, Larsen S, Hey-Mogensen M, et al. Decreased mitochondrial oxidative phosphorylation capacity in the human heart with left ventricular systolic dysfunction. *Eur J Heart Fail.* 2013;15(2):150-157.
311. Athithan L, Gulsin GS, McCann GP, Levelt E. Diabetic cardiomyopathy: Pathophysiology, theories and evidence to date. *World J Diabetes.* 2019;10(10):490-510.
312. Lowell BB, Shulman GI. Mitochondrial dysfunction and type 2 diabetes. *Science.* 2005;307(5708):384-387.
313. Fritz T, Krämer DK, Karlsson HK, et al. Low-intensity exercise increases skeletal muscle protein expression of PPARdelta and UCP3 in type 2 diabetic patients. *Diabetes Metab Res Rev.* 2006;22(6):492-498.
314. Montgomery MK, Turner N. Mitochondrial dysfunction and insulin resistance: an update. *Endocr Connect.* 2015;4(1):R1-r15.
315. Mogensen M, Sahlin K, Fernström M, et al. Mitochondrial Respiration Is Decreased in Skeletal Muscle of Patients With Type 2 Diabetes. *Diabetes.* 2007;56(6):1592-1599.
316. Krumschnabel G, Fontana-Ayoub M, Sumbalova Z, et al. Simultaneous high-resolution measurement of mitochondrial respiration and hydrogen peroxide production. *Methods Mol Biol.* 2015;1264:245-261.
317. Kuznetsov AV, Veksler V, Gellerich FN, Saks V, Margreiter R, Kunz WS. Analysis of mitochondrial function in situ in permeabilized muscle fibers, tissues and cells. *Nat Protoc.* 2008;3(6):965-976.
318. Zweck E, Scheiber D, Schultheiss H-P, et al. Impaired Myocardial Mitochondrial Respiration in Humans With Prediabetes: A Footprint of Prediabetic Cardiomyopathy. *Circulation.* 2022;146(15):1189-1191.
319. Yu T, Sheu SS, Robotham JL, Yoon Y. Mitochondrial fission mediates high glucose-induced cell death through elevated production of reactive oxygen species. *Cardiovasc Res.* 2008;79(2):341-351.
320. Li SY, Sigmon VK, Babcock SA, Ren J. Advanced glycation endproduct induces ROS accumulation, apoptosis, MAP kinase activation and nuclear O-GlcNAcylation in human cardiac myocytes. *Life Sci.* 2007;80(11):1051-1056.
321. Gawlowski T, Suarez J, Scott B, et al. Modulation of dynamin-related protein 1 (DRP1) function by increased O-linked-β-N-acetylglucosamine modification (O-GlcNAc) in cardiac myocytes. *J Biol Chem.* 2012;287(35):30024-30034.
322. Anderson EJ, Kypson AP, Rodriguez E, Anderson CA, Lehr EJ, Neufer PD. Substrate-Specific Derangements in Mitochondrial Metabolism and Redox Balance in the Atrium of the Type 2 Diabetic Human Heart. *Journal of the American College of Cardiology.* 2009;54(20):1891-1898.
323. Monga S, Valkovič L, Tyler D, et al. Insights Into the Metabolic Aspects of Aortic Stenosis With the Use of Magnetic Resonance Imaging. *JACC: Cardiovascular Imaging.* 2022.

324. Iung B, Delgado V, Rosenhek R, et al. Contemporary Presentation and Management of Valvular Heart Disease: The EURObservational Research Programme Valvular Heart Disease II Survey. *Circulation.* 2019;140(14):1156-1169.
325. Cruz-Jentoft AJ, Baeyens JP, Bauer JM, et al. Sarcopenia: European consensus on definition and diagnosis: Report of the European Working Group on Sarcopenia in Older People. *Age Ageing.* 2010;39(4):412-423.
326. Janssen I, Heymsfield SB, Ross R. Low relative skeletal muscle mass (sarcopenia) in older persons is associated with functional impairment and physical disability. *J Am Geriatr Soc.* 2002;50(5):889-896.
327. Wang S, Xie H, Gong Y, et al. The value of L3 skeletal muscle index in evaluating preoperative nutritional risk and long-term prognosis in colorectal cancer patients. *Scientific Reports.* 2020;10(1):8153.
328. Miyamoto Y, Baba Y, Sakamoto Y, et al. Sarcopenia is a Negative Prognostic Factor After Curative Resection of Colorectal Cancer. *Ann Surg Oncol.* 2015;22(8):2663-2668.
329. Bertschi D, Kiss CM, Schoenenberger AW, Stuck AE, Kressig RW. Sarcopenia in Patients Undergoing Transcatheter Aortic Valve Implantation (TAVI): A Systematic Review of the Literature. *The journal of nutrition, health & aging.* 2021;25(1):64-70.
330. Heidari B, Al-Hijji MA, Moynagh MR, et al. Transcatheter aortic valve replacement outcomes in patients with sarcopaenia. *EuroIntervention.* 2019;15(8):671-677.
331. Banovic M, Athithan L, McCann GP. Aortic stenosis and diabetes mellitus: An ominous combination. *Diabetes and Vascular Disease Research.* 2019;16(4):310-323.
332. Larsson SC, Wallin A, Håkansson N, Stackelberg O, Bäck M, Wolk A. Type 1 and type 2 diabetes mellitus and incidence of seven cardiovascular diseases. *Int J Cardiol.* 2018;262:66-70.
333. Ram E, Kogan A, Levin S, et al. Type 2 diabetes mellitus increases long-term mortality risk after isolated surgical aortic valve replacement. *Cardiovascular Diabetology.* 2019;18(1):31.
334. Abramowitz Y, Vemulapalli S, Chakravarty T, et al. Clinical Impact of Diabetes Mellitus on Outcomes After Transcatheter Aortic Valve Replacement. *Circulation: Cardiovascular Interventions.* 2017;10(11):e005417.
335. Jaiswal N, Gavin MG, Quinn WJ, 3rd, et al. The role of skeletal muscle Akt in the regulation of muscle mass and glucose homeostasis. *Mol Metab.* 2019;28:1-13.
336. Sylow L, Tokarz VL, Richter EA, Klip A. The many actions of insulin in skeletal muscle, the paramount tissue determining glycemia. *Cell Metab.* 2021;33(4):758-780.
337. Park SW, Goodpaster BH, Strotmeyer ES, et al. Decreased muscle strength and quality in older adults with type 2 diabetes: the health, aging, and body composition study. *Diabetes.* 2006;55(6):1813-1818.
338. Wang CP, Hazuda HP. Better glycemic control is associated with maintenance of lower-extremity function over time in Mexican American and European American older adults with diabetes. *Diabetes Care.* 2011;34(2):268-273.
339. Wong E, Backholer K, Gearon E, et al. Diabetes and risk of physical disability in adults: a systematic review and meta-analysis. *Lancet Diabetes Endocrinol.* 2013;1(2):106-114.
340. Lee CG, Boyko EJ, Barrett-Connor E, et al. Insulin sensitizers may attenuate lean mass loss in older men with diabetes. *Diabetes Care.* 2011;34(11):2381-2386.
341. Mahmod M, Francis JM, Pal N, et al. Myocardial perfusion and oxygenation are impaired during stress in severe aortic stenosis and correlate with impaired

energetics and subclinical left ventricular dysfunction. *Journal of Cardiovascular Magnetic Resonance.* 2014;16(1):29.
342. Yang YX, Chong MS, Lim WS, et al. Validity of estimating muscle and fat volume from a single MRI section in older adults with sarcopenia and sarcopenic obesity. *Clin Radiol.* 2017;72(5):427.e429-427.e414.
343. Brown E, Williams A, Hakim O, et al. MRI thigh measurements predict whole-body skeletal muscle mass in patients with type 2 diabetes: a comparison with DXA. *JCSM Rapid Communications.* 2022;5(2):149-153.
344. Yamauchi K, Suzuki S, Kato C, Kato T. Atrophy of individual thigh muscles measured by MRI in older adults with knee osteoarthritis: A cross-sectional study. *Annals of Physical and Rehabilitation Medicine.* 2020;63(1):38-45.
345. Garg L, Agrawal S, Pew T, et al. Psoas Muscle Area as a Predictor of Outcomes in Transcatheter Aortic Valve Implantation. *The American Journal of Cardiology.* 2017;119(3):457-460.
346. Kittiskulnam P, Carrero JJ, Chertow GM, Kaysen GA, Delgado C, Johansen KL. Sarcopenia among patients receiving hemodialysis: weighing the evidence. *Journal of Cachexia, Sarcopenia and Muscle.* 2017;8(1):57-68.
347. Janssen I, Heymsfield SB, Wang Z, Ross R. Skeletal muscle mass and distribution in 468 men and women aged 18–88 yr. *Journal of Applied Physiology.* 2000;89(1):81-88.
348. Shimura T, Yamamoto M, Kano S, et al. Impact of the Clinical Frailty Scale on Outcomes After Transcatheter Aortic Valve Replacement. *Circulation.* 2017;135(21):2013-2024.
349. Baumgartner RN, Stauber PM, McHugh D, Koehler KM, Garry PJ. Cross-sectional age differences in body composition in persons 60+ years of age. *J Gerontol A Biol Sci Med Sci.* 1995;50(6):M307-316.
350. Rantanen T, Harris T, Leveille SG, et al. Muscle strength and body mass index as long-term predictors of mortality in initially healthy men. *J Gerontol A Biol Sci Med Sci.* 2000;55(3):M168-173.
351. Kim Y-S, Lee Y, Chung Y-S, et al. Prevalence of Sarcopenia and Sarcopenic Obesity in the Korean Population Based on the Fourth Korean National Health and Nutritional Examination Surveys. *The Journals of Gerontology: Series A.* 2012;67(10):1107-1113.
352. Phielix E, Mensink M. Type 2 diabetes mellitus and skeletal muscle metabolic function. *Physiol Behav.* 2008;94(2):252-258.
353. Cheng Z, Tseng Y, White MF. Insulin signaling meets mitochondria in metabolism. *Trends Endocrinol Metab.* 2010;21(10):589-598.
354. Coen PM, Jubrias SA, Distefano G, et al. Skeletal muscle mitochondrial energetics are associated with maximal aerobic capacity and walking speed in older adults. *J Gerontol A Biol Sci Med Sci.* 2013;68(4):447-455.
355. Siegel MP, Wilbur T, Mathis M, et al. Impaired adaptability of in vivo mitochondrial energetics to acute oxidative insult in aged skeletal muscle. *Mech Ageing Dev.* 2012;133(9-10):620-628.
356. Michael N, Gupta V, Sadananthan SA, et al. Determinants of intramyocellular lipid accumulation in early childhood. *Int J Obes (Lond).* 2020;44(5):1141-1151.